AN INVESTIGATION OF TURBULENT FLOW IN A CORRUGATED PIPE

A Thesis

Presented to

the Faculty of the Department of Chemical Engineering

University of Houston

In Partial Fulfillment

of the Requirements for the Degree

Master of Science in Chemical Engineering

---

by

Wuu-nan Chen

August, 1973

ACKNOWLEDGEMENTS

My most sincere thanks are extended to my advisor, Dr. A. E. Dukler, for his advice and guidance during the course of this study.

Thanks also for many friends, especially for Mr. K. J. Chu, Who have given me counsel and assistance during my study and thanks for Mr. Roy Priest and Mr. Mike Smith for their valuable assistance in designing and constructing the experimental equipment.

Loving and heartfelt thanks due my wife, Monica, who not only provided me with continuous encouragment, but also type this thesis.

AN INVESTIGATION OF TURBULENT FLOW IN A CORRUGATED PIPE

An Abstract of a Thesis

Presented to

the Faculty of the

Cullen College of Engineering

University of Houston

Houston, Texas

In Partial Fulfillment

of the Requirements for the Degree

Master of Science in Chemical Engineering

by

Wuu-nan Chen

August, 1973

ABSTRACT

Today turbulent measurement with hot wire anemometer is a routine procedure but the conventional equations require a knowledge of the direction of the mean velocity. For flow over peripheral corrugations where the mean velocity vector is changing in direction with radial and axial positions the conventional equations are not valid. Therefore, new equations were derived. These show that the simple sum and differencing techniques useful for parallel flow no longer can be applied.

Experiments were made in a corrugated pipe. This corrugated pipe approximates a sine wave in shape and has the wavelength, 2.75", the amplitude, 0.437", and the smallest radius, 4.275". Experimental data shows that the conventional commercial X-wire boundary layer probe support system interference to the flow. A special type of X-wire was designed and called "Boundary Layer Probe." Using this probe, the radial velocity vector can be easily determined along with the axial component from the derived equations. The system of equations is complex requiring computer solution of data digitized from analog tape.

Data show that the turbulent intensities in longitudinal and radial direction across the pipe radius are higher than those measured from the smooth circular pipe. This is so even at the centerline. The local relative turbulent intensities show that a sharp jump occurs around the tip line (line connecting the tips of the peaks) at certain section which seems to indicate a "separation flow" existing in that region.

CONTENT

I INTRODUCTION

The purpose of this work was to study turbulent flow in a rough corrugated pipe to try to understand the mechanism for increased shear and pressure drop.

In order to do this a constant temperature hot wire* anemometer was used. But in a system like this techniques for using hot wire anemometer systems have not been fully established. This is due to the fact that most existing equations require a knowledge of the direction of the mean velocity vector in order to use them. For flow over corrugated surface the direction of this velocity is an unknown quantity. As a result it has been necessary to develop new equations for the mean velocity, its direction, and the auto and cross correlations of the velocity fluctuations. The resulting equations are complex so it was necessary to develop new software to solve for the flow quantities of interest. As part of the work fast fourier transform programs were developed to permit calculation of spectra and correlation directly from the constant temperature hot wire anemometer signal.

In order to apply the new method to the problem of flow over peripheral corrugations it was necessary to design a probe with a new geometry and test its performance.

* Hot wire anemometer is the general terminology for this kind of instrument despite the fact that the heated element used in this work was a quartz cylinder coated with platinum or tungsten.

The resulting probe and response equations were used to measure flow over a corrugated surface and the variation in both the mean flow and in the turbulent quantities were measured.

II PREVIOUS STUDIES AND ANALYTICAL CONSIDERATION

Previous Studies

Prandtl[1], Jones[2] and Sears[3] established that for laminar flow past an infinitely long cylinder oblique to a uniform velocity field, the two velocity components in a plane normal to the axis of the cylinder are independent of the axial component. If the cylinder is heated uniformly along its axis, consideration of the energy equation shows that the rate of heat loss per unit length depends only on the normal velocity component. From these facts the cosine law of directional sensitivity can be established for an infinitely long hot wire anemometer, and this result is generally assumed to apply to wires of finite length. The cosine law is expressed as:

$$Ve = V_I \cdot \cos\beta_3 \qquad \text{(II-1)}$$

where Ve is the effective cooling velocity of the stream, V_I is the instantaneous velocity, δ is the angle between the instantaneous velocity vector and the wire axis, and $\beta_3 + \delta = 90^\circ$. (see Figure II-1) Schrbauer and Klebanoff[4] experimentally tested the cosine law and concluded that it held for finite wire for angles of yaw less than 70°.

Kronauer[5] suggested that the deviation from the cosine law depended on the length-to-diameter ratio of the wire and is substantially independent of the Reynolds number. Kronauer expressed his results in the form:

$$Ve(\beta_3) = V_I \cdot \cos\beta_3 + 1.2(D/L)^{\frac{1}{2}} \cdot \sin^2\beta_3 \qquad \text{(II-2)}$$

where D and L are sensor diameter and length respectively.

Champagne and Sleicher[6] observed that there is considerable disagreement as to the directional sensitivity of a sensor and to the accuracy of measurements made with wire oblique to the flow when cosine law cooling is assumed. They, therefore, made extensively theoretical and experimental research and derived the following equation,

$$Ve^2 = V_I^2 \ (\cos^2\beta_3 + k^2 \cdot \sin^2\beta_3) \qquad \text{(II-3)}$$

where the value of k is a constant depending primarily upon the length-to-diameter ratio (L/D) of the sensor. Equations (II-2) and (II-3) both indicate that an inclined sensor is sensitive to the tangential velocity component along the sensor. This sensitivity must be taken into consideration when interpreting data from an inclined sensor. Champagne and Sleicher[7] meanwhile derived the equations which included the effects of non-linearity caused by high intensity turbulence. However, those equations were applied for one-dimensional flow only where the mean flow direction is known.

If the direction of the mean velocity is not known or if it varies with position across the flow, the directional sensitivity of the X-wire (wires in the form of X array) changes, and the conventional equations are not valid. One method of overcoming this problem would be to use two identical wires and a traversing mechanism that allows the X array to be rotated about its center until the output voltage in each wire is equal. The rotation can then be measured mechanically and measured velocity fluctuations can be resolved along the desired coordinates. The three undesirable features of this method are that it is very difficult to make identical wires, that the traversing mechanism can become too complex, and that if the fluctuations are large, it is impossible to tell practically whether the two output voltage are equal or not.

Bullock and Bremhorst(8) suggested a method for measuring statistics of the turbulence and the direction of the mean velocity vector when changes in the direction take place along a traverse. In principle the method is sound but in practice it is limited. Error in measuring wire current in commercially available hot wire equipment are such that the calculated angle for the velocity vector can be expected to be in error by at least 5 degrees.

Mccroskey and Durbin(9) proposed a new type of two sensor probe to measure flow angle. Their system consisted of two sensor in a "V" configuration. Equations were developed for extracting the direction of the mean velocity when it lies in the plane of the V. Their work demonstrated that very high precision in measurement was necessary to interpret the results and this made it necessary to develop a new high precision control circuit. The method thus requires special circuits and is not useful when the plane in which the mean velocity vector lies is not known.

In 1968, Yost[28] carried out extensive measurements of flow over roughnesses. The basic equation he used in calculating the mean velocity is,

$$\overline{Ve} = \overline{V_I}\,(\sin\alpha)^{1/k_o}$$

where k_o is a factor which allows the deviation from the sine law and is measured to be 1.1. He, then, linearized the relation between bridge voltage from anemometer and the effective cooling velocity. The equation is,

$$\overline{Eb} = C_3\,\overline{Ve}$$

With $\alpha = 45^\circ$ and $\overline{V_I} = \overline{V_{Io}}$ at centerline,

$$C_3 = \overline{Ve}/(0.73\overline{V_{Io}})$$

C_3 is calculated once $\overline{Ve}$ and $\overline{V_{Io}}$ be measured. Then for any unknown velocity vector, there are two equations corresponding to the two wires, i.e.

$$\overline{V_A} = \overline{V_I}(\sin\alpha_A)^{0.909}$$

$$\overline{V_B} = \overline{V_I}(\sin\alpha_B)^{0.909}$$

where $\alpha_A + \alpha_B = 90$. Dividing $\overline{V_A}$ by $\overline{V_B}$ gives,

$$\alpha_A = \text{arc}\tan(\overline{V_A}/\overline{V_B})^{1.1}$$

also, $$\overline{V_I} = \overline{V_A}/(\sin\alpha_A)^{0.909}$$

Finally, $$\overline{Vn} = \overline{V_I}\,\sin(90^\circ - \alpha_A)$$

The factor k_o which accounts for the deviation from sine law is not a constant. It depends on the sensor geometry and varies with angle of inclination, α. This equation with k_o measured at $\alpha=45$ can only be used within $\alpha = 45^\circ \pm 10^\circ$.

The factor k in equation (II-3) depends on sensor geometry and also varies with the angle of inclination. But extensive[(6)(29)] measurements have been made using equation (II-3) and found that the value of k measured at $\alpha=60^\circ$ has a maximum error for the determination of mean velocity between 1 to 3% at $0^\circ < \alpha < 60^\circ$. For a film type of sensor which has less end loss due to the support, the maxmimum error will be improved.

In measurements of turbulence and Reynolds shear stress, Yost did not include the contribution of radial velocity component. The contribution of radial velocity to the turbulent quantities may not be negligible especially when radial velocity is large.

Aware of these difficulties we derived new equations using equation (II-3) and the geometrical relations of the wires and their three independent coordinates. These equations can be applied in two-dimensional flow without requiring the mean velocity vector to be known.

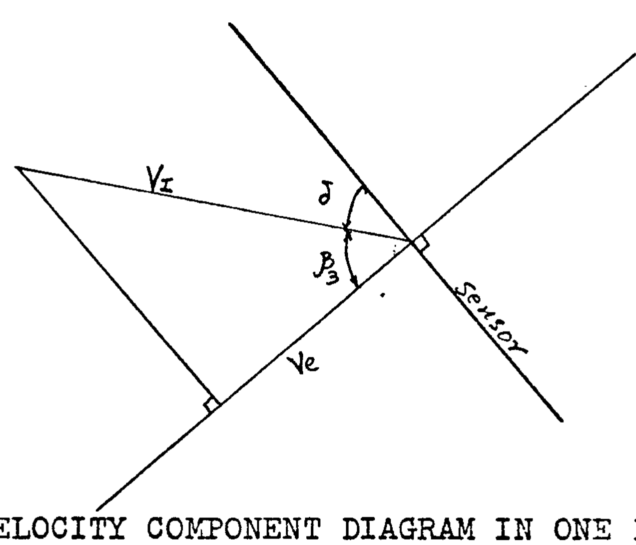

FIGURE II-1. VELOCITY COMPONENT DIAGRAM IN ONE DIMENSION.

Analytical Considerations

Define intrinsic coordinates S, N, T with Es as a unit vector tangent to the mean streamline, where En and Et coincide with the principal normal and binormal direction, respectively, of the mean streamline as shown in Figure II-2. Let $\overline{Vs}$, $\overline{Vn}$, and $\overline{Vt}$ be the resulting mean velocities and Vs', Vn', and Vt' be the velocity component fluctuations in the S, N, and T direction, respectively.

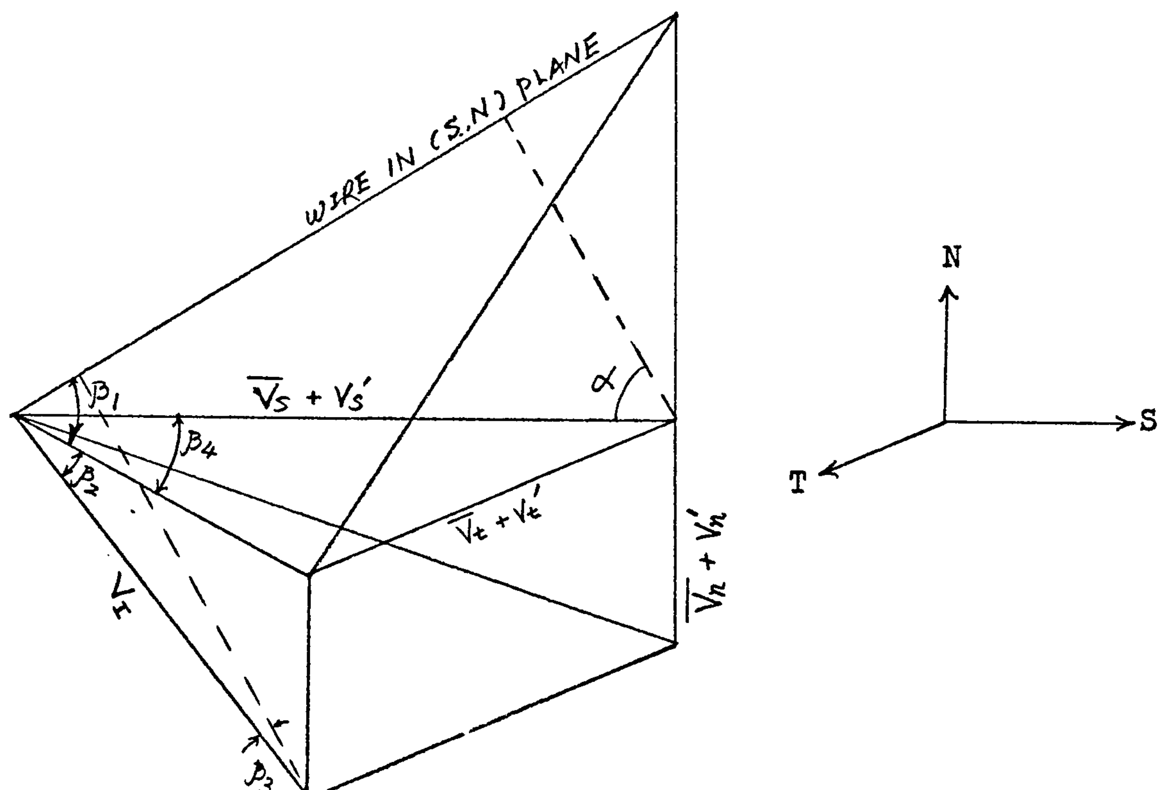

FIGURE II-2. VELCCITY COMPONENT DIAGRAM IN THREE DIMENSIONS.

The magnitude of the instantaneous velocity vector is (see Figure II-2)

$$V_I = ((\overline{Vs} + Vs')^2 + (\overline{Vn} + Vn')^2 + (\overline{Vt} + Vt')^2)^{\frac{1}{2}} \qquad \text{(II-4)}$$

The instantaneous effective cooling velocity is given by

$$Ve^2 = V_I^2(\cos^2\beta_3 + k^2\cdot\sin^2\beta_3) \qquad \text{(II-5)}$$

where k is a constant depend primarily upon the length-to-diameter ratio of the wire, β_3 is the angle between the instantaneous velocity vector and the normal to the wire axis. β_3 can be expressed in terms of α, the angle between the normal to the wire and the longitudinal, $\bar{S}$, direction, and the velocity component as follows. Applying the cosine law of trigonometry (see Figure II-2) yields:

$$-\sin\beta_3 = (\cos^2\alpha + \frac{2\sin\alpha\cdot\cos\alpha\cdot\tan\beta_2}{\cos\beta_4} + \frac{\sin^2\alpha\cdot\tan^2\beta_2}{\cos^2\beta_4} + \sin^2\alpha\cdot\tan^2\beta_4$$
$$- 1 - \frac{\sin^2\alpha}{\cos^2\beta_3\cdot\cos^2\beta_4})(\frac{\cos\beta_2\cdot\cos\beta_4}{2\sin\alpha}) \qquad \text{(II-6)}$$

The angle β_2 and β_4 are defined by

$$\sin\beta_2 = (\overline{Vn} + Vn')((\overline{Vs} + Vs')^2 + (\overline{Vn} + Vn')^2 + (\overline{Vt} + Vt')^2)^{-\frac{1}{2}}$$
$$\cos\beta_2 = ((\overline{Vs} + Vs')^2 + (\overline{Vt} + Vt')^2)^{\frac{1}{2}}((\overline{Vs} + Vs')^2 + (\overline{Vn} + Vn')^2 + (\overline{Vt} + Vt')^2)^{-\frac{1}{2}}$$
$$\sin\beta_4 = (\overline{Vt} + Vt')((\overline{Vs} + Vs')^2 + (\overline{Vt} + Vt')^2)^{-\frac{1}{2}} \qquad \text{(II-7)}$$
$$\cos\beta_4 = (\overline{Vs} + Vs')((\overline{Vs} + Vs')^2 + (\overline{Vt} + Vt')^2)^{-\frac{1}{2}}$$

Now consider a situation of two-dimensional flow only, ie. $\overline{Vt} = 0.$ and assume $Vt' \cong 0.$ Set $\beta_4 = 0$, or $\tan\beta_4 = 1$, and $\cos\beta_4 = 1$. Substitute into (II-6) and (II-7), we have

$$-\sin\beta_3 = (-\sin\alpha + \cos\alpha\cdot\tan\beta_2)\cdot\cos\beta_2$$

$$\sin\beta_2 = (\overline{Vn}+Vn')((\overline{Vs}+Vs')^2 + (\overline{Vn}+Vn')^2)^{-\frac{1}{2}}$$

$$\cos\beta_2 = (\overline{Vs}+Vs')((\overline{Vs}+Vs')^2 + (\overline{Vn}+Vn')^2)^{-\frac{1}{2}} \qquad (II-9)$$

$$\tan\beta_2 = (\overline{Vn}+Vn')/(\overline{Vs}+Vs')$$

Substitute (II-9) into (II-8) gives

$$-\sin\beta_3 = (-\sin\alpha + \cos\alpha\,\frac{(\overline{Vn}+Vn')}{(\overline{Vs}+Vs')})\left(\frac{(\overline{Vs}+Vs')}{((\overline{Vs}+Vs')^2 + (\overline{Vn}+Vn')^2)^{\frac{1}{2}}}\right) \qquad (II-10)$$

Squaring (II-10) gives,

$$\sin^2\beta_3 = (\sin^2\alpha\,(1+\frac{Vs'}{\overline{Vs}})^2 + \cos^2\alpha\,(\frac{\overline{Vn}}{\overline{Vs}}+\frac{Vn'}{\overline{Vs}})^2 - 2\sin\alpha\cos\alpha\,(1+\frac{Vs'}{\overline{Vs}})$$

$$(\frac{\overline{Vn}}{\overline{Vs}}+\frac{Vn'}{\overline{Vs}}))\left(\frac{1}{(1+\frac{Vs'}{\overline{Vs}})^2 + (\frac{\overline{Vn}}{\overline{Vs}}+\frac{Vn'}{\overline{Vs}})^2}\right) \qquad (II-11)$$

Define $R = \overline{Vn}/\overline{Vs}$; $\gamma n = Vn'/\overline{Vs}$; $\gamma s = Vs'/\overline{Vs}$ (II-12)

Then (II-11) becomes,

$$\sin^2\beta_3 = (\sin^2\alpha\,(1+\gamma s)^2 + \cos^2\alpha\,(R+\gamma n)^2 - 2\sin\alpha\cdot\cos\alpha\,(1+\gamma s)(R+\gamma n))$$

$$*((1+\gamma s)^2 + (R+\gamma n)^2)^{-1} \qquad (II-13)$$

The denominator of this equation may be expanded in a power series to give

$$((1+\gamma s)^2 + (R+\gamma n)^2)^{-1} = 1 - 2\gamma s + 3\gamma s^2 - (R+\gamma n)^2 - 4\gamma s^3 + 4\gamma s(R+\gamma n)^2$$

$$+ \text{4th. order terms} \qquad (II-14)$$

Substituting (II-14) into (II-13) and collecting terms gives

$$\sin^2\beta_3 = (-(R+\gamma n)^2 + 2\gamma s(R+\gamma n)^2)\cdot\sin^2\alpha + \sin^2\alpha + ((R+\gamma n)^2 - 2\gamma s(R+\gamma n)^2)\cos^2\alpha$$

$$- 2\sin\alpha\cdot\cos\alpha\cdot((R+\gamma n) - \gamma s(R+\gamma n) + \gamma s^2(R+\gamma n) - (R+\gamma n)^3)$$

$$(II-15)$$

Thus

$$\cos^2\beta_3 + k^2\cdot\sin^2\beta_3 = \cos^2\alpha\cdot(1 + k^2\cdot\tan^2\alpha + (k^2-1)((\tan^2\alpha-1)J_1 - 2J_3\cdot\tan\alpha)) \quad \text{(II-16)}$$

where

$$J_1 = (-(R+\gamma n)^2 + 2\gamma s(R+\gamma n)^2)$$

$$J_3 = ((R+\gamma n) - \gamma s(R+\gamma n) + \gamma s^2(R+\gamma n) - (R+\gamma n)^3)$$

From (II-4) we have

$$V_I^2 = \overline{Vs}^2\cdot((1+\gamma s)^2 + (R+\gamma n)^2) \quad \text{(II-17)}$$

substituting (II-17) and (II-16) into (II-5) gives

$$Ve^2 = \overline{Vs}^2\cdot\cos^2\alpha\,((1+\gamma s)^2 + (R+\gamma n)^2)(1 + k^2\cdot\tan^2\alpha + (k^2-1)((J_1/\cos^2\alpha) - 2J_1 - 2J_3\tan\alpha)) \quad \text{(II-18)}$$

Substituting J_1 and J_3 and rearranging,

$$\frac{Ve_1}{\overline{Vs}\cdot\cos\alpha} = (S_1 + S_2 + S_3)^{\frac{1}{2}} \quad \text{(II-19)}$$

where

$$\begin{aligned}
S_1 &= (1+k^2\cdot\tan^2\alpha) + 2R(1-k^2)\tan\alpha + R^2(k^2+\tan^2\alpha)\\
S_2 &= 2A_1\cdot\gamma s + 2A_2\cdot\gamma n\\
&\quad A_1 = (1+k^2\tan^2\alpha) - R\cdot\tan\alpha\,(k^2-1)\\
&\quad A_2 = (1-k^2)\tan\alpha + R(k^2+\tan^2\alpha)\\
S_3 &= A_3\gamma n^2 + A_4\gamma s^2 + A_5\gamma s\,\gamma n\\
&\quad A_3 = k^2 + \tan^2\alpha\\
&\quad A_4 = 1 + k^2\cdot\tan^2\alpha\\
&\quad A_5 = 2(1-k^2)\tan\alpha
\end{aligned} \quad \text{(II-20)}$$

R, γs and γn are defined in equation (II-12)

Similarly for wire #2, we have

$$Ve_2^2 = V_I^2 (\cos^2\gamma_3 + k^2 \sin^2\gamma_3) \qquad \text{(II-21)}$$

where $r_3 = 90^\circ - \beta_3$

Finally we have

$$\frac{Ve_2}{\overline{Vs}\cdot\cos\alpha} = (T_1 + T_2 + T_3)^{\frac{1}{2}} \qquad \text{(II-22)}$$

where

$$T_1 = (k^2 + \tan^2\alpha) - 2R(1-k^2)\tan\alpha + R^2(1+k^2\tan^2\alpha)$$

$$T_2 = 2B_1\gamma s + 2B_2\gamma n$$

$$B_1 = (k^2 + \tan^2\alpha) + R(k^2-1)\tan\alpha$$

$$B_2 = (k^2-1)\tan\alpha + R(1+k^2\tan^2\alpha)$$

$$T_3 = B_3\gamma n^2 + B_4\gamma s^2 + B_5\gamma s\gamma n \qquad \text{(II-23)}$$

$$B_3 = 1 + k^2\tan^2\alpha$$

$$B_4 = k^2 + \tan^2\alpha$$

$$B_5 = 2(k^2-1)\tan\alpha$$

Equations (II-19) and (II-22) provide relationship between the instantaneous effective velocity across each wire (Ve_1, Ve_2), the wire orientation, α, the tangent of the mean velocity vector, R, the influence coefficient for cooling along the film, k, and values of the instantaneous fluctuating velocity ratios, γs, γn, $\gamma s \gamma n$. Now it is clear that if a hot wire anemometer can be used to find these instantaneous cooling velocities then by manipulation of the equations it could be possible to extract information on the mean velocity, $\overline{Vs}$, the vector direction, R, and the correlation coefficients γs , γn and $\gamma s \gamma n$. The use of the hot wire system is discussed in the next section and development of the equations for finding these quantities is then treated.

III HOT WIRE ANEMOMETRY THEORY

A. GENERAL REMARKS:

The hot wire anemometer is an instrument used for measuring instantaneous velocities in a fluid stream, through the stream's instantaneous cooling effect on a very thin, electrically heated wire filament or film.

The first major application was in the study of turbulence in air streams. The use of hot-wire, or hot-film probes permitted, not only oscilloscope portrayal of turbulent velocity fluctuations but also a numerical investigation of their magnitude. Today turbulence measurement with the hot wire anemometer is a routine procedure, and with special x-wire, x-film or v-wire, v-film arrays longitudinal and transverse components of turbulence can be measured separately and the correlation between them can be investigated. The hot wire anemometer is also used in the measurement of temperature and temperature fluctuations.

B. BASIC PRINCIPLE:

A hot sensor(wire or film) probe has at its working end a thin wire or film through which an electric heating current is passed. The voltage across the hot wire or hot film depends on its electrical resistance, which depends on its temperature. In turn, its temperature depends on the cooling effect of the air stream. Because the sensor is small (typically about 0.04" long and 0.0003" diameter for wire and 0.04" long and 0.002" diameter for film), the instrument is able to respond very rapidly to fluctuations in air velocity. The hot wire itself is usually tungsten or platinum alloy while a film is a quartz rod coated with platinum, soldered or welded at each end to supporting needles.

Two type of electric circuity, "constant current" and "constant temperature", have been used. (see Figure III-1)

1. In the constant current system, the heating current is kept constant and the voltage across the hot wire or hot film is examined. In such a system the response of the sensor to a velocity fluctuation is modified by its own internal heat capacity, which becomes important for fluctuating frequencies above about fifty cycles per second. Thus special circuitry is necessary to compensate for this "storage" effect of the wire or film.

2. In the constant temperature type of instrument, a feedback circuit maintains the resistance constant and thus the temperature of the sensor is constant. The energy input to the sensor must then go entirely into the air stream. The internal capacity is no longer of importance, because its temperature is constant, and consequently this energy input is a measure of the instantaneous air velocity.

C. OPERATING PRINCIPLE:

Consider a long thin wire which is heated by an electric

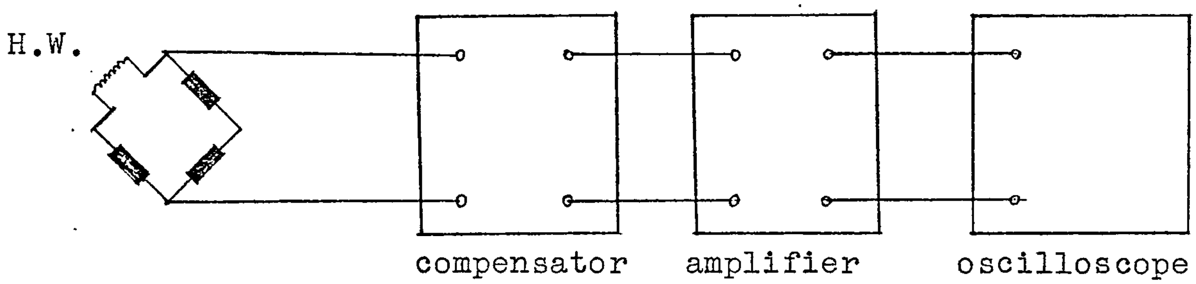

(a)

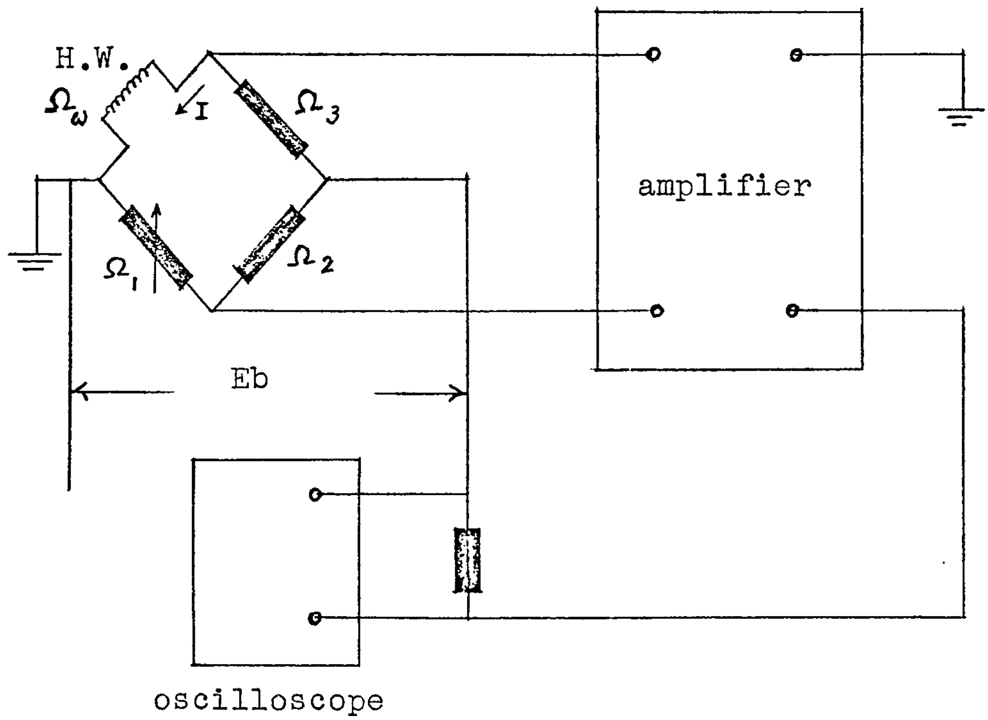

(b)

FIGURE III-1. BLOCK DIAGRAMS OF (a) CONSTANT CURRENT METHOD AND (b) CONSTANT TEMPERATURE METHOD.

circuit and cooled by a moving stream of air, the velocity of which is to be measured. The rate at which heat is transferred to the air stream in steady flow has been studied by a number of investigators.[10 TO 16] Although there are various heat transfer relations for a cylinder in cross flow, the recommended relation for air is that by Collis and Williams.[14] However, King's equation[10] is also a good approximation for hot wire and hot film measurements with long cylinders and is simpler. We found that it is in very good agreement with our experiment.

The total amount of heat transferred depends on:

1. The flow velocity
2. The difference in temperature between the wire, or film and the fluid
3. The physical properties of the fluid
4. The dimensions and physical properties of the cylinder

Generally 2 and 4 are known. So 1 or 3 can be measured if either one is known or kept constant. The sensor is cooled by heat conduction, free and forced convection, and radiation. Under usual operating conditions, where wire or film temperature do not exceed 300° C, the radiation effects are negligibly small. For air and a wire of 0.005" diameter, Van Der Hegge Zijnen[17] showed that free convection is negligible.

In 1914, an approximate theoretical calculation due to King[10] gave,

$$Nu = \left(\frac{2}{\pi}\cdot\frac{C_v}{C_p}\cdot Pr\cdot Re\right)^{\frac{1}{2}} + \frac{1}{\pi} \qquad \text{(III-1)}$$

where Nu = Nusselt number, $H/\pi \cdot Kg \cdot (Ts-Te)$

Pr = Prandtl number, $\mu Cp/Kg$

Re = Reynold number, $\rho VeD/\mu$

H = Rate of heat transfer to stream per unit length of sensor

Kg = Thermal conductivity of fluid

Cp = Specific heat at constant pressure

Cv = Specific heat at constant volume

Ve = Effective cooling velocity

ρ = Density of fluid

D = Diameter of sensor

μ = Viscosity of fluid

Ts = sensor temperature

Te = Static stream temperature far from sensor

For thermal-equilibrium conditions, the heat per unit time transferred to the ambient fluid from a sensor must be equal to the heat generated per unit time by the electric current through the sensor, thus We have,

$$I^2\Omega_w = \left(\pi K_g L \left(\frac{2}{\pi}\,\frac{C_v}{C_p}\,P_r\,\frac{\rho D}{\mu}\right)^{\frac{1}{2}}\sqrt{V_e} + \frac{\pi K_g L}{\pi}\right)(T_s - T_e) \qquad \text{(III-2)}$$

where I = The sensor heating current

Ω_w = The total electric resistance of the sensor

For the purpose of hot wire or hot film anemometer it is convenient and usual to write this relation in the form

$$I^2 \Omega_w = (C_1 + C_2 \sqrt{V_e}) (T_s - T_e) \qquad \text{(III-3)}$$

where $C_1 = \frac{1}{\pi}(\pi KgL)$

$C_2 = (\pi KgL)\left(\frac{2C_v}{\pi C_p} Pr \frac{\rho D}{\mu}\right)^{\frac{1}{2}}$ (III-4)

Furthermore, equation (III-4) can be written as

$$Eb^2 \frac{\Omega_w}{(\Omega_w + \Omega_3)^2} = (C_1 + C_2 \sqrt{Ve})(Ts-Te) \qquad \text{(III-5)}$$

where Eb = Bridge voltage, $I(\Omega_w + \Omega_3)$

Ω_3 = Electric resistance in serie with (see figure III-1,(b))

In the practice of hot wire anemometry the factors C and C are not calculated according to the known functions of the known physical properties of the fluid, but are determined experimently by calibration. Although in King's[10] derivation, the air was assumed to be incompressible and inviscid, and the experimental study by King[10] showed fair agreement with (III-1) for low velocities which are not suitable for practical applications. The equation (III-5) is exactly same as given by Kramers[18] except the expression for C_1 and C_2 differ appreciably. For air and diatomic gases Kramers'[18] empirical relation has proved to be valid in the range $0.01 < Re < 10000$. So that if We determine C_1 and C_2 by experiment other than by known functions as given by equation (III-4), then equation (III-5) will be suitable for practical applications in a gas stream.

In the constant temperature system used in this work, Ts and Ω_3 is kept constant. Ω_3 is a built-in constant electric resistance. Eb is measured experimently. So equation (III-5) leads to one unknown, Ve. Any change in Ve is uniquely determined by Eb. Recall from equation (II-5)

$$Ve^2 = V_I^2\,(\cos^2\beta_3 + k^2 \sin^2\beta_3)$$

substituted into equation (III-5), we have

$$Eb^2 \frac{\Omega_w}{(\Omega_3+\Omega_w)^2} = \left(C_1 + C_2 \sqrt{V_I (\cos^2\beta_3 + k^2 \sin^2\beta_3)^{1/2}} \right)(T_s - T_e) \tag{III-6}$$

An equation such as this exists for each sensor. There are two sensors used simultaneously, then we have two simultaneous equations, and there are only two independent variables, V_I and β_3. Theoretically, V_I and β_3 can be solved. If we let $Eb = \overline{Eb} + Eb'$, $V_I = \overline{V_I} + V_I'$, and $\beta_3 = \overline{\beta_3} + \beta_3'$ where $\overline{Eb}$, $\overline{V_I}$, and $\overline{\beta_3}$ represent time-mean variables, Eb', V_I' and β_3' represent fluctuation variables with $\overline{Eb'} = 0$, $\overline{V_I'} = 0$, and $\overline{\beta_3'} = 0$, and substituted into equation (III-6) for each sensor then there are four equations and there exists four unknown variables, $\overline{V_I}$, V_I', $\overline{\beta_3}$ and β_3'. Therefore, by combining one another among them, the turbulent intensity, turbulent shear stress and other turbulent quantities can be calculated.

IV EXPERIMENTAL EQUIPMENT

A. Hot Wire Anemometer System

All data are obtained with a two-channel, constant temperature anemometer system manufactured by Thermo-System, Inc. This constant temperature anemometer is of model 1010A, and has a frequency response of 0 to 50000 cps. The anemometer produces a voltage signal, Eb, proportional to the effective cooling velocity, Ve, according to equation (III-5).

There are two types of probes used in this experiment. One is the single film, model 1210 with sensor type 20 manufactured by Thermo-System Inc. The sensor type 20 has a sensing size 0.002" diameter and 0.04" long, a relative frequency response 40000 cps, and has low end losses. It is a standard film sensor for air and low velocity water measurement. This single film was used to evaluate the value of k in equation (II-5). The value measured was 0.35.

The other is the X-film type with sensor type 20. This type of probe is specially designed so that the axes of the sensor are parallel to vertical plane, and they are perpendicular to each other, ie $\alpha = 45^\circ$. All the sensors used were calibrated in a reference channel. This channel is a 3" diameter commercial aluminum smooth pipe. Probes were placed at the center position and a pitot tube inserted to independently measure the velocity at the center position of this smooth pipe.

B. Reference Channel

This is a commercial, 6061 T6 alloy, Aluminum pipe. The dimensions of the pipe and the position of hot film probe and the pitot tube are shown in figure (IV-1). As is well known, the radial velocities in such a pipe is very small if they are not zero. The calibration curve which has as a criterion $\overline{Vn}=0$ is drawn from measurements in this pipe at the center line position. The air flow is supplied by a compressor.

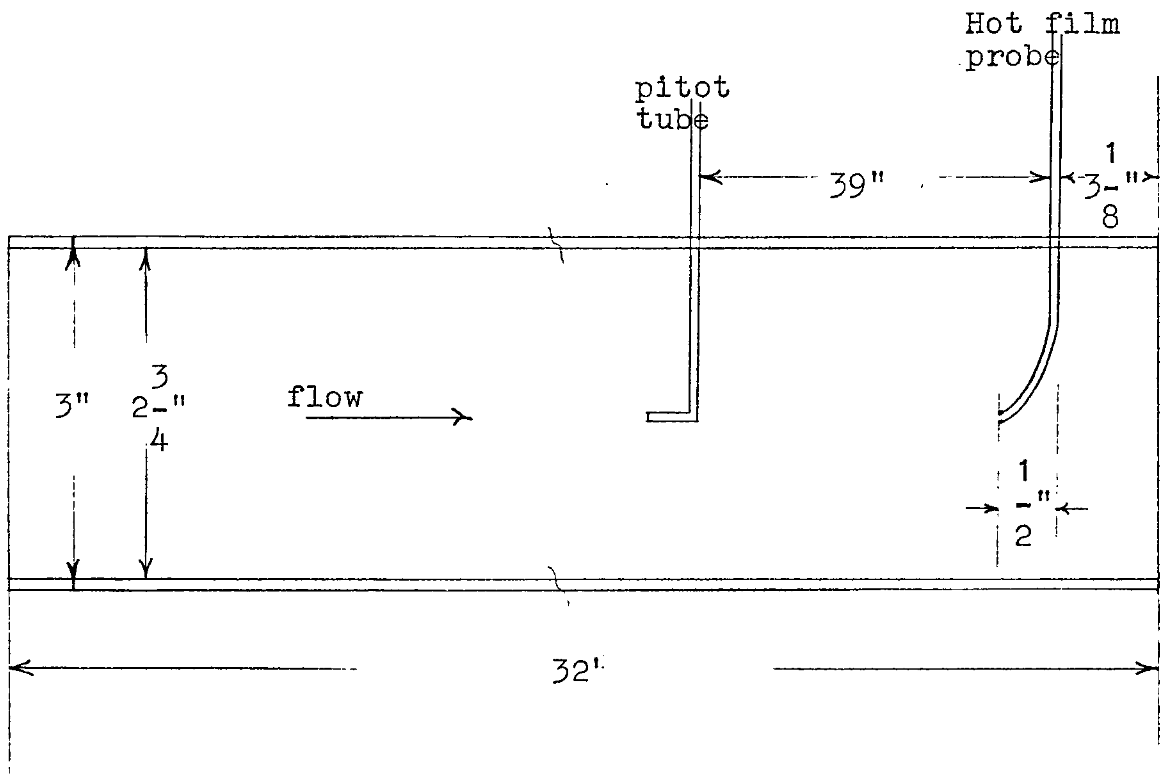

FIGURE IV-1. SCHEMATIC DIAGRAM OF REFERENCE CHANNEL.

C. Flow Channel

The flow channel is a galvanized corrugated pipe. Figure IV-2 shows its longitudinal view. Experiments are made at y/r=1.0 (center), 0.5, 0.25, 0.10, 0.05, 0.0187 of VL2, ML2, VS, ML1 respectively. The air flow is supplied by a blower with a screen gate through which the ambient air passes.

D. Pitot Tube And Micro Manometer

Mean velocities used in the calibration curve fit were obtained with ordinary pitot tube with a 1/8" diameter. All pressure measurements were obtained with a Merian micro manometer. This manometer had a range of 10" of water and the pressure difference could be measured to an accuracy of 0.0005".

E. DC Offset

This is electronic equipment used to subtract a constant mean voltage with accuracy of $\pm 0.06\%$. This equipment is used to subtract a constant mean voltage from the output of the hot

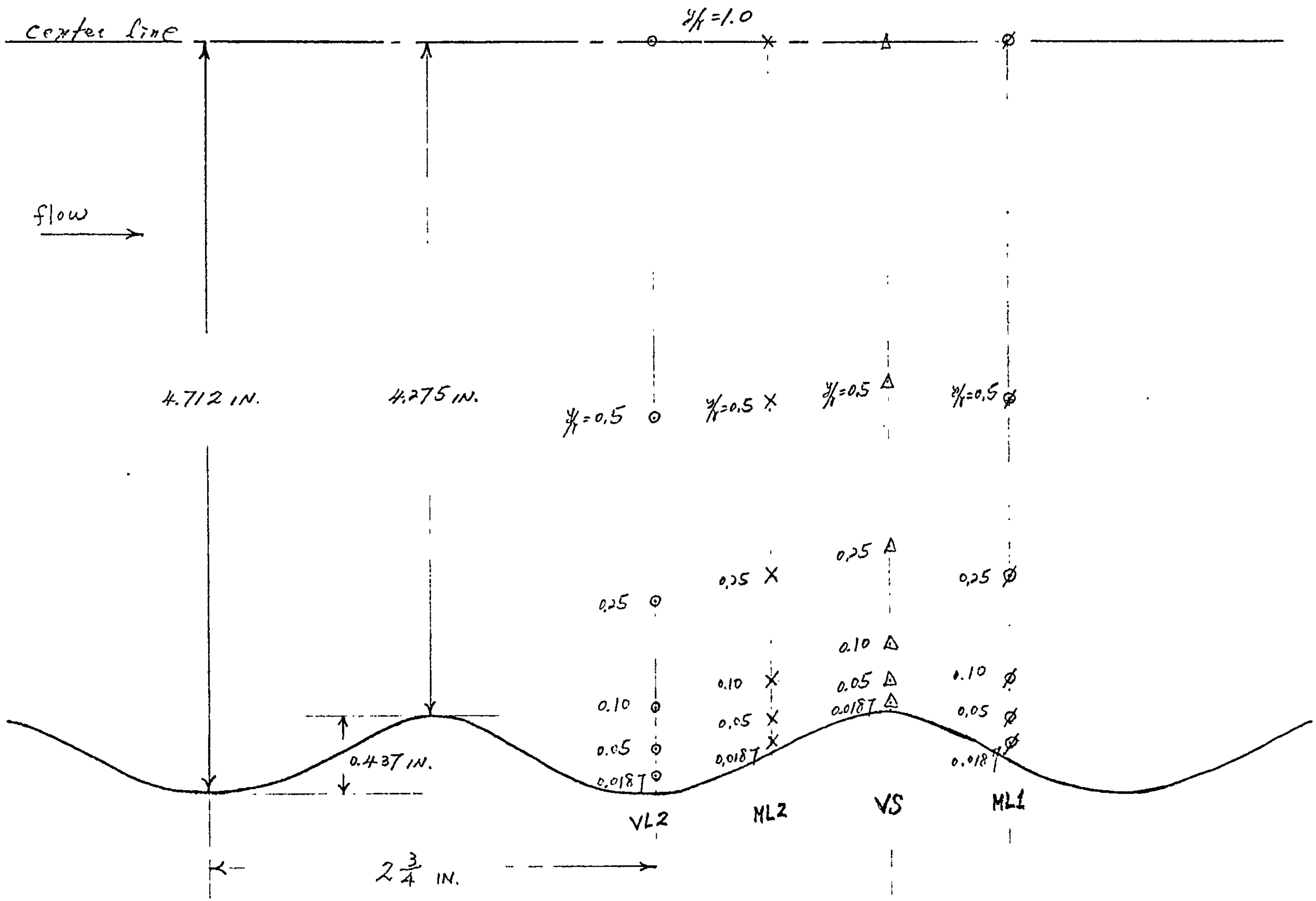

FIGUREIV-2. SCHEMATIC DIAGRAM OF FLOW CHANNEL.

wire anemometer to increase the signal-to-noise ratio when recorded on magnetic tape. By this method the accuracy of turbulence intensity measurements are greatly increased.

F. Tape Recorder

All data are recorded on AMPEX instrumentation tape. The tape recorder is AMPEX 1300 which has seven simultaneous channels and has center carrier frequencies from 1000 to 5700 HZ. The highest frequency of the experimental signal is estimated to be 10000 HZ. The tape speed used is 30 ips with center carrier frequency at 2700 HZ when recorded. In data processing the tape speed is reduced to 15 ips with center carrier frequency at 1500 HZ.

V DEVELOPMENT OF COMPUTATIONAL ALGORITHM

In this chapter we develop the computational algorithm for the Final Program and the Calibration Program. The Final Program was used to evaluate R, Vs, $\overline{\gamma s^2}$, $\overline{\gamma n^2}$, and $\overline{\gamma s \gamma n}$. The Calibration Program was used to calibrate the hot film used in experiments.

A. The Computational Algorithm For The Final Program:

The right side of equation (II-19) is expanded using the binomial theorem. Neglecting third order and higher terms, gives

$$\frac{Ve_1}{\overline{Vs}\cdot\cos\alpha} = (S_1 + S_2 + S_3)^{\frac{1}{2}}$$

$$\cong S_1^{\frac{1}{2}}\left(1 + \frac{S_2}{2S_1} + \frac{S_3}{2S_1} - \frac{1}{8}\frac{S_2^2}{S_1}\right) \qquad (V-1)$$

If we decompose Ve into a mean and a fluctuation part, we have

$$Ve = \overline{Ve} + Ve' \qquad \text{with } \overline{Ve'} = 0$$

Take the time-mean of equation (V-1), gives

$$\overline{Ve} = \overline{Vs}\cdot\cos\alpha\cdot S_1^{\frac{1}{2}}\left(1 + \frac{\overline{S_3}}{2S_1} - \frac{1}{8}\frac{\overline{S_2^2}}{S_1}\right) \qquad (V-2)$$

Equation (V-1) minus equation (V-2), gives

$$Ve' = \overline{Vs}\cdot\cos\alpha\cdot S_1^{\frac{1}{2}}\left(\frac{S_2}{2S_1} + \frac{1}{2S_1}(S_3 - \overline{S_3}) - \frac{1}{8}\cdot\frac{1}{S_1^2}(S_2^2 - \overline{S_2^2})\right)$$

S_3 and S_2^2 contain terms in γs^2, γn^2, and $\gamma s\gamma n$, and γs^2, γn^2, $\gamma s\gamma n$ are all of higher order than γs and γn, so that $(S_2^2 - \overline{S_2^2})$ and $(S_3 - \overline{S_3})$ are negligibly small compared to S_2.

Then we have

$$Ve' = \overline{Vs}\cdot\cos\alpha\cdot S_1^{\frac{1}{2}}\left(\frac{S_2}{2S_1}\right) \qquad (V\text{-}3)$$

Substituted (II-20) into (V-2) and (V-3) for wire #1, gives

$$\overline{Ve_1} = \overline{Vs}\cdot\cos\alpha\cdot S_1^{\frac{1}{2}}\left(1 + \overline{\gamma s^2}\left(\frac{A_4}{2S_1} - \frac{A_1}{2S_1^2}\right) + \overline{\gamma n^2}\left(\frac{A_3}{2S_1} - \frac{A_2^2}{2S_1^2}\right) + \overline{\gamma s\gamma n}\left(\frac{A_5}{2S_1} - \frac{A_1A_2}{S_1^2}\right)\right) \qquad (V\text{-}4)$$

$$Ve' = \overline{Vs}\cdot\cos\alpha\cdot S_1^{\frac{1}{2}}\left(\frac{A_1}{S_1}\gamma s + \frac{A_2}{S_1}\gamma n\right) \qquad (V\text{-}5)$$

Similarly for equation (II-22), We have

$$\overline{Ve_2} = \overline{Vs}\cdot\cos\alpha\cdot T_1^{\frac{1}{2}}\left(1 + \overline{\gamma s^2}\left(\frac{B_4}{2T_1} - \frac{B_1^2}{2T_1^2}\right) + \overline{\gamma n^2}\left(\frac{B_3}{2T_1} - \frac{B_2^2}{2T_1^2}\right) + \overline{\gamma s\gamma n}\left(\frac{B_5}{2T_1} - \frac{B_1B_2}{T_1^2}\right)\right) \qquad (V\text{-}6)$$

$$Ve_2' = \overline{Vs}\cdot\cos\alpha\cdot T_1^{\frac{1}{2}}\left(\frac{B_1}{T_1}\gamma s + \frac{B_2}{T_1}\gamma n\right) \qquad (V\text{-}7)$$

Now define,

$$1 + F_1 = 1 + \overline{\gamma s^2}\left(\frac{A_4}{2S_1} - \frac{A_1^2}{2S_1}\right) + \overline{\gamma n^2}\left(\frac{A_3}{2S_1} - \frac{A_2^2}{2S_1^2}\right) + \overline{\gamma s\gamma n}\left(\frac{A_5}{2S_1} - \frac{A_1A_2}{S_1^2}\right) \qquad (V\text{-}8)$$

$$1 + F_2 = 1 + \overline{\gamma s^2}\left(\frac{B_4}{2T_1} - \frac{B_1^2}{2T_1}\right) + \overline{\gamma n^2}\left(\frac{B_3}{2T_1} - \frac{B_2^2}{2T_1^2}\right) + \overline{\gamma s\gamma n}\left(\frac{B_5}{2T_1} - \frac{B_1B_2}{T_1^2}\right) \qquad (V\text{-}9)$$

equations (V-4) and (V- 6) become,

$$\overline{Ve_1} = \overline{Vs}\cdot\cos\alpha\cdot S_1^{\frac{1}{2}}(1 + F_1) \qquad (V\text{-}10)$$

$$\overline{Ve_2} = \overline{Vs}\cdot\cos\alpha\cdot T_1^{\frac{1}{2}}(1 + F_2) \qquad (V\text{-}11)$$

If F_1 and F_2 are small (the measured values of F_1 and F_2 are, in fact, very small) then it is clear that between these two equations, once $\overline{Ve_1}$ and $\overline{Ve_2}$ are determined from the hot wire anemometer, then we have two equations in the two unknowns, $\overline{Vs}$ and R.

Define
$$\phi^2 = \left(\frac{\overline{Ve_1}\,(1 + F_2)}{\overline{Ve_2}\,(1 + F_1)}\right)^2 = \frac{S_1}{T_1}$$
$$= \frac{(1 + k^2\cdot\tan^2\alpha) + 2R(1 - k^2)\tan\alpha + R^2(k^2 + \tan^2\alpha)}{(k^2 + \tan^2\alpha) - 2R(1 - k^2)\tan\alpha + R^2(1 + k^2\tan^2\alpha)}$$

For an 90° arry set at 45° to the S-direction $\alpha = 45^\circ$, then
$$R = \frac{1}{2}\left(\frac{1 + k^2}{1 - k^2}\right)\left(\frac{\phi^2 - 1}{\phi^2 + 1}\right) \tag{V-12}$$

It is then straightforward to evaluate Vs from either equation (V-10) or (V-11) above. As will be shown below, with a computational algorithm it is possible to solve the equation exactly including the terms F_1 and F_2 by a system of sequential solutions once the terms for the correlations included in F_1 and F_2 have been found.

From equations (V-5) and (V-7), We have
$$\frac{Ve_1'}{\overline{Vs}\cdot\cos\alpha\cdot S_1^{\frac{1}{2}}} = \frac{A_1}{S_1}\gamma s + \frac{A_2}{S_1}\gamma n$$
$$\frac{Ve_2'}{\overline{Vs}\cdot\cos\alpha\cdot T_1^{\frac{1}{2}}} = \frac{B_1}{T_1}\gamma s + \frac{B_2}{T_1}\gamma n$$

or
$$\frac{Ve_1'}{\overline{Ve_1}/(1 + F_1)} = \frac{A_1}{S_1}\gamma s + \frac{A_2}{S_1}\gamma n \tag{V-13}$$
$$\frac{Ve_2'}{\overline{Ve_2}/(1 + F_2)} = \frac{B_1}{T_1}\gamma s + \frac{B_2}{T_1}\gamma n \tag{V-14}$$

It is now possible to obtain for γs^2, γn^2 and $\gamma s\gamma n$ by working with these equations. But notice that the simple sum and differencing techniques useful for parallel flow no longer can be applied here. Adding or subtracting, equations (V-13) and (V-14) will not produce signal proportional only to γs or γn except for the special case where R = 0. For a general case, these relationships must be used.

$$\gamma s(t) = \frac{\dfrac{Ve_1'}{\overline{Ve_1}/(1+F_1)} B_2 S_1 - \dfrac{Ve_2'}{\overline{Ve_2}/(1+F_2)} A_2 T_1}{A_1 B_2 - A_2 B_1} \qquad \text{(V-15)}$$

$$\gamma n(t) = \frac{\dfrac{Ve_1'}{\overline{Ve_1}/(1+F_1)} B_1 S_1 - \dfrac{Ve_2'}{\overline{Ve_2}/(1+F_2)} A_1 T_1}{-(A_1 B_2 - A_2 B_1)} \qquad \text{(V-16)}$$

and

$$\overline{\gamma s^2} = \frac{\left(\dfrac{B_2 S_1}{\overline{Ve_1}/(1+F_1)}\right)^2 \overline{Ve_1'^2} - \left(\dfrac{2A_2 B_2 S_1 T_1}{\overline{Ve_1}\,\overline{Ve_2}/(1+F_1)(1+F_2)}\right)\overline{Ve_1' Ve_2'} + \left(\dfrac{A_2 T_1}{\overline{Ve_2}/(1+F_2)}\right)^2 \overline{Ve_2'^2}}{(A_1 B_2 - A_2 B_1)^2} \qquad \text{(V-17)}$$

$$\overline{\gamma n^2} = \frac{\left(\dfrac{B_1 S_1}{\overline{Ve_1}/(1+F_1)}\right)^2 \overline{Ve_1'^2} - \left(\dfrac{2A_1 B_1 S_1 T_1}{\overline{Ve_1}\,\overline{Ve_2}/(1+F_1)(1+F_2)}\right)\overline{Ve_1' Ve_2'} + \left(\dfrac{A_1 T_1}{\overline{Ve_2}/(1+F_2)}\right)^2 \overline{Ve_2'^2}}{(A_1 B_2 - A_2 B_1)^2} \qquad \text{(V-18)}$$

$$\overline{\gamma s \gamma n} = \frac{B_1 B_2 \left(\dfrac{S_1}{\overline{Ve_1}/(1+F_1)}\right)^2 \overline{Ve_1'^2} - (A_1 B_2 + A_2 B_1)\left(\dfrac{S_1 T_1}{\overline{Ve_1}\,\overline{Ve_2}/(1+F_1)(1+F_2)}\right)\overline{Ve_1' Ve_2'} + A_1 A_2 \left(\dfrac{T_1}{\overline{Ve_2}/(1+F_2)}\right)^2 \overline{Ve_2'^2}}{-(A_1 B_2 - A_2 B_1)^2} \qquad \text{(V-19)}$$

Thus, if the signals $Ve_1'(t)$, and $Ve_2'(t)$ are available either in analog or digital form, the above two equations can be used to calculate $\gamma s(t)$, and $\gamma n(t)$ and from this the calculations of $\overline{\gamma s^2}$, $\overline{\gamma n^2}$ and $\overline{\gamma s \gamma n}$ can be found. The calculation must be sequential since F includes these correlations but the calculation can proceed schematively as in Figure V-1 and the value of k and α are known and the value of $\overline{Ve}$ and Ve'(t) are obtained from the hot wire anemometer. (see Appendix D)

B. The Computational Algorithm For Calibration Program

Recall from equation (III-5)

$$Eb\frac{\Omega_\omega}{(\Omega_\omega + \Omega_3)^2} = (C_1 + C_2\sqrt{Ve})(Ts - Te)$$

where C_1 and C_2 are constants determined experimently. Ω_3 is a built-in constant electric resistance. In the constant temperature hot wire anemometry system which we used in this thesis the resistance - and so the temperature - of the hot wire is kept constant, ie Ω_3 and Ts are constants. Te is ambient temperature which is a known quantity. Therefore the signal from the constant temperature anemometer, Eb(t), is related uniquely to Ve(t), the effective cooling velocity. Solving equation (III-5) for Ve for wire #1, gives

$$Ve_1 = \alpha_{s1} + \alpha_{s2}(Eb_1^2) + \alpha_{s3}(Eb_1^4) \qquad (V-20)$$

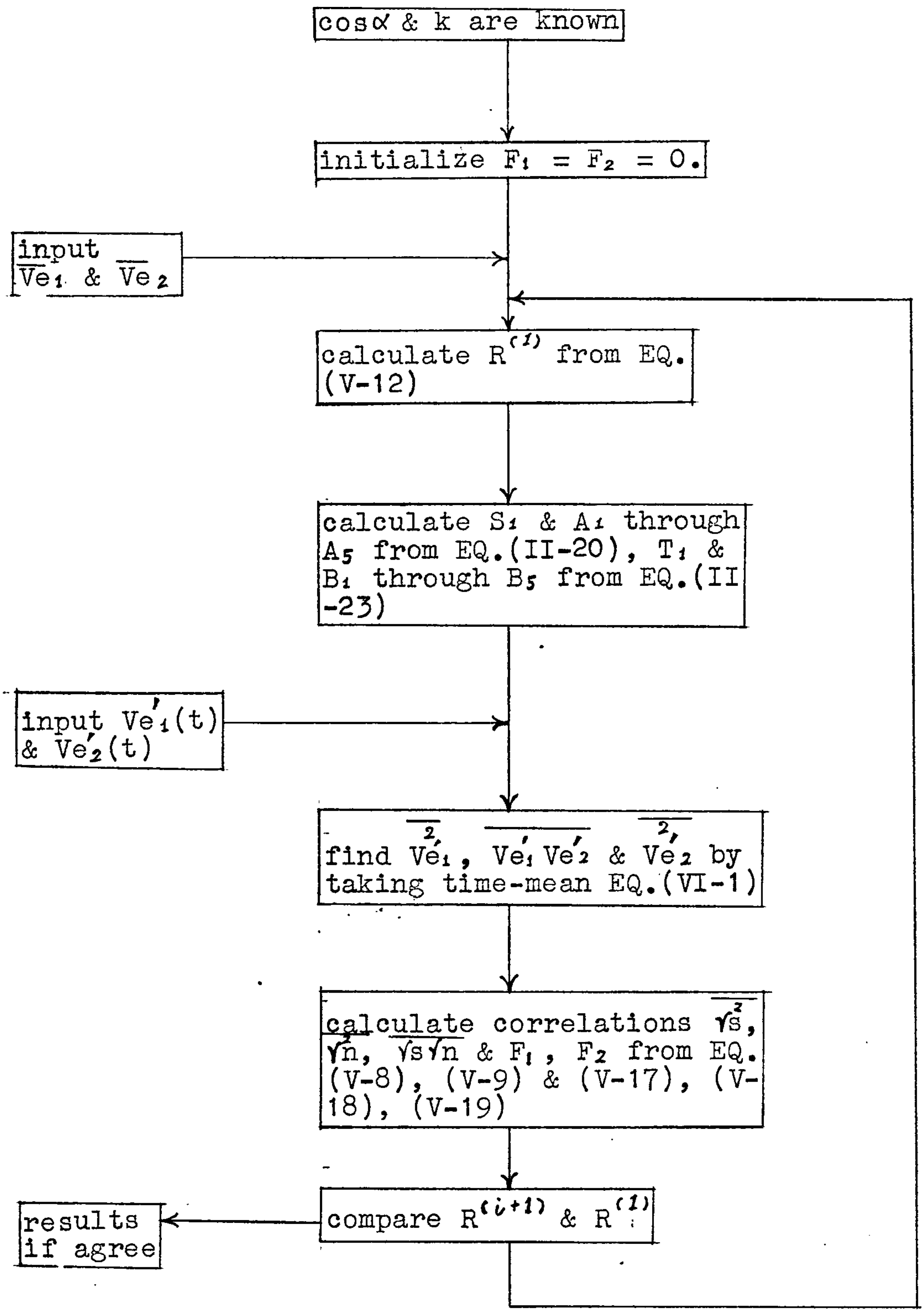

FIGURE V-1. COMPUTER FLOW DIAGRAM FOR FINAL PROGRAM. (WITHOUT CALIBRATION CONSTANTS) where $\alpha s_1 = (C_1/C_2)^2$

$$\alpha s_2 = -2\frac{C_1}{C_2}\frac{\Omega_\omega}{(\Omega_\omega+\Omega_3)^2}\frac{1}{(Ts - Te)} \qquad \text{(V-21)}$$

$$\alpha s_3 = \frac{1}{C_2^2}\frac{\Omega_\omega^2}{(\Omega_\omega+\Omega_3)^4}\frac{1}{(Ts - Te)^2}$$

Ve_1 can be obtained via linearization by using an analog linearizer but since data processing in this study was through a hybrid computer with very accurate electronics, it was more reliable to record Eb (or rather the fluctuation in Eb) and use equation (V-20) to solve for Ve_1.

Take time-mean of equation (V-8), gives

$$\overline{Ve_1} = \alpha s_1 + \alpha s_2(\overline{Eb_1^2}) + \alpha s_3(\overline{Eb_1^4}) \qquad \text{(V-22)}$$

equation (V-8) minus (V-10), gives

$$Ve_1' = \alpha s_2(Eb_1^2 - \overline{Eb_1^2}) + \alpha s_3(Eb_1^4 - \overline{Eb_1^4}) \qquad \text{(V-23)}$$

Similarly, for wire #2, we have

$$\overline{Ve_2} = \alpha t_1 + \alpha t_2(\overline{Eb_2^2}) + \alpha t_3(\overline{Eb_2^4}) \qquad \text{(V-24)}$$

$$Ve_2' = \alpha t_2(Eb_2^2 - \overline{Eb_2^2}) + \alpha t_3(Eb_2^4 - \overline{Eb_2^4}) \qquad \text{(V-25)}$$

Combine equations (V-10), (V-11) and (V-22), (V-24), we have

$$\overline{Ve_1} = \alpha s_1 + \alpha s_2(\overline{Eb_1^2}) + \alpha s_3(\overline{Eb_1^4}) = \overline{Vs}\cdot\cos\alpha\cdot S_1^{\frac{1}{2}}(1+F_1) \qquad \text{(V-26)}$$

$$\overline{Ve_2} = \alpha t_1 + \alpha t_2(\overline{Eb_2^2}) + \alpha t_3(\overline{Eb_2^4}) = \overline{Vs}\cdot\cos\alpha\cdot T_1^{\frac{1}{2}}(1+F_2) \qquad \text{(V-27)}$$

where α and k are known. If the X-array of hot film is placed at the centerline of a uniform smooth pipe R is zero, thus $S_1\cdot\cos\alpha$ and $T_1\cdot\cos\alpha$ are known. If the centerline velocity $\overline{Vs}$ is measured with an accurate pitot tube for a variety of flow rates and the bridge voltages recorded then the coefficients, αs_j and αt_j, can be found from a polynomial curve fit if the values of F_1 and F_2 have been evaluated for each velocity. These equations clearly showed that the correlation of the velocity fluctuations (which determined F_1 and F_2) enter into the calibration calculation and if neglected can introduce serious error.

The fluctuating velocity is related to these coefficients by,

$$Ve_1' = \alpha s2(Eb_1^2 - \overline{Eb_1^2}) + \alpha s3(Eb_1^4 - \overline{Eb_1^4}) = \overline{Vs}\cdot\cos\alpha\cdot S_1^{\frac{1}{2}}\left(\frac{A_1}{S_1}\gamma s + \frac{A_2}{S_1}\gamma n\right) \quad (V-28)$$

$$Ve_2' = \alpha t2(Eb_2^2 - \overline{Eb_2^2}) + \alpha t3(Eb_2^4 - \overline{Eb_2^4}) = \overline{Vs}\cdot\cos\alpha\cdot T_1^{\frac{1}{2}}\left(\frac{B_1}{T_1}\gamma s + \frac{B_2}{T_1}\gamma n\right) \quad (V-29)$$

These equations can now be incorporated along with a polynomial curve fit in a sequential calculations to obtain the coefficients, αs_j and αt_j. This is shown in the Figure V-2. (see Appendix C)

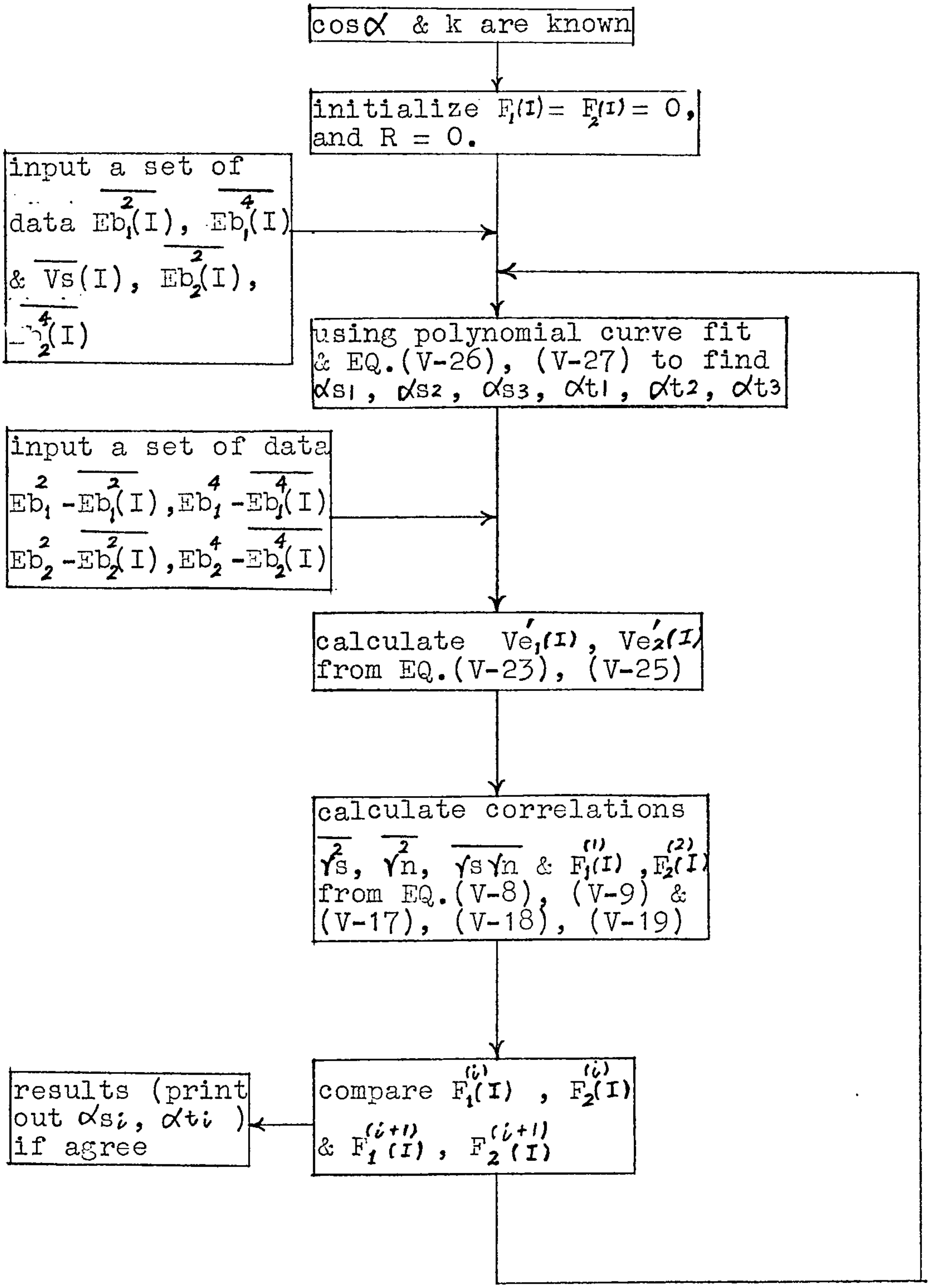

FIGURE V-2. COMPUTER FLOW DIAGRAM FOR CALIBRATION CURVE PROGRAM.

VI DATA PROCESSING SYSTEM

The signal from the constant temperature hot wire anemometer is an analog signal. This analog signal is processed through a hybrid computer to give digital data, then the digital computer is used to process these digital data. This data processing system consists of these programs:

A. Hybrid digitizing and time-mean program

B. Calibration program

C. Final program

The flow chart of this system is as follow:

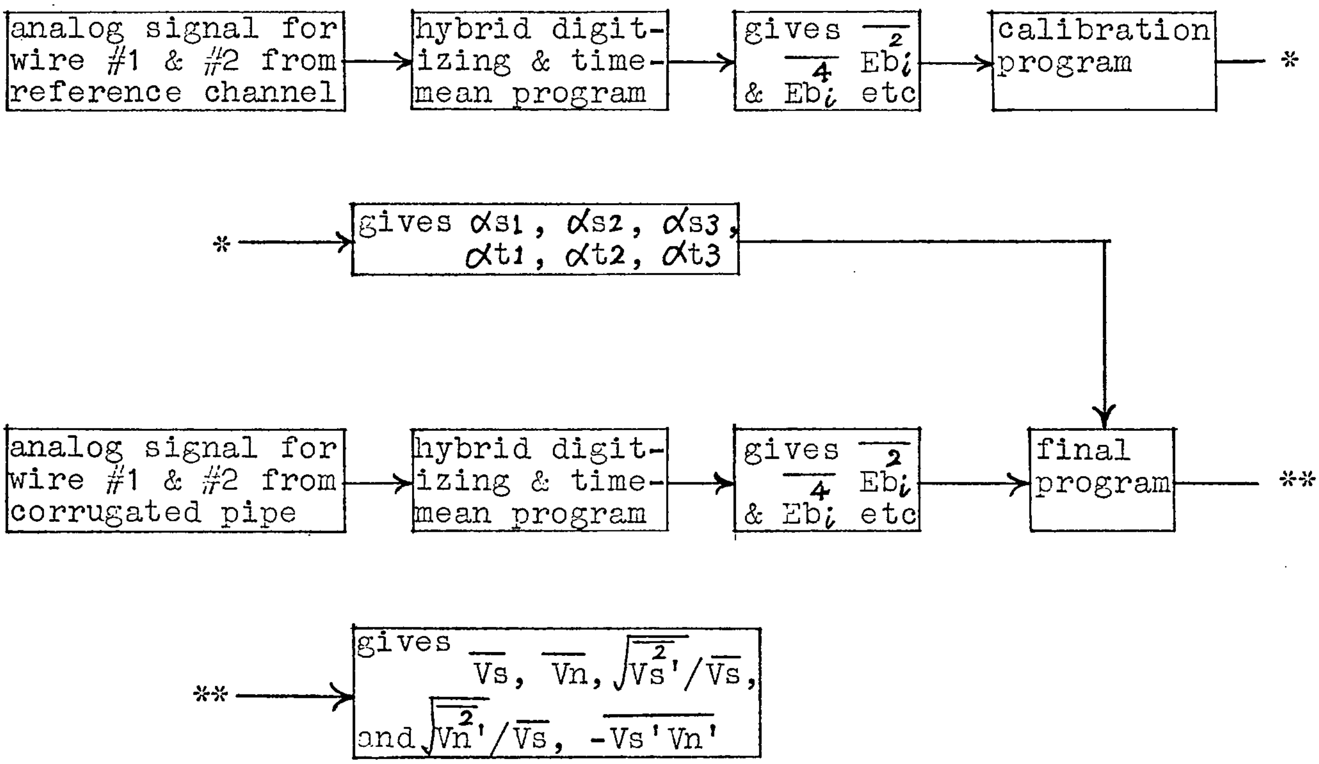

FIGURE VI-1. DATA PROCESSING SYSTEM.

A. Hybrid Digitizing And Time-mean Program

Analog data from magnetic tape records are processed through a hybrid computer. This equipment consists of a Hybrid System Inc. SS-100 analog, a specially designed interface HS-1044 and an IBM 360-44 digital computer.

This program is used to digitize the input analog data into digital numeric values, and to find its time-mean value. The time-mean value is calculated according to the formula

$$\overline{f(t_i)} = \frac{1}{N} \sum_{i=1}^{N} f(t_i) \qquad \text{(VI-1)}$$

where $f(t_i)$ is any function of discrete time t_i, N is the total number of discrete time t_i.

In order to solve the simultaneous equations (V-10), and (V-11), it was necessary to obtain simultaneous values of Eb_1 and Eb_2 . A signle input channel was used to execute the digitizing function, thus it was necessary to use a synchronization technique. The synchronize devise is called the "sample-hold", and functions as follows:

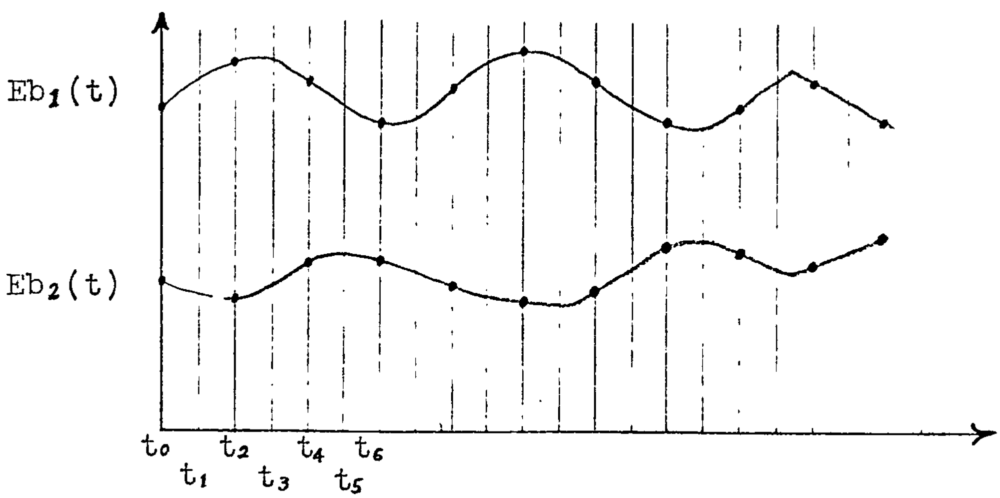

FIGURE VI-2. SYNCHRONIZATION OF DISCRETE TIME SERIES.

The computer "read" the true signal at any time, say, t_i, simultaneously, $Eb_1(t_i)$ and $Eb_2(t_i)$, but the true signals are digitized alternately. Thus, for example, the values $Eb_1(t_o)$ and $Eb_2(t_o)$ are sampled at time t_o. At time, t_o, $Eb_1(t_o)$ is digitized, and at time t_1, $Eb_2(t_o)$ is digitized. At time t_2, two new reading are obtained. The effect is to feed into digital storage pairs of corresponding values of Eb_1 and Eb_2 sampled at time intercals 2(1/f) apart, where f is the sampling frequency.

Every computer has its limitation of capacity. In this program we used a capacity of 8000 locations for storing the digitized values for each channel. For two channels we have 16000 locations. The maximum frequency of the turbulence of interest in this work is less than 8000 cps (cycles per second). Recording tape speed of 30 ips (inch per second) was used which has a frequency response from 0 to 10000 cps. In reproducing the signal through the hybrid computer, a tape speed of 15 ips was used because of the limitation of the digitizing frequency available. For the accurate spectral representation of the analog signal by the discrete data, the digitizing frequency should be at least twice the maximum frequency of interest. For the reason of the economy, the factor is usually chosen as two. If the signal is processed through the digitizer at the same speed as recorded and if two channels are to be sampled then the required digitizing frequency is (2 * 8000)*2 = 32000 cps. In this work tape playback of 15 ips was used. This is one half the reading speed. Therefore, an effective digitizing frequency of 16000 cps was used. Because computer capacity is limited to 8000 locations, the sampling time for each run is limited to that which will generate 4000 data points at the digitizing frequency of 16000 cps for each channel. This time length of 1/4 seconu is not long enough for sufficiently statistical accuracy of the result. In order to achieve the required accuracy, 15 separate runs, each of 1/4 second duration, were taken at the same condition and processed through the same computational program. It gives the total digitizing time for each channel 3.75 second. For a high frequency measurement 3.75 second is quite enough. (see Appendix B) The analog patch panel chart and the logic patch panel chart are as follows:

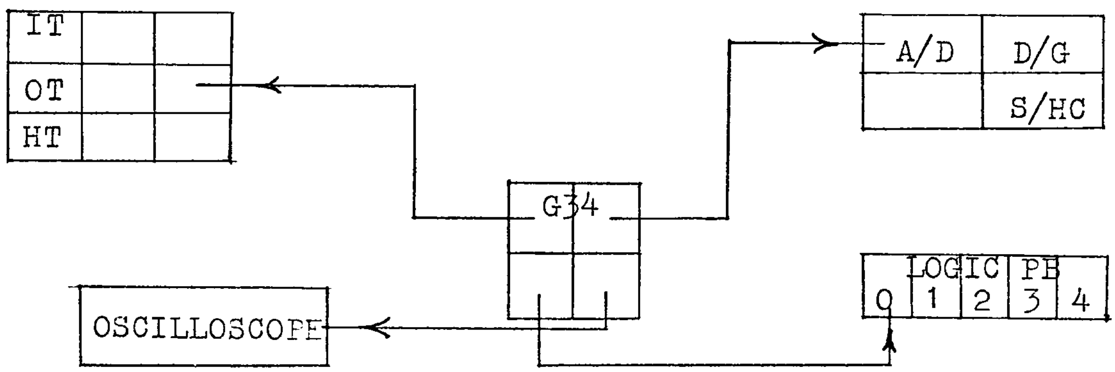

The Logic patch panel chart

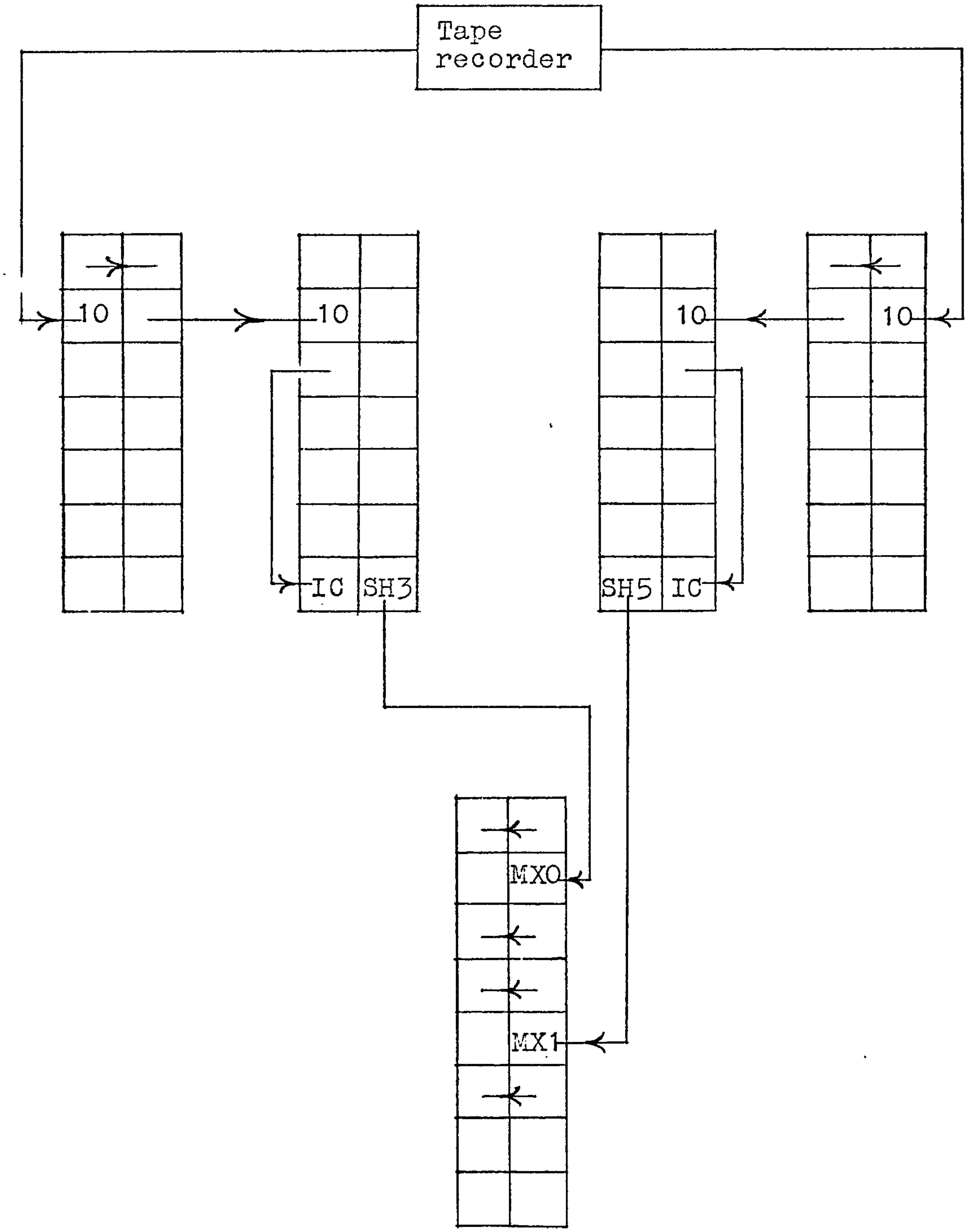

The analog patch panel chart.

FIGURE VI-3. THE LOGIC PATCH PANEL CHART AND THE ANALOG PATCH PANEL CHART.

B. Calibration Curve Program

All the sensors used have to be calibrated, and this is the fundamental procedure that all the measurements relied on. Usually, the calibration procedure assumed the mean flow direction is known, and the stream velocity is not fluctuating. However, there is always some degrees of fluctuation existing in the stream. Therefore, in calibrating sensors to this fluctuating components needs to be considered.

This program is used to evaluate the coefficients of the calibration curve, αs_1, αs_2, αs_3, αt_1, αt_2, and αt_3, by solving equations (V-26) and (V-27). This program consisted of a polynomial curve fit to fit a set of data, (Eb_i, Vs), where Eb_i is obtained from hot wire anemometer output, and $\overline{Vs}$ from pitot tube measurement placed in the center position of a smooth pipe. From the program output, R ($R = \overline{Vn}/\overline{Vs}$) calculated is really quite small, so that we just let R = 0 in this calibration curve program. The value of α, the angle between the normal to the sensor and the longitudinal direction, is a manufactured constant, which is 45°. Also we let

$$1 + F_1 = 1 + \overline{\gamma s^2}\left(\frac{A_4}{2S_1} - \frac{A_1^2}{2S_1^2}\right) + \overline{\gamma n^2}\left(\frac{A_3}{2S_1} - \frac{A_2^2}{2S_1^2}\right) + \overline{\gamma s \gamma n}\left(\frac{A_5}{2S_1} - \frac{A_1 A_2}{S_1^2}\right) \quad \text{(V-8)}$$

$$1 + F_2 = 1 + \overline{\gamma s^2}\left(\frac{B_4}{2T_1} - \frac{B_1^2}{2T_1^2}\right) + \overline{\gamma n^2}\left(\frac{B_3}{2T_1} - \frac{B_2^2}{2T_1^2}\right) + \overline{\gamma s \gamma n}\left(\frac{B_5}{2T_1} - \frac{B_1 B_2}{T_1^2}\right) \quad \text{(V-9)}$$

The flow chart of this program is listed in Figure (V-2).

C. Final program

The purpose of this program is to provide the mean velocity and turbulent intensity in the longitudinal and radial direction and their cross correlation of the velocities, $\overline{Vs}$, $\overline{Vn}$, $\sqrt{\overline{Vs'^2}}/Vs$, $\sqrt{\overline{Vn'^2}}/Vs$, and $\overline{Vs'Vn'}$. This program essentially is solving the simultaneous equations of (V-4), (V-6), (V-17), (V-18), and (V-19). The flow chart of this program is as follows:

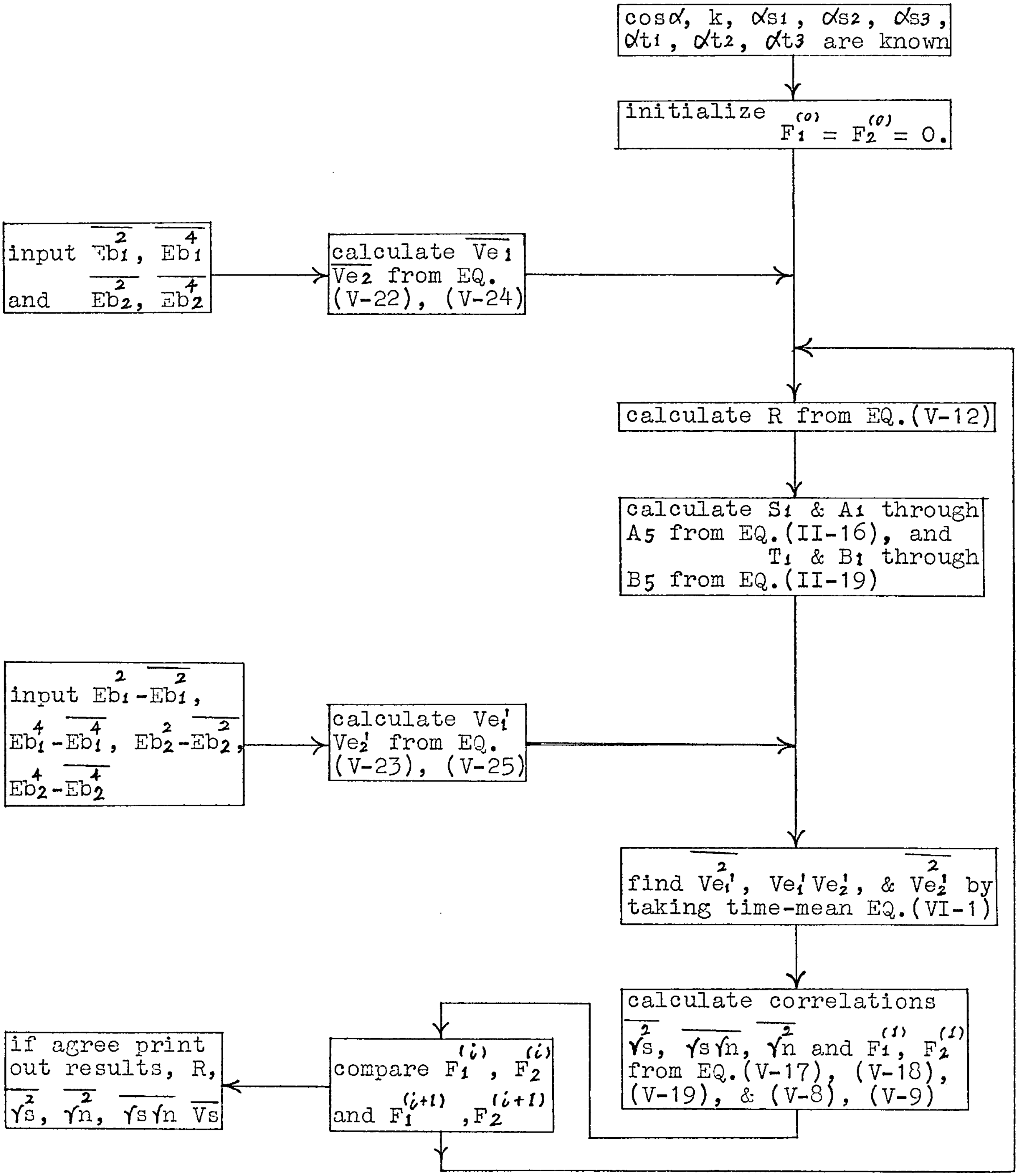

FIGURE VI-4. COMPUTER FLOW DIAGRAM FOR FINAL PROGRAM. (WITH CALIBRATION CONSTANTS)

VII ERROR ANALYSIS

A. Calibration Signal From Bridge Voltage To Computer Output

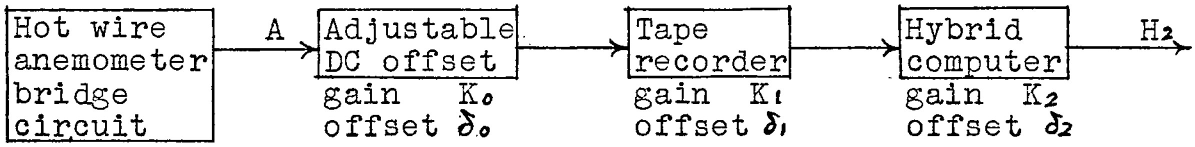

FIGURE VII-1. SIGNAL FLOW DIAGRAM FROM HOT WIRE ANEMOMETER TO HYBRID COMPUTER.

In processing the analog signal from hot wire anemometer to the hybrid computer output, the signal is processed through an adjustable DC offset and tape recorder as in Figure VII-1 . Each electronic unit has its own gain and offset value and this must be taken into consideration during processing the data in order to obtain accurate results. The following method was used in our data processing.

Let A = Instantaneous Bridge voltage from hot wire anemometer

K_0 = Gain value of adjustable DC offset

δ_0 = Adjustable DC offset value

δ_1 = Offset value of tape recorder

δ_2 = Offset value of hybrid computer

K_1 = Gain value of tape recorder

K_2 = Gain value of hybrid computer

H_2 = Hybrid computer output

then $K_0(A+\delta_0)$ = Output of DC offset

$K_0 \cdot K_1 (A+\delta_0)+\delta_1$ = Output of tape recorder and $\quad H_2 = K_2(K_0 K_1(A+\delta_0)+\delta_1)+\delta_2 =$ Output of hybrid computer

Our object was to find A, so that

$$H_2 = K_2(K_0 K_1 (A+\delta_0)+\delta_1)+\delta_2$$
$$= K_3(A+\delta_0) + K_4$$

where $\quad K_3 = K_0 K_1 K_2 \quad ; \quad K_4 = K_2\delta_1 + \delta_2$

$$A = \left(\frac{H_2 - K_4}{K_3}\right) - \delta_0 \qquad \text{(VII-1)}$$

By this way, the signal A can be found in terms of hybrid computer output and those gain and offset values. Now, we know δ_0, because this offset is readable directly from the setting of a precision potentiometer. We can find K_3 and K_4 by putting two known signals H_0 and H_1 of constant amplitude onto the tape recorder and observing the output of the hybrid computer. This is as follows:

Let $\quad H_0, H_1$ = Known input signal to tape recorder

H_{00}, H_{10} = The corresponding output of H_0, H_1, respectively, from hybrid computer

then

$$H_{00} = H_0 K_3 + K_4 \qquad \text{(VII-2)}$$
$$H_{10} = H_1 K_3 + K_4 \qquad \text{(VII-3)}$$

solving (VII-2) and (VII-3), gives

$$K_3 = \frac{H_{00} - H_{10}}{H_0 - H_1} \qquad \text{(VII-4)}$$

$$K_4 = \frac{-H_{00}H_1 + H_{10}H_0}{H_0 - H_1} \qquad \text{(VII-5)}$$

By this method, the constants K_3, K_4 and δ_o can be found for any setting of the tape unit and adjustable offset unit. With this correction the true signal from the hot wire anemometer can be calculated ignoring the gain and offset introduced from the individual electronic instruments used in data processing.

B. The Tape Recorder Signal-To-Noise Ratio And DC Offset

Input signals to the tape recorder are amplified or attenuated so that the maximum or minimum voltage is + 1.414 volts. The signal-to-noise ratio of the recorder at 30 ips (inch per second) speed is 44 DB or Es/en = 160. Thus the noise level can be expected to be 0.62% of 1.414 or +0.009 volts. Consider a bridge voltage signal of 1.414 volts maximum with 5% fluctuation due to turbulence. It is clear that the noise is of the order of 0.6/5 or 12% of the fluctuating signal. With fluctuation of the order of 2.5% of the mean, the noise can be over 20%. However, if the noise voltage is eliminated to a maximum of 1.414 volts then the error in the fluctuating quantity is of the order of 0.6%.

This procedure was, in fact, followed and errors due to tape recorder noise can be expected to be less than 1.0%. The DC offset potentiometer are readable within 0.001 volt.

C. The Sensitivity Of Radial Velocity Determination To The Measured Value Of Bridge Voltage

Recall from equations (V-1) and (V-20),

$$Ve_1 = \alpha_{s1} + \alpha_{s2}(Eb_1^2) + \alpha_{s3}(Eb_1^4) \tag{VII-12}$$

$$= \overline{Vs}\cdot\cos\alpha\cdot S_1^{\frac{1}{2}}\left(1 + \frac{S_2}{2S_1} + \frac{S_3}{2S_1} - \frac{1}{8}\frac{S_2^2}{S_1^2}\right) \tag{VII-13}$$

$$Ve_2 = \alpha_{T1} + \alpha_{T2}(Eb_2^2) + \alpha_{T3}(Eb_2^4) \tag{VII-14}$$

$$= \overline{Vs}\cdot\cos\alpha\cdot T_1^{\frac{1}{2}}\left(1 + \frac{T_2}{2T_1} + \frac{T_3}{2T_1} - \frac{1}{8}\frac{T_2^2}{T_1^2}\right) \tag{VII-15}$$

let

$$1 + G_1 = 1 + \frac{S_2}{2S_1} + \frac{S_3}{2S_1} - \frac{1}{8}\frac{S_2^2}{S_1^2} \tag{VII-16}$$

$$1 + G_2 = 1 + \frac{T_2}{2T_1} + \frac{T_3}{2T_1} - \frac{1}{8}\frac{T_2^2}{T_1^2} \tag{VII-17}$$

Because S_2 and S_3 contain r_s and r_n terms, so it is negligible compared to S_1. As first approximation, we assume $1+G_1$ and $1+G_2$ are constant.

(VII-14) divided by (VII-15), gives

$$\frac{Ve_1}{Ve_2} = \frac{S_1^{\frac{1}{2}}(1 + G_1)}{T_1^{1/2}(1 + G_2)}$$

or
$$\frac{Ve_1(1 + G_2)}{Ve_2(1 + G_1)} = \left(\frac{S_1}{T_1}\right)^{\frac{1}{2}}$$

defined
$$\Phi = \frac{Ve_1(1 + G_2)}{Ve_2(1 + G_1)} \qquad \text{(VII-18)}$$

$$\therefore \quad \Phi^2 = \frac{S_1}{T_1} = \frac{(1 + k^2) + 2(1 - k^2)R + (1 + k^2)R^2}{(1 + k^2) + 2(1 - k^2)R + (1 + k^2)R^2}$$

with $\alpha = 45^\circ$.

If $R = 0$ then $\Phi = 1$. Now assume $R \neq 0$, solving the above equation, gives

$$R^2 - \left(\frac{\Phi^2 + 1}{\Phi^2 - 1}\right)\left(\frac{2(1 - k^2)}{(1 + k^2)}\right)R + 1 = 0$$

or
$$R = \left(\frac{\Phi^2 + 1}{\Phi^2 - 1}\right)\left(\frac{1 - k^2}{1 + k^2}\right) \pm \sqrt{\left(\left(\frac{\Phi^2 + 1}{\Phi^2 - 1}\right)\left(\frac{1 - k^2}{1 + k^2}\right)\right)^2 - 1} \qquad \text{(VII-19)}$$

define
$$\psi = \left(\frac{\Phi^2 + 1}{\Phi^2 - 1}\right)\left(\frac{1 - k^2}{1 + k^2}\right) \qquad \text{(VII-20)}$$

$$\therefore \quad R = \psi + (\psi^2 - 1)^{\frac{1}{2}}$$

$$= \psi \pm \left(\psi - \frac{1}{2\psi} - \frac{1}{8\psi^3} - \frac{1}{16\psi^5} - \cdots\right)$$

$$= \pm\left(\frac{1}{2\psi} + \frac{1}{8\psi^3} + \frac{1}{16\psi^5} + \cdots\right)$$

The sign of R indicated the direction of radial velocity, we take positive sign in order to simplify the discussion.

$$R = \frac{1}{2\psi} + \frac{1}{8\psi^3} + \frac{1}{16\psi^5} + \cdots$$

From experimental measurements, Φ is usually between 0.8 and 1.3 for k=0.35, so that ψ is large.

Therefore, $$\frac{1}{2\psi} \gg \frac{1}{8\psi^3}$$

We have, $$R \cong \frac{1}{2\psi} = \frac{1}{2}\left(\frac{\Phi^2 - 1}{\Phi^2 + 1}\right)\left(\frac{1 + k^2}{1 - k^2}\right)$$

$$= \frac{1}{2}\left(1 + \frac{-2}{\Phi^2 + 1}\right)\left(\frac{1 + k^2}{1 - k^2}\right) \qquad \text{(VII-21)}$$

differentiating (VII-21), gives

$$dR = 2\left(\frac{1 + k^2}{1 - k^2}\right)\left(\frac{\Phi \, d\Phi}{(\Phi^2 + 1)}\right) \qquad \text{(VII-22)}$$

differentiated (VII-18), (VII-12) and (VII-14) individually, gives

$$d\Phi = \left(\frac{1 + G_2}{1 + G_1}\right)\left(\frac{Ve_2 \, dVe_1 - Ve_1 \, dVe_2}{Ve_2^2}\right) \qquad \text{(VII-23)}$$

$$dVe_1 = 2(\alpha s2 Eb_1 + 2\alpha s3 Eb_1^3) dEb_1 \qquad \text{(VII-24)}$$

$$dVe_2 = 2(\alpha t2 Eb_2 + 2\alpha t3 Eb_2^3) dEb_2 \qquad \text{(VII-25)}$$

Therefore, We have the following equations:

$$Ve_1 = \alpha s1 + \alpha s2 (Eb_1^2) + \alpha s3 (Eb_1^4) \qquad \text{(VII-12)}$$

$$Ve_2 = \alpha t1 + \alpha t2 (Eb_2^2) + \alpha t3 (Eb_2^4) \qquad \text{(VII-14)}$$

$$dVe_1 = 2(\alpha s_2 Eb_1 + 2\alpha s_3 Eb_1^3)dEb_1 \quad \text{(VII-24)}$$

$$dVe_2 = 2(\alpha t_2 Eb_2 + 2\alpha t_3 Eb_2^3)dEb_2 \quad \text{(VII-25)}$$

$$\Phi = \frac{Ve_1}{Ve_2}\left(\frac{1 + G_2}{1 + G_1}\right) \quad \text{(VII-18)}$$

$$d\Phi = \left(\frac{Ve_2 dVe_1 - Ve_1 dVe_2}{Ve_2^2}\right)\left(\frac{1 + G_2}{1 + G_1}\right) \quad \text{(VII-23)}$$

$$dR = 2\left(\frac{1 + k^2}{1 - k^2}\right)\left(\frac{\Phi\, d\Phi}{(\Phi^2 + 1)^2}\right) \quad \text{(VII-22)}$$

Consider these calculations;

$k = 0.35$, $Ve_1 = 26.10981$, $Ve_2 = 20.21416$, $Eb_1 = 1.29166$,

$Eb_2 = 4.21687$, $G_1 = G_2 = 0$

substituted into above equations, We have

$$\Phi = 1.29166 \quad , \quad 2\left(\frac{1 + k^2}{1 - k^2}\right) = 2.5584$$

$$2Ve_2(\alpha s_2 Eb_1 + 2\alpha s_3 Eb_1^3)/Ve_2^2 = 1.65743$$

$$2Ve_1(\alpha t_2 Eb_2 + 2\alpha t_3 Eb_2^3)/Ve_2^2 = 1.81317$$

Therefore

$$dR = 0.46411(1.65743dEb_1 - 1.81317dEb_2)$$

dEb can occur as a result of

A. hot wire anemometer drift

B. error in reading of DC offset

C. goodness of polynomial curve fit

Hot wire anemometer drift is + 0.005 volts in 15 hours or , say, 0.003 volts over the period of a complete experiment. (about 7 hours) The DC offset reading is read from a digital volt meter which is readable within 0.001 volt.

The standard deviation of the curve fit is 0.004 volts in Eb_1 or Eb_2. Therefore, the maximum error is 0.008 volts.

So, for $dEb_1 < 0$, $dEb_2 < 0$,

$$dR = 0.46411(-1.65743 + 1.81317)(0.008)$$
$$= 0.000578$$

for $dEb_1 > 0$, $dEb_2 < 0$,

$$dR = (0.46411)(1.65743)(0.008)$$
$$= 0.01289$$

Also $\tan\theta = R$, and at small angle $d\theta \sim dR$. So a dR of 0.000578 $\sim$ 0.01289 radiam or θ can be resolved to be

$$d\theta = (0.000578)(3000/2\ ) = 0.02760 \text{ degree}$$

and $$d\theta = (0.01289)(300/2\ ) = 0.61550 \text{ degree}$$

For this calculation,

$$R = \frac{1}{2}\left(\frac{1 + 0.35}{1 - 0.35}\right)\left(\frac{1.29166 - 1}{1.29166 + 1}\right) = 0.16021$$

the percentage error is

$$\frac{dR}{R} = \frac{0.000578}{0.16021} = 0.36\%$$

and $$\frac{dR}{R} = \frac{0.01289}{0.16021} = 8.05\%$$

$dR/R = 8.05\%$ is the maximum error with $dEb_1 > 0$ and $dEb_2 < 0$. Usually, dEb_1 and dEb_2 have the same sign. Therefore, the percentage error is always less than 8.05%. If dEb_1 and dEb_2 have the same sign, the error in R (ie dR) is decreased rapidly.

The total turbulent energy in longitudinal and radial direction as calculated by two different methods are listed in Table VII-1. Method A is calculated from the power spectrum, and method B is calculated directly from the time series of the velocity.

The power spectrum is first calculated from the signal then the turbulent energy is calculated from

$$\overline{V_i^{2}{}'} = \int_0^{\infty} E_i(f)\,df \qquad \text{METHOD A}$$

where $E_i(f)$ is the auto-power-spectrum in i-direction. The turbulent energy is calculated by method B from the following equation,

$$\overline{V_i^{2}{}'} = \int_0^{\infty} (V_i(t))^2 ft \qquad \text{METHOD B}$$

Table VII-1 shows that the measured values, $Vs')_A$, $Vs')_B$, $Vn')_A$, and $Vn')_B$, are almost same, except for a few points. This, along with the discussion in chapter VII, gives us the confidence that the methods used in this work are correct.

TABLE VII-1.

COMPARISON OF TURBULENT INTENSITIES BY METHOD A AND METHOD B

Method A is by Power Spectrum Measurement.

Method B is by Time-Series Measurement.

		$Re_{Max}=2.53*10^5$			$Re_{Max}=2.53*10^5$		
Posi-tion	y/r	$\overline{Vs'^2})_A$	$\overline{Vs'^2})_B$	Devi-ation	$\overline{Vn'^2})_A$	$\overline{Vn'^2})_B$	Devi-ation
	1.0	30.1	31.1	3.3%	22.8	23.5	2.8%
	0.5	71.1	69.2	3.6	34.0	31.2	9.0
	0.25	75.8	79.4	4.9	32.0	33.2	3.7
ML2	0.10	69.6	76.5	9.2	33.5	34.4	2.7
	0.05	92.6	74.1	25.0	28.2	29.5	4.7
	0.0187	63.5	66.8	5.3	32.7	34.8	6.4
	1.0	30.4	30.7	1.3	22.8	23.4	2.5
	0.5	57.5	66.7	16.0	29.2	29.1	0.4
	0.25	66.4	77.9	17.2	30.3	31.8	5.1
VS	0.10	84.5	80.4	5.5	32.8	32.8	0.0
	0.05	81.8	81.6	0.4	39.6	35.8	10.8
	0.0187	78.7	82.9	5.4	27.7	27.5	0.9
	1.0	30.0	31.7	5.9	23.3	23.5	0.9
	0.5	62.4	66.3	6.3	30.4	32.1	5.9
	0.25	77.5	76.9	0.8	31.1	31.8	0.2
ML2	0.10	78.2	81.5	4.2	26.7	26.8	0.0
	0.05	63.4	65.0	2.6	25.0	24.7	1.3
	0.0187	65.1	56.2	16.0			
	1.0	30.6	35.7	16.7	23.1	26.9	16.3
	0.5	73.5	70.6	4.1	32.2	32.5	0.8
	0.25	75.3	80.8	7.3	30.6	34.3	12.1
VL2	0.10	74.0	81.9	10.6	25.3	28.1	11.0
	0.05	51.6	55.2	6.9	20.7	21.5	4.1
	0.0187	36.6	37.3	1.8	9.4	10.1	7.6

VIII PROBE CONFIGURATION

The sensor itself is usually tungsten or platinum alloy or film (quartz coated with platinum), soldered or welded at each end to supporting needles. All the work done earlier by others attempted to minimize the degree of the interference of the flow caused by the wire support. However, there have been no good criterion to judge the results.

At first, we used the probe manufactured by Thermo-system Inc. for commercial use in cross flow. This is a film probe with dimensions 0.002" diameter and 0.04" long. The constant value of k measured was 0.35 and α is $45^\circ \pm 1^\circ$. (see Appendix I) This probe was placed in a rectangular channel. The probe configuration and the dimensions of this rectangular channel are shown in Figure VIII-1 and VIII-2.

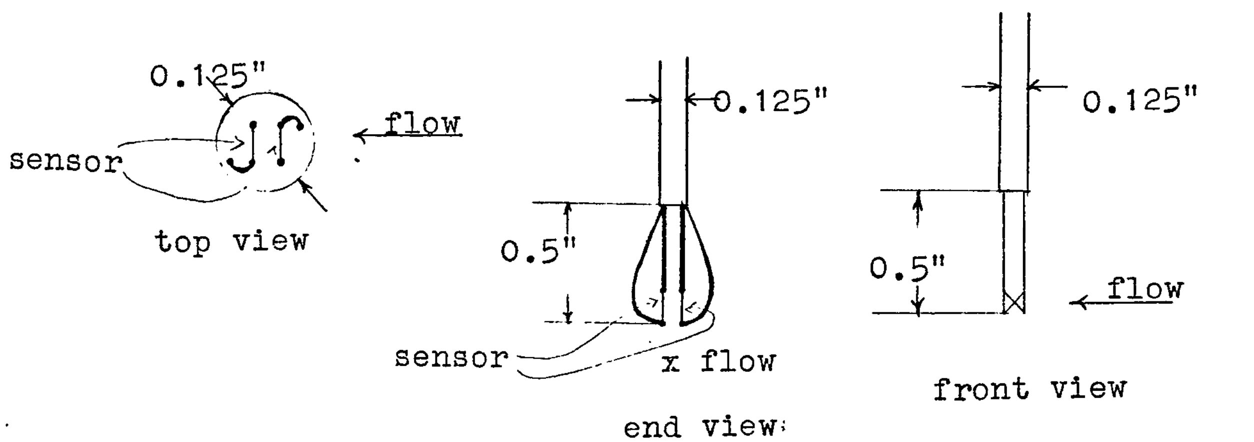

FIGURE VIII-1. SCHEMATIC DIAGRAM OF X-FILM PROBE IN CROSS FLOW.

The probe was positioned as shown in Figure VIII - 2 and measurements made at the centreline (y/r = 1.0) and at various positions between the centerline and the lower wall. The measured mean and fluctuating quantities are tabulated in Table VIII-1. The transverse velocities across th smooth channel diameter should, of course, be zero. But the calculated transverse velocities in Table VIII-1 showed significant non-zero values, except those measured at the centerline position. This result raised some questions as to the possibility of wire support interference.

This same probe was than placed at the axis of a smooth circular pipe but this time with the alignment as shown in Figure VIII-3 and Figure VIII-4.

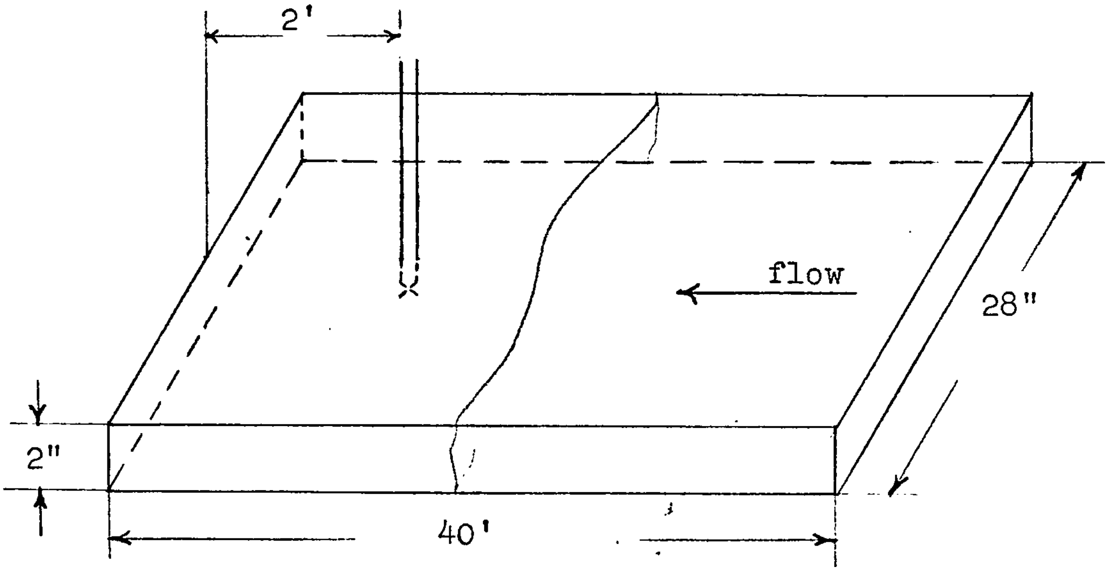

FIGURE VIII-2. SCHEMATIC DIAGRAM OF RECTANGULAR CHANNEL AND PROBE POSITION.

TABLE VIII-1.

(Cross Flow)

At centerline (y/r = 1.0)

pitot tube velocity	$\overline{Vs}$	$\overline{Vn}$	$\sqrt{\overline{Vs'^2}}/\overline{Vs}$	$\sqrt{\overline{Vn'^2}}/\overline{Vs}$	$-\overline{Vs'Vn'}$
62.30	62.70	-0.176	3.02 %	3.06 %	-0.011
56.18	55.65	0.245	3.00	3.16	-0.126
49.12	49.14	0.048	3.02	3.22	-0.073
41.25	41.44	0.000	3.01	3.31	-0.086
34.38	34.61	-0.223	3.08	3.43	-0.071
24.49	24.44	0.000	3.20	3.60	-0.064
20.62	20.61	0.122	3.28	3.68	-0.048
11.97	12.02	-0.021	3.51	3.84	-0.036

Y/r	$\overline{Vs}$	$\overline{Vn}$	$\sqrt{\overline{Vs'^2}}/\overline{Vs}$	$\sqrt{\overline{Vn'^2}}/\overline{Vs}$	$-\overline{Vs'Vn'}$
1.0	62.70	-0.176	3.02 %	3.06 %	-0.011
0.75	63.22	2.190	3.64	3.37	-1.189
0.50	60.88	2.654	4.88	3.97	-2.918
0.25	56.73	3.203	5.97	4.45	-4.231
0.125	53.35	3.757	6.42	4.49	-4.400
0.025	52.06	3.822	6.48	4.48	-4.733

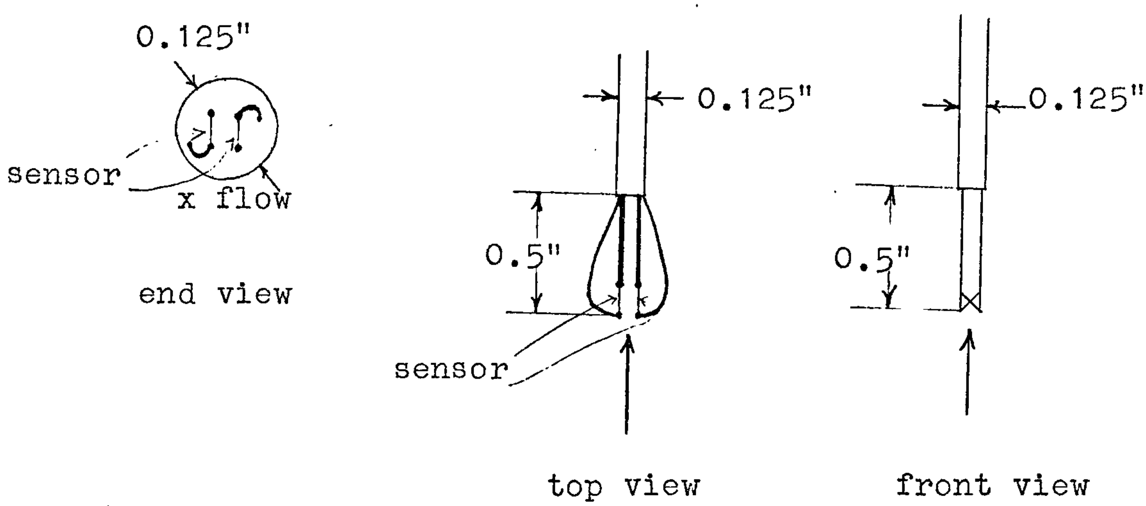

FIGURE VIII-3. SCHEMATIC DIAGRAM OF X-FILM PROBE IN END FLOW.

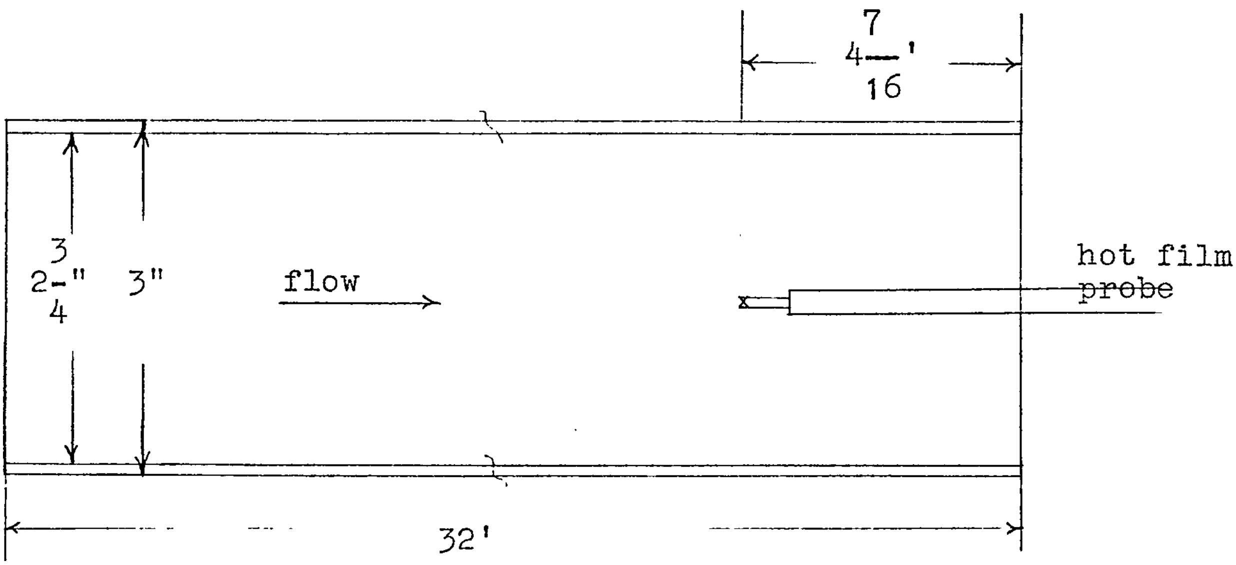

FIGURE VIII-4. SCHEMATIC DIAGRAM OF REFERENCE CHANNEL AND PROBE POSITION.

In such an orientation the possibility of wire supprot interference is decreased for a probe of this design. The measured quantities obtained in the experiment are tabulated in Table VIII-2. These results are also plotted in Figure VIII-7, VIII-8, & VIII-9 which compare the Laufer's[19] data, the end flow data and the Boundary Layer Probe data. From the Table VIII-2 it is now seen that $\overline{Vn}$ is quite small at all radial positions across the pipe. The longitudinal turbulent intensities are slightly higher than those of Laufer's[19] data, and the radial ones are lower than those of Laufer's[19] data. This could because the probe used by Laufer in his experiment was the one we used at the very begining and with the same arrangement. This increase in longitudinal energy and decrease in radial energy is reasonable because the interference of the wire support is reduced to some extent. This reduction of interference prevents the longitudinal turbulence energy from becoming radial turbulence energy by the interference of the wire support. The Reynolds shear stress agree well with the linear relationship. The result thus clearly suggest that wire support interference takes place with this configuration with some arrangement in flow.

From the knowledge obtained in these experiments a special probe was designed. This probe is such that its wires are parallel to each other and lie in a vertical plane with all wire support downstream of the wire. Its three views

TABLE VIII-2.

(End Flow)

AT centerline ($y/r = 1.0$)

pitot tube velocity	$\overline{Vs}$	$\overline{Vn}$	$\sqrt{\overline{Vs'^2}}/Vs$	$\sqrt{\overline{Vn'^2}}/Vs$	$-\overline{Vs'Vn'}$
45.44	45.39	-0.054	3.29 %	2.52 %	-0,052
42.99	42.86	-0.026	3.32	2.53	-0.049
41.03	41.15	0.065	3.29	2.54	-0.040
39.07	39.11	0.069	3.32	2.55	-0.051
37.24	37.17	0.036	3.31	2.58	-0.043
34.81	34.89	-0.023	3.31	2.58	-0.046
32.82	32.79	-0.017	3.34	2.59	-0.046
30.41	30.34	-0.023	3.29	2.61	-0.052
28.03	28.06	-0.003	3.35	2.73	-0.063
25.34	25.37	-0.030	3.36	2.65	-0.027
23.31	23.21	0.026	3.39	2.79	-0.041
19.42	19.51	0.003	3.33	2.69	-0.014
17.08	17.05	0.008	3.39	2.81	-0.032

y/r	$\overline{Vs}$	$\overline{Vn}$	$\sqrt{\overline{Vs'^2}}/Vs$	$\sqrt{\overline{Vn'^2}}/Vs$	$-\overline{Vs'Vn'}$
1.0	37.17	0.036	3.31 %	2.58 %	-0.043
0.8	35.77	-0.08	4.05	2.72	-0.534
0.6	33.81	-0.13	5.18	3.17	-0.985
0.5	32.60	-0.12	5.60	3.30	-1.142
0.4	31.32	-0.11	5.99	3.45	-1.298
0.3	29.64	-0.09	6.52	3.60	-1.511
0.2	27.69	-0.09	6.78	3.63	-1.541
0.128	25.30	-0.07	7.00	3.64	-1.506

are shown in figure VIII-5.

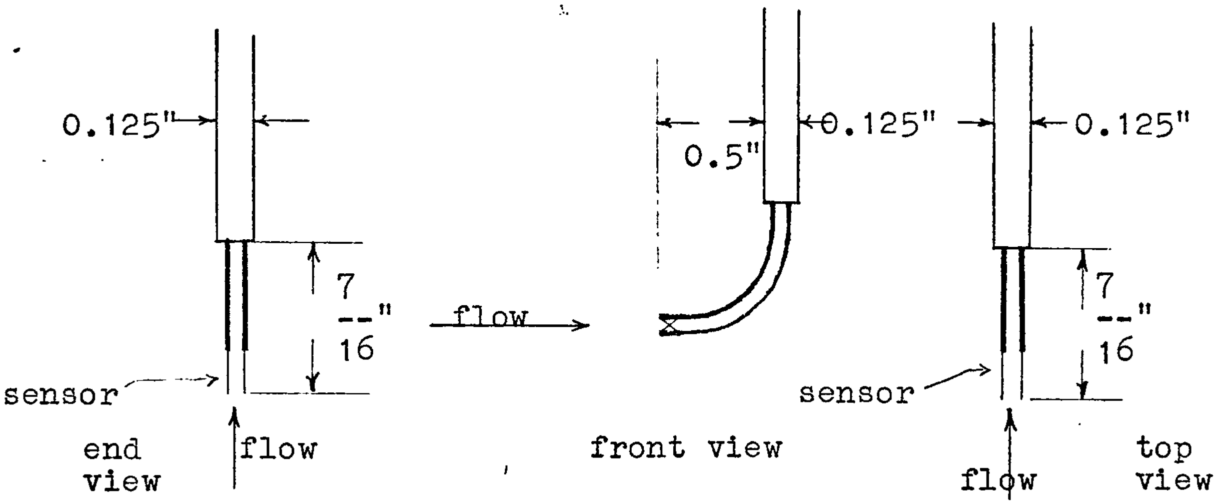

FIGURE VIII-5. SCHEMATIC DIAGRAM OF BOUNDARY LAYER PROBE.

Comparing the probes in Figures VIII-3 & VIII-5 it is seen that the big difference between them is the mounting configuration of the support. Also the minor difference between them is that the probe of Figure VIII-3 is a straight one, but Figure VIII-5 is a curved one. We called this special designed probe the "Boundary Layer Probe". This probe was placed in the same smooth circular pipe as shown in igure VIII-6.

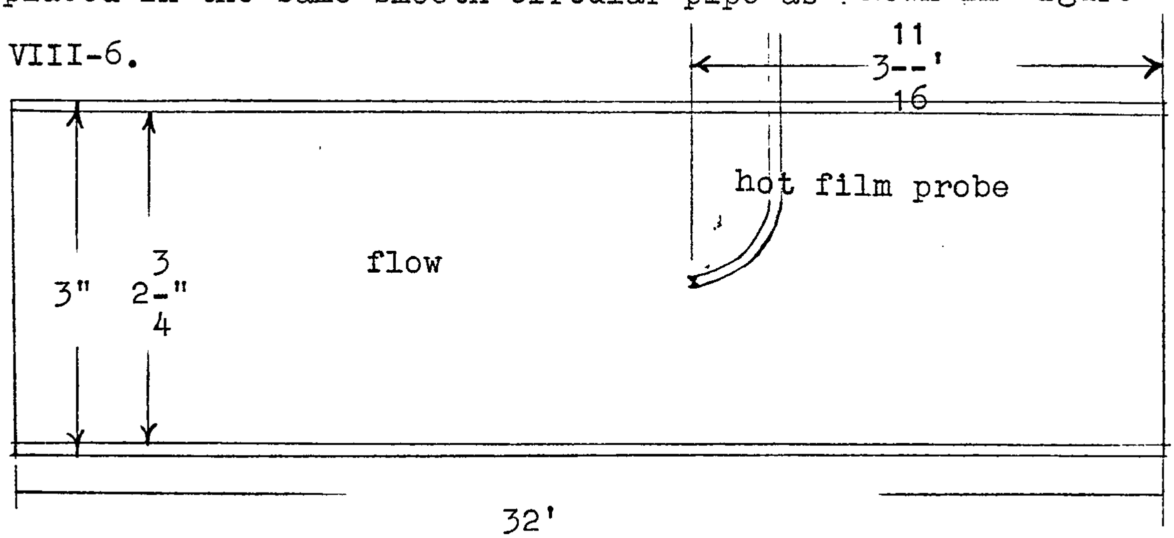

FIGURE VIII-6. SCHEMATIC DIAGRAM OF REFERENCE CHANNEL AND PROBE POSITION.

The measured quantities obtained in the experiment were tabulated in Table VIII-3 and also plotted in Figures VIII-7, VIII-8, and VIII-9. Again, the calculated $\overline{Vn}$'s are very small at all radial positions across the pipe. The longitudinal and radial turbulent intensities have similar values to those in end flow. Reynolds shear stress agrees well with the linear relationship.

The results found in end flow and boundary layer probe flow experiments assures us that the wire support really causes some interference in flow and data of other investigations which used the type of probe (including Laufer) are open to some question.

TABLE VIII-3.

(Boundary Layer Probe Flow)

At centerline ($y/r = 1.0$)

pitot tube velocity	$\overline{Vs}$	$\overline{Vn}$	$\sqrt{\overline{Vs'^2}}/Vs$	$\sqrt{\overline{Vn'^2}}/Vs$	$-\overline{Vs'Vn'}$
56.25	56.28	0.024	3.52 %	2.92 %	-0.348
53.83	53.87	-0.022	3.50	2.91	-0.270
50.60	50.66	-0.048	3.48	2.95	-0.257
47.81	47.82	-0.016	3.51	2.96	-0.257
44.75	44.73	-0.067	3.51	3.00	-0.240
40.92	40.89	-0.002	3.50	3.04	-0.184
37.65	37.63	0.049	3.47	3.00	-0.147
33.88	33.91	0.038	3.52	3.03	-0.130
29.85	29.99	0.049	3.59	3.10	-0.118
25.72	25.55	-0.048	3.60	3.15	-0.081
21.32	21.29	-0.025	3.59	3.14	-0.055
15.44	15.50	0.008	3.65	3.16	-0.026

y/r	$\overline{Vs}$	$\overline{Vn}$	$\sqrt{\overline{Vs'^2}}/Vs$	$\sqrt{\overline{Vn'^2}}/Vs$	$-\overline{Vs'Vn'}$
1.0	36.17	0.021	3.50 %	3.01 %	-0.135
0.9	36.06	0.006	3.57	3.04	-0.158
0.8	35.62	0.021	4.04	3.17	-0.414
0.7	34.81	-0.004	4.62	3.38	-0.681
0.6	33.89	-0.015	5.11	3.59	-0.871
0.5	32.75	0.028	5.59	3.83	-1.081
0.4	31.55	0.008	6.08	4.00	-1.250
0.3	30.20	0.017	6.42	4.14	-1.387

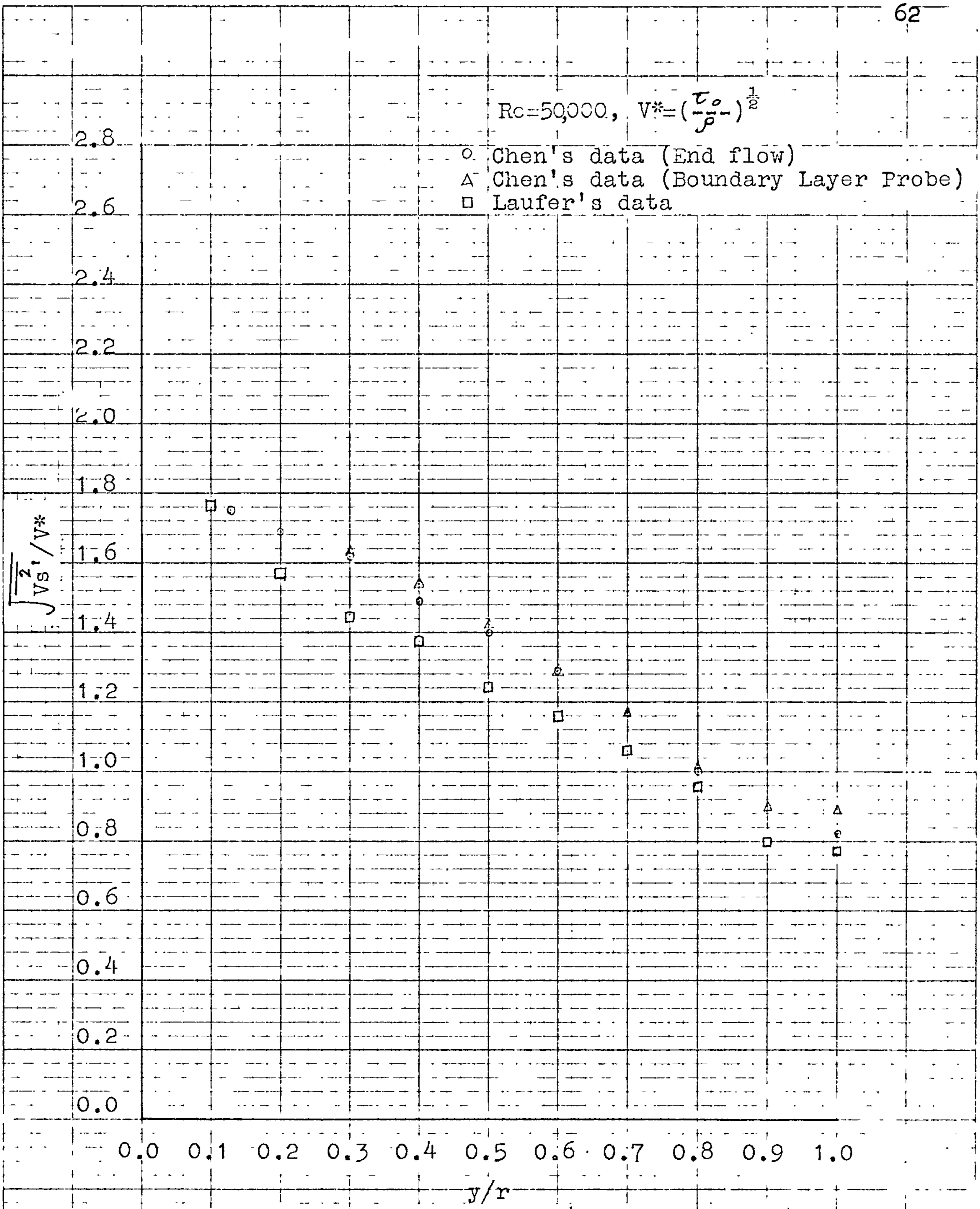

FIGURE VIII-7. LONGITUDIANL TURBULENT INTENSITY.

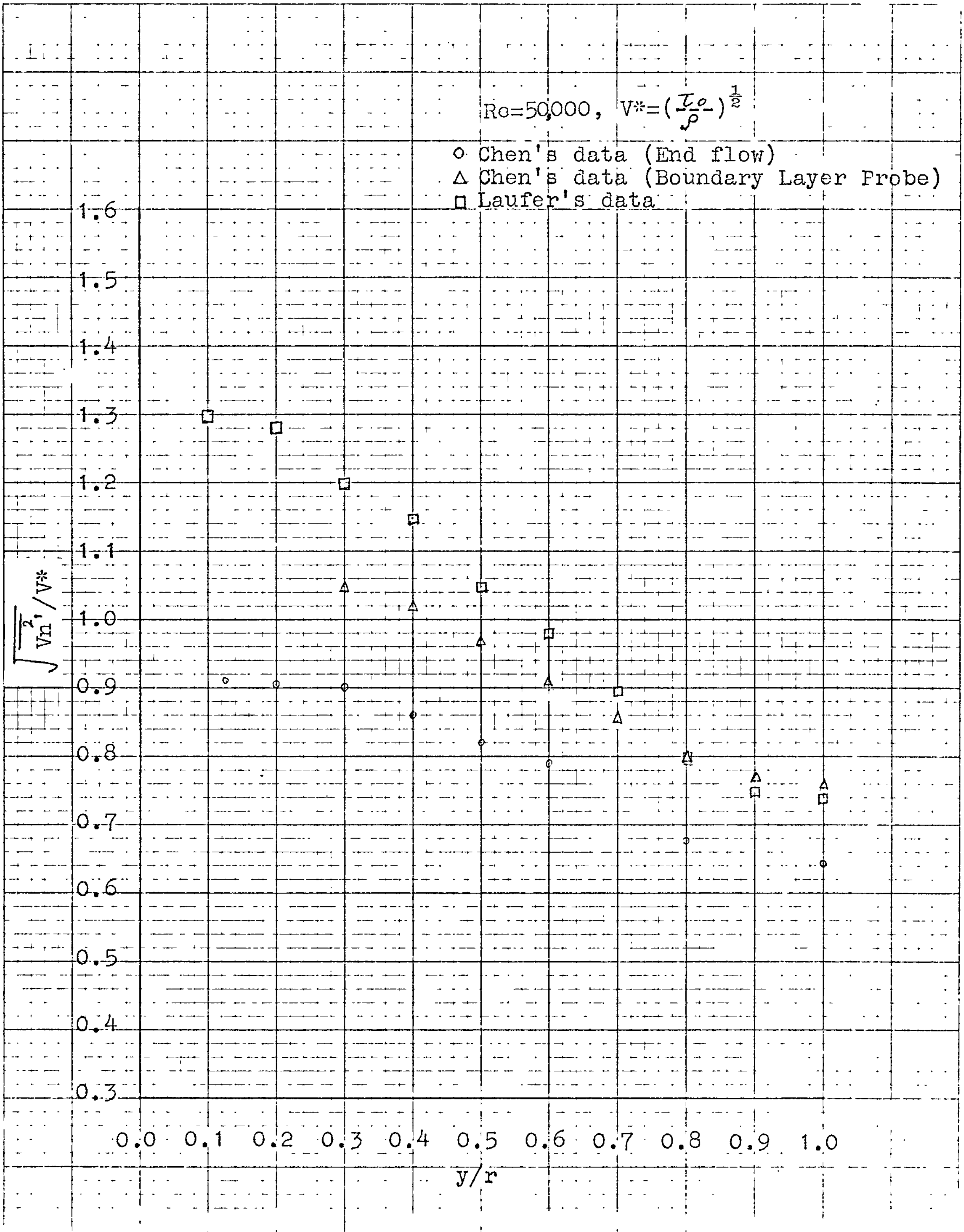

FIGURE VIII-8. RADIAL TURBULENT INTENSITY.

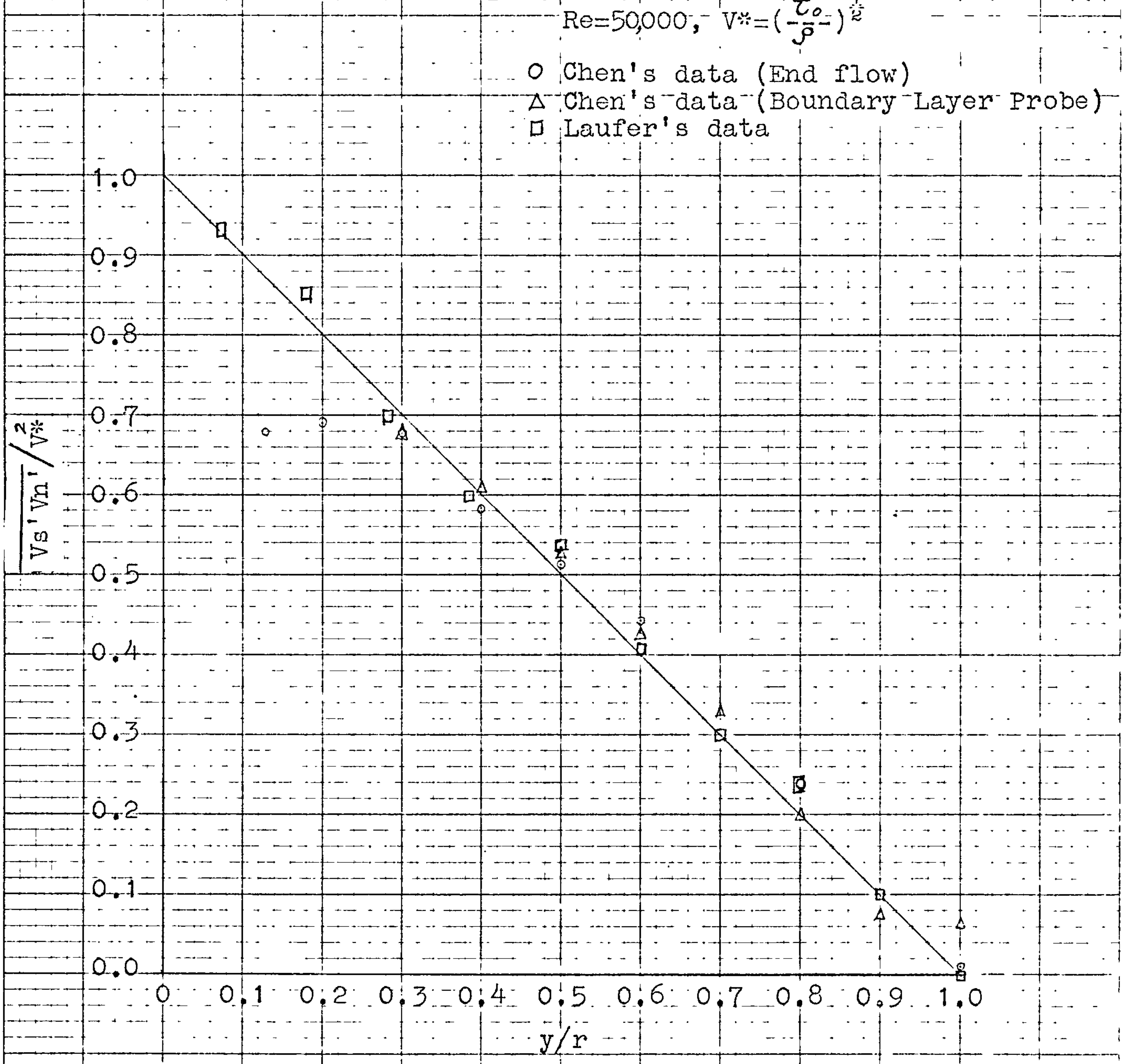

FIGURE VIII-9. REYNOLD"S STRESS.

IX PRESENTATION OF DATA

The experiments were made in the corrugated pipe (see Figure IV-2). Data were taken at y/r = 1.0, 0.5, 0.25, 0.10, 0.05 and 0.0187 where r is the radius and y is the distance from wall. The calibration curve was made in the reference channel (see Figure IV-1).

A. Distribution of Mean Velocities

Mean velocity measurements and all the other turbulent quantities were carried out at y/r = 1.0, 0.5, 0.25, 0.10, 0.05, 0.0187 at different sections designated as VS, ML1, ML2, VL2, as shown in Figure IV-2. Because the corrugated pipe is not a pipe of uniform diameter equal values of y/r at different sections does not mean the equal position from centerline. Due to the non-uniform diameter of the corrugated pipe, the Reynold number is defined as:

$$Re_{Max} = \frac{D \cdot \overline{Vso}}{\nu}$$

where D is the diameter of the pipe measured at VS section, ie.8.550", and $\overline{Vso}$ is the longitudinal velocity at the centerline measured at VS section. For $\overline{Vso}$ = 25.40 ft/sec, $Re_{Max} = 1.15 * 10^5$, and for $\overline{Vso}$ = 56.22 ft/sec, $Re_{Max} = 2.53*10^5$. These are the two Reynold numbers used in this work.

1. Distribution of longitudinal velocity, $\overline{Vs}$

Longitudinal velocity data are tabulated in Table IX-1 and Table IX-2. They are also plotted in Figure IX-1 and Figure IX-2. The diagrams show no difference in $\overline{Vs}$ for all the sections from y/r = 1.0 to y/r = 0.5 but closer to the wall there

TABLE IX-1

$Re_{Max}=1.15*10^5$

Position	y/r	$\overline{Vs}$	$\overline{Vn}$	$\sqrt{\overline{Vs'^2}}/\overline{Vs}_{local}$	$\sqrt{\overline{Vn'^2}}/\overline{Vs}_{local}$	$-\overline{Vs'Vn'}$
ML1	1.0	25.74	0.21	9.52%	7.96%	0.05
	0.5	20.53	0.06	18.19	11.24	3.38
	0.25	18.28	0.46	19.92	12.20	2.88
	0.10	14.89	0.92	24.38	14.16	3.31
	0.05	13.14	1.49	26.36	14.46	3.41
	0.0187	9.07	0.93	23.52	17.36	2.28
VS	1.0	25.40	0.29	9.09	7.88	0.06
	0.5	21.81	0.23	15.58	10.35	2.70
	0.25	18.68	0.26	19.94	12.14	3.08
	0.10	16.37	0.04	23.31	12.79	2.65
	0.05	15.56	-0.12	22.82	13.76	2.03
	0.0187	15.51	-0.42	21.61	12.35	0.63
ML2	1.0	25.27	0.29	9.39	7.93	-0.21
	0.5	21.79	0.35	15.98	10.31	2.82
	0.25	17.37	0.06	21.59	12.68	3.25
	0.10	14.10	-0.16	24.13	13.02	2.10
	0.05	11.62	-0.35	24.40	13.73	0.73
	0.0187	10.32	-0.54	23.07	12.97	-0.84
VL2	1.0	25.33	0.30	9.20	8.01	-0.02
	0.5	20.94	0.29	17.56	10.89	3.23
	0.25	17.50	0.46	21.15	12.70	3.28
	0.10	12.31	1.09	26.54	15.19	3.00
	0.05	8.86	0.60	22.64	15.82	1.51
	0.0187	8.06	-0.00	16.23	10.34	-0.25

TABLE IX-2.

$Re_{Max}=2.53*10^5$

Position	y/r	$\overline{Vs}$	$\overline{Vn}$	$\sqrt{\overline{Vs'^2}}/\overline{Vs}_{local}$	$\sqrt{\overline{Vn'^2}}/\overline{Vs}_{local}$	$-\overline{Vs'Vn'}$
ML1	1.0	55.79	0.88	10.00%	8.68%	-2.05
	0.5	47.22	0.95	17.62	11.82	18.42
	0.25	40.66	1.71	21.92	14.16	20.67
	0.10	33.98	3.81	25.74	17.26	20.92
	0.05	30.58	5.14	28.15	17.77	21.43
	0.0187	21.47	5.18	38.07	27.49	31.17
VS	1.0	56.22	0.82	9.86	8.60	-0.06
	0.5	47.26	0.57	17.28	11.42	15.75
	0.25	41.03	0.51	21.51	13.75	20.47
	0.10	39.17	0.45	22.89	14.61	18.18
	0.05	37.77	0.02	23.91	15.83	14.94
	0.0187	39.87	-0.35	22.84	13.14	4.96
ML2	1.0	57.20	0.75	9.85	8.48	0.01
	0.5	46.24	0.53	17.61	12.26	17.45
	0.25	41.24	0.61	21.26	13.67	18.72
	0.10	33.17	-2.08	27.21	15.60	14.71
	0.05	28.02	-3.67	28.77	17.73	6.16
	0.0187	24.37	-4.59	30.76	17.52	-5.87
VL2	1.0	56.94	0.82	10.49	9.11	3.20
	0.5	46.19	0.74	18.19	12.34	17.84
	0.25	37.78	0.56	23.79	15.49	23.08
	0.10	30.93	1.83	29.26	17.13	18.74
	0.05	18.76	2.37	39.59	24.73	15.77
	0.0187	15.27	0.32	39.99	20.83	0.76

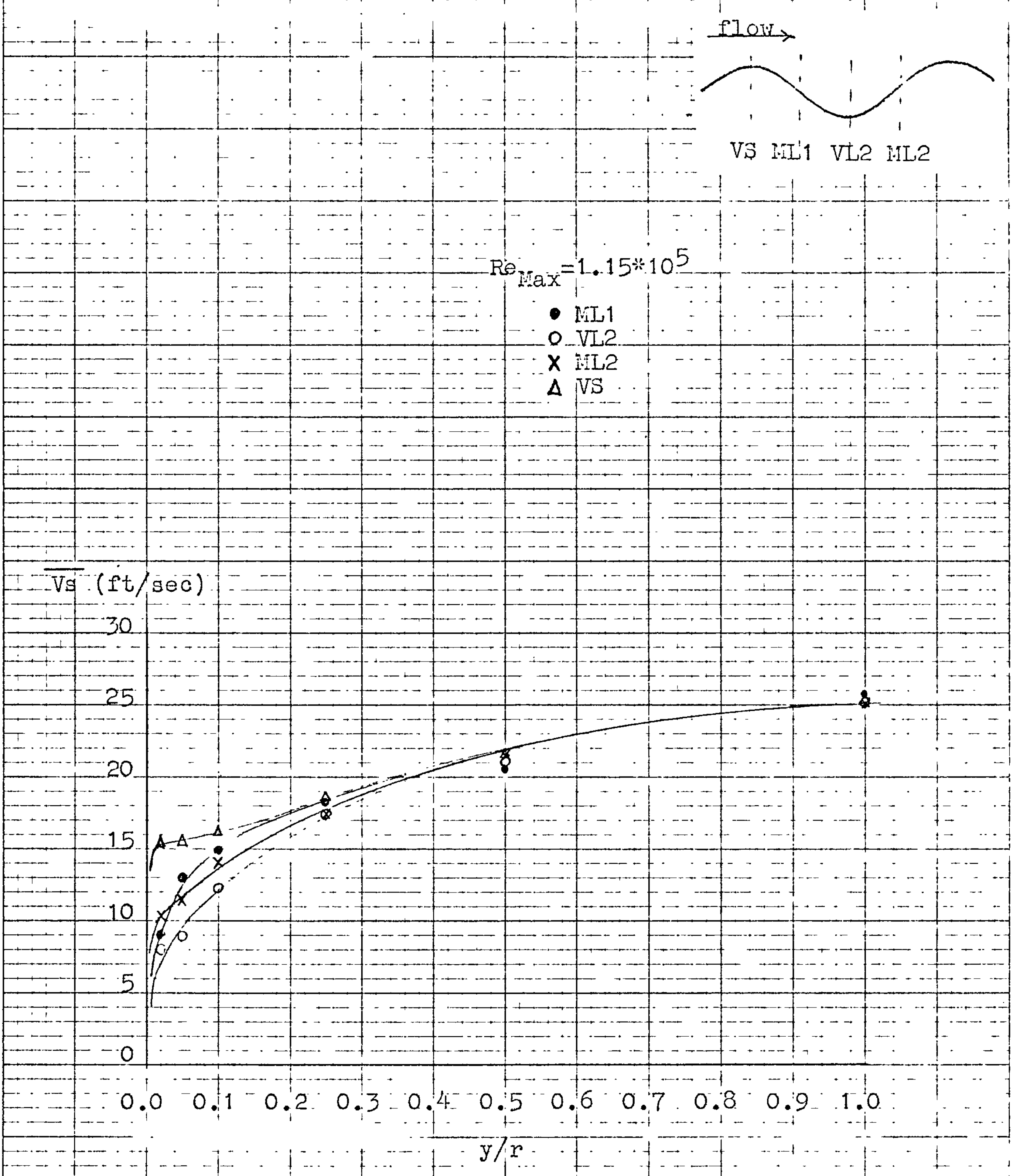

FIGURE IX-1. LONGITUDINAL MEAN VELOCITY DISTRIBUTION ACROSS FLOW CHANNEL.

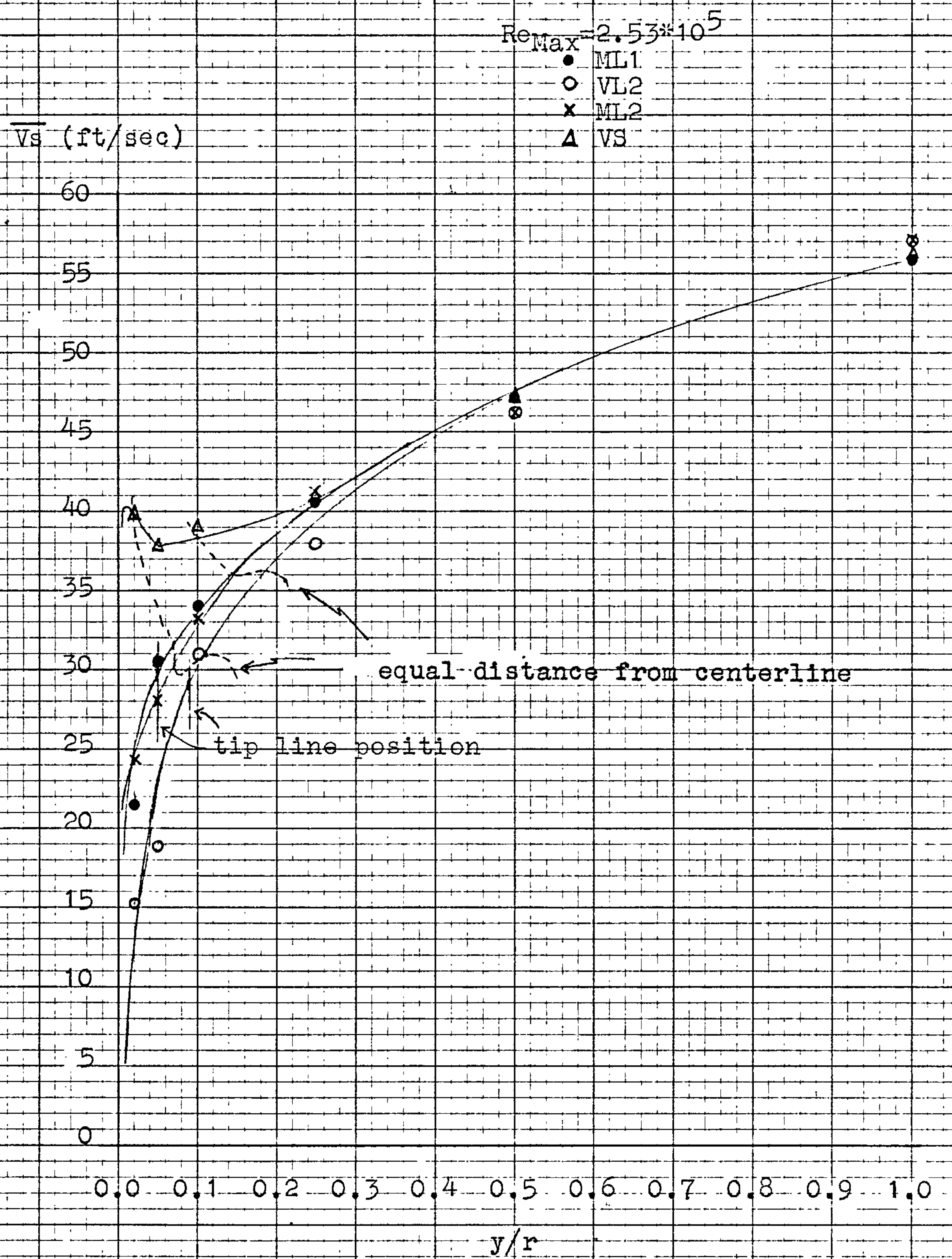

FIGURE IX-2. LONGITUDINAL MEAN VELOCITY DISTRIBUTION ACROSS FLOW CHANNEL.

are difference. At $Re_{Max}=1.15*10^5$ the curves show less deviation. However, at $Re_{Max}=2.53*10^5$ there is a sharp decrease in the region of y/r=0.0 to y/r=0.1. If we draw the line connecting the tips of the peak then the sharp change in $\overline{Vs}'$ occurs near this line. This would suggest that the flow is suddenly trapped beneath this line by the valley. The longitudinal velocity is higher in wall region (from y/r=0.0 to y/r=0.2) at the VS section than at other sections. This is due to the fact that VS section has the small cross-sectional area. Also, notice that between y/r=0.05 and y/r= 0.0, there appears a peak in the velocity for the VS section. This could be due to a local jet flow in this wall region. Such a jet could exist because the flow at ML2 section is forced to pass the smaller area of VS section then open to a larger area of the ML1 section.

2. Distribution of radial velocity, $\overline{Vn}$

The sign of radial velocity indicates the direction of the velocity vector. For the region below the centerline, the positive sign means the velocity vector is toward the wall and the negative sign means toward the center.

The radial velocity data are tabulated in Table IX-1 and Table IX-2. They are also plotted in Figure IX-3 and Figure IX-4.

At $Re_{Max}=1.15*10^5$, $\overline{Vn}$ is zero from y/r=1.0 down to y/r= 0.3 independent of the sections chosen. For ML2 and VS,

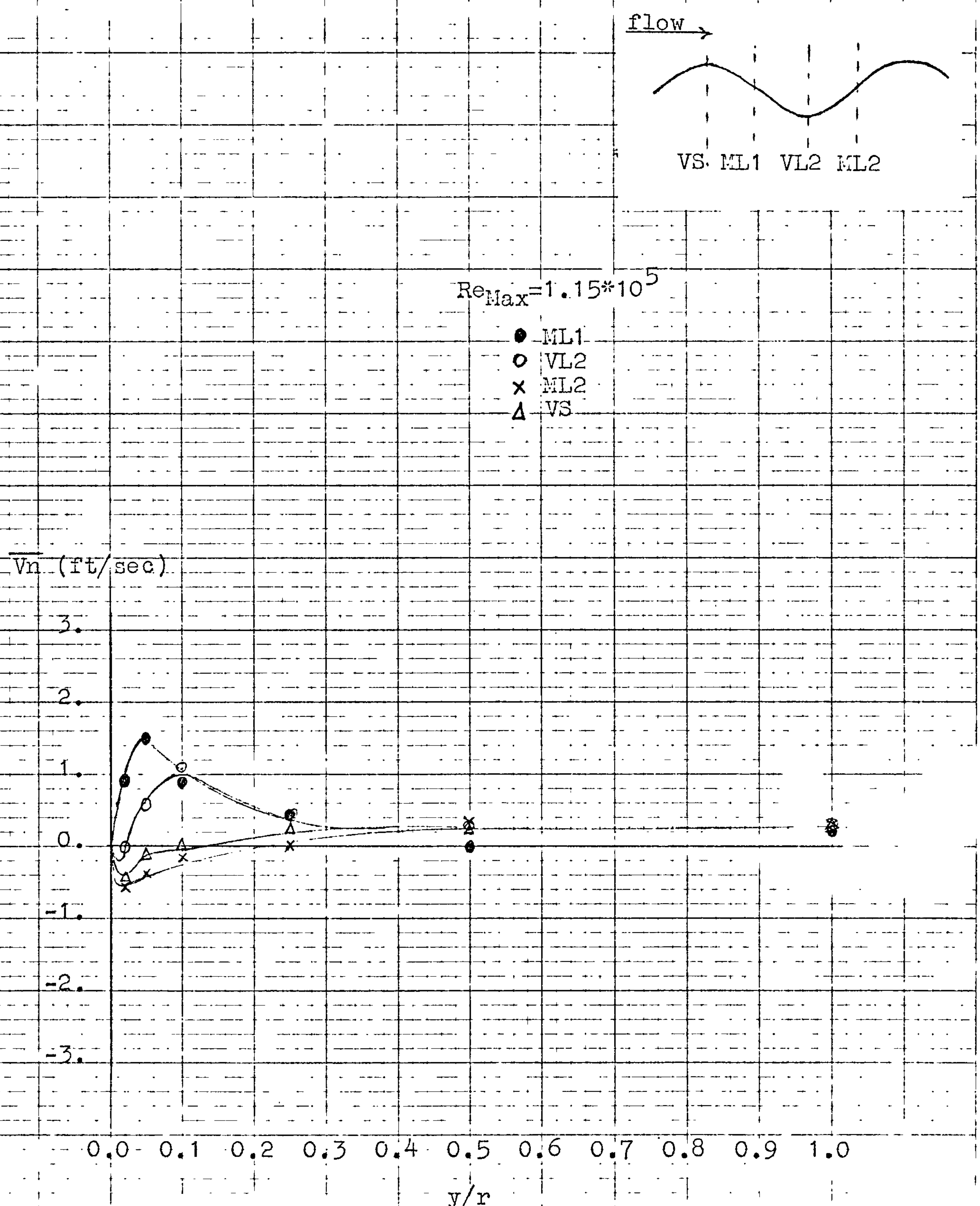

FIGURE IX-3. RADIAL MEAN VELOCITY DISTRIBUTION ACROSS FLOW CHANNEL

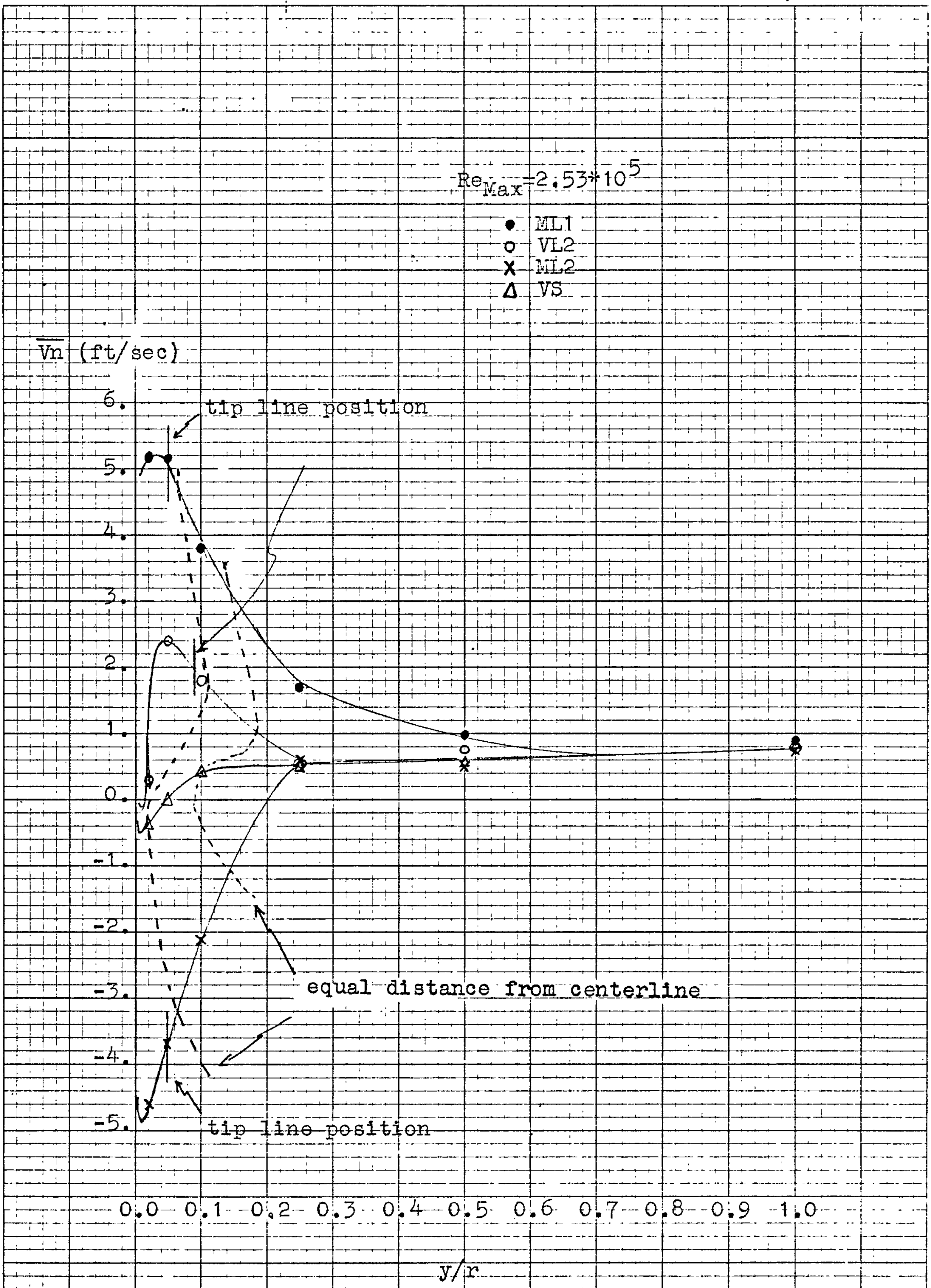

FIGURE IX-4. RADIAL MEAN VELOCITY DISTRIBUTION ACROSS FLOW CHANNEL.

$\overline{Vn}$ is zero even down to the wall, but for ML1 and VL2, they show higher values. At Re_{Max}=2.53*10^5 the observation for $\overline{Vn}$ is the same. However, $\overline{Vn}$ is not zero for all sections at y/r= 1.0 but has a value of about 0.6 ft/sec, we think that this is due to the fact that the corrugated pipe is not perfectly symmetric. We will artificially adjust the zero line upward to give a radial velocity at centerline which is zero. From y/r=1.0 to y/r=0.25 $\overline{Vn}$ is zero for all sections. For ML1 and VL2, $\overline{Vn}$ has a positive sign, this means that the velocity vector is flowing toward the wall. For ML2 and VS, $\overline{Vn}$ has a negative sign which means the flow is going up toward the center. This is reasonable because the fluid should follow the curve of the wall boundary. When fluid passes the VS point, its direction should diverge from the wall slope and change direction toward the wall passing the VL2 point.

Smoke trace experiments showed that there really exists a degree of secondary motion as described above. But such observations are only qualitative. Therefore, the measurement of radial velocity is important.

B. Distribution Of Vs' And Vn'

Three relative turbulent intensities were calculated, one relative to the centerline longitudinal mean velocity at each section, one relative to the local mean velocity, and one relative to the friction velocity, V*, for $Re_{Max}=1.15*10^5$ and $Re_{Max}=2.53*10^5$. Turbulent intensities relative to centerline axial velocity for radial and longitudinal direction are tabulated in Table IX-3 and IX-4 and are also plotted in Figure IX-5, IX-6, IX-7, and IX-8, where they are compared to the Laufer's data.[19] Those data show that all the turbulent intensities measured in the corrugated pipe are much higher than those measured in smooth pipe. The second relative turbulent intensity data are also tabulated in Table IX-3 and Table IX-4, and are also plotted in Figure IX-9, IX-10, IX-11, and IX-12. These relative turbulent intensities give information about the local turbulence because they provide an indication of the ratio of the kinetic energy of turbulence and the kinetic energy of mean motion. Between y/r=1.0 to y/r=0.25 these two local turbulent intensities, longitudinal and radial local turbulent intensities, show almost no difference for all sections. We think the dispersion from one another at y/r=0.5 in Figure IX-10 could be due to experimental error. At $Re_{Max}=1.15*10^5$ the curves increase smoothly along the pipe radius, then have a tendency to increase rapidly near the wall. As velocity increases, at $Re_{Max}=2.53*10^5$, there is the same behavior as at low velocity but a sharp increase exists at

TABLE IX-3

$Re_{Max}=1.15*10^5$

Posi-yion	y/r	$\sqrt{\overline{Vs'^2}}/\overline{Vs}_{local}$	$\sqrt{\overline{Vs'^2}}/\overline{Vs}_{center}$	$\sqrt{\overline{Vn'^2}}/\overline{Vs}_{local}$	$\sqrt{\overline{Vn'^2}}/\overline{Vs}_{center}$
	1.0	9.52%	9.52%	7.96%	7.96%
	0.5	18.19	14.51	11.24	8.97
	0.25	19.96	14.16	12.20	8.66
ML1	0.10	24.38	14.10	14.16	8.19
	0.05	26.36	13.46	14.46	7.38
	0.0187	23.52	8.29	17.36	6.12
	1.0	9.09	9.09	7.88	7.88
	0.5	15.58	13.38	10.35	8.89
	0.25	19.94	14.67	12.14	8.93
VS	0.10	23.31	15.02	12.79	8.24
	0.05	22.82	13.98	13.76	8.43
	0.0187	21.61	13.20	12.35	7.54
	1.0	9.39	9.39	7.93	7.93
	0.5	15.98	13.78	10.31	8.89
	0.25	21.59	14.84	12.68	8.72
ML2	0.10	24.13	13.46	13.02	7.27
	0.05	24.40	11.22	13.73	6.31
	0.0187	23.07	9.42	12.97	5.30
	1.0	9.20	9.20	8.01	8.01
	0.5	17.56	14.52	10.89	9.00
	0.25	21.15	14.61	12.70	8.77
VL2	0.10	26.54	12.90	15.19	7.38
	0.05	22.64	7.92	15.82	5.53
	0.0187	16.23	5.16	10.34	3.29

TABLE IX-4

$Re_{Max}=2.53*10^5$

Position	y/r	$\sqrt{\overline{Vs'^2}}/\overline{Vs}_{local}$	$\sqrt{\overline{Vs'^2}}/\overline{Vs}_{center}$	$\sqrt{\overline{Vn'^2}}/\overline{Vs}_{local}$	$\sqrt{\overline{Vn'^2}}/\overline{Vs}_{center}$
	1.0	10.00%	10.00%	8.68%	8.68%
	0.5	17.62	14.91	11.82	10.00
	0.25	21.92	15.98	14.16	10.32
ML1	0.10	25.74	15.68	17.26	10.51
	0.05	28.15	15.43	17.77	9.74
	0.0187	38.07	14.65	27.49	10.58
	1.0	9.86	9.86	8.60	8.60
	0.5	17.28	14.53	11.42	9.60
	0.25	21.51	15.70	13.75	10.03
VS	0.10	22.89	15.95	14.61	10.18
	0.05	23.91	16.06	15.83	10.64
	0.0187	22.84	16.20	13.14	9.32
	1.0	9.85	9.85	8.48	8.48
	0.5	17.61	14.24	12.26	9.91
	0.25	21.26	15.33	13.67	9.86
ML2	0.10	27.21	15.78	15.60	9.05
	0.05	28.77	14.09	17.77	8.69
	0.0187	30.76	13.11	17.52	7.47
	1.0	10.49	10.49	9.11	9.11
	0.5	18.19	14.76	12.34	10.01
	0.25	23.79	15.79	15.49	10.28
VL2	0.10	29.26	15.89	17.13	9.31
	0.05	39.59	13.04	24.73	8.15
	0.0187	39.99	10.72	20.83	5.59

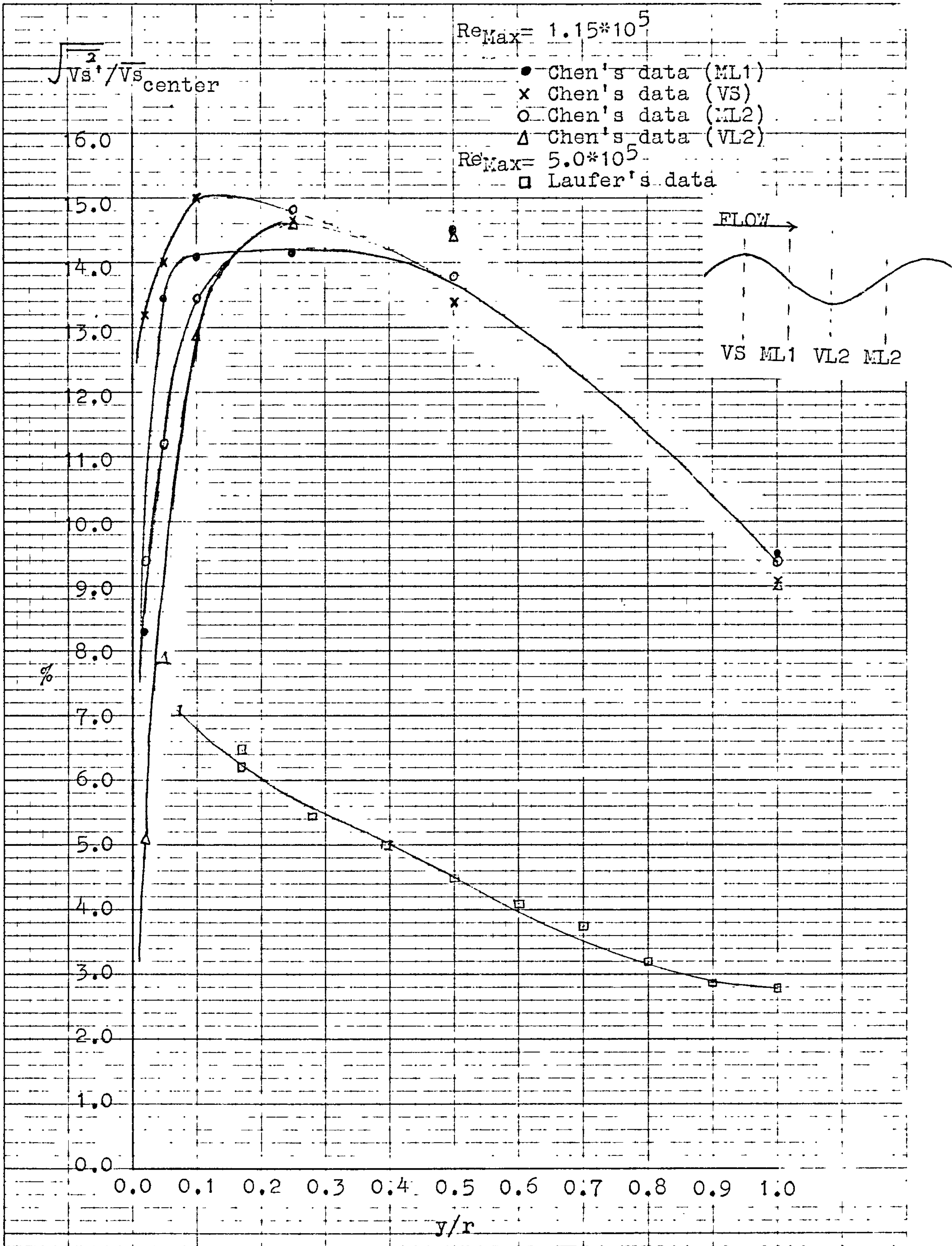

FIGURE IX-5. LONGITUDINAL TURBULENT INTENSITIES RELATIVE TO CENTERLINE MEAN VELOCITY ACROSS FLOW CHANNEL

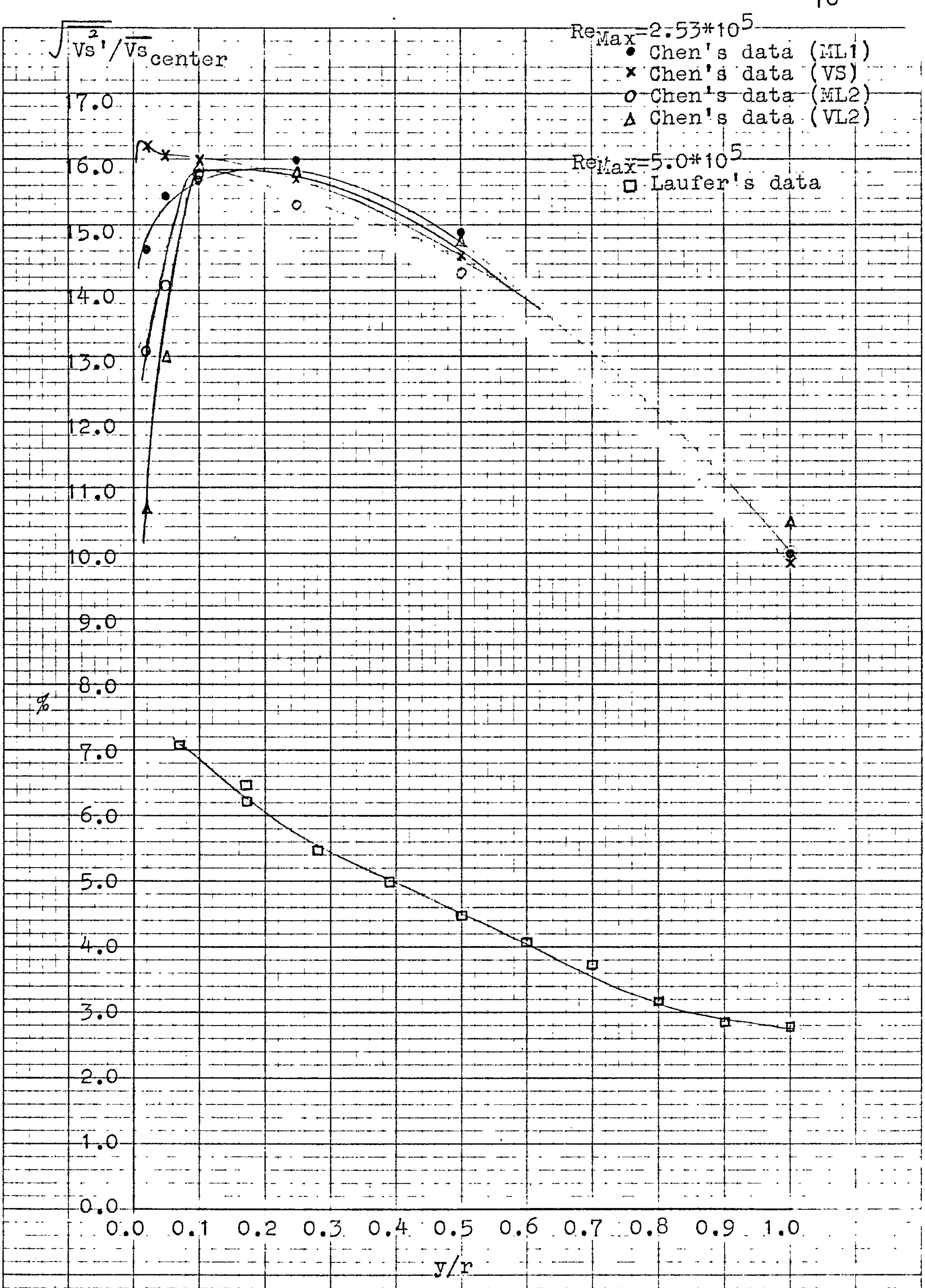

FIGURE IX-6. LONGITUDINAL TURBULENT INTENSITIES RELATIVE TO CENTERLINE MEAN VELOCITY ACROSS FLOW CHANNEL.

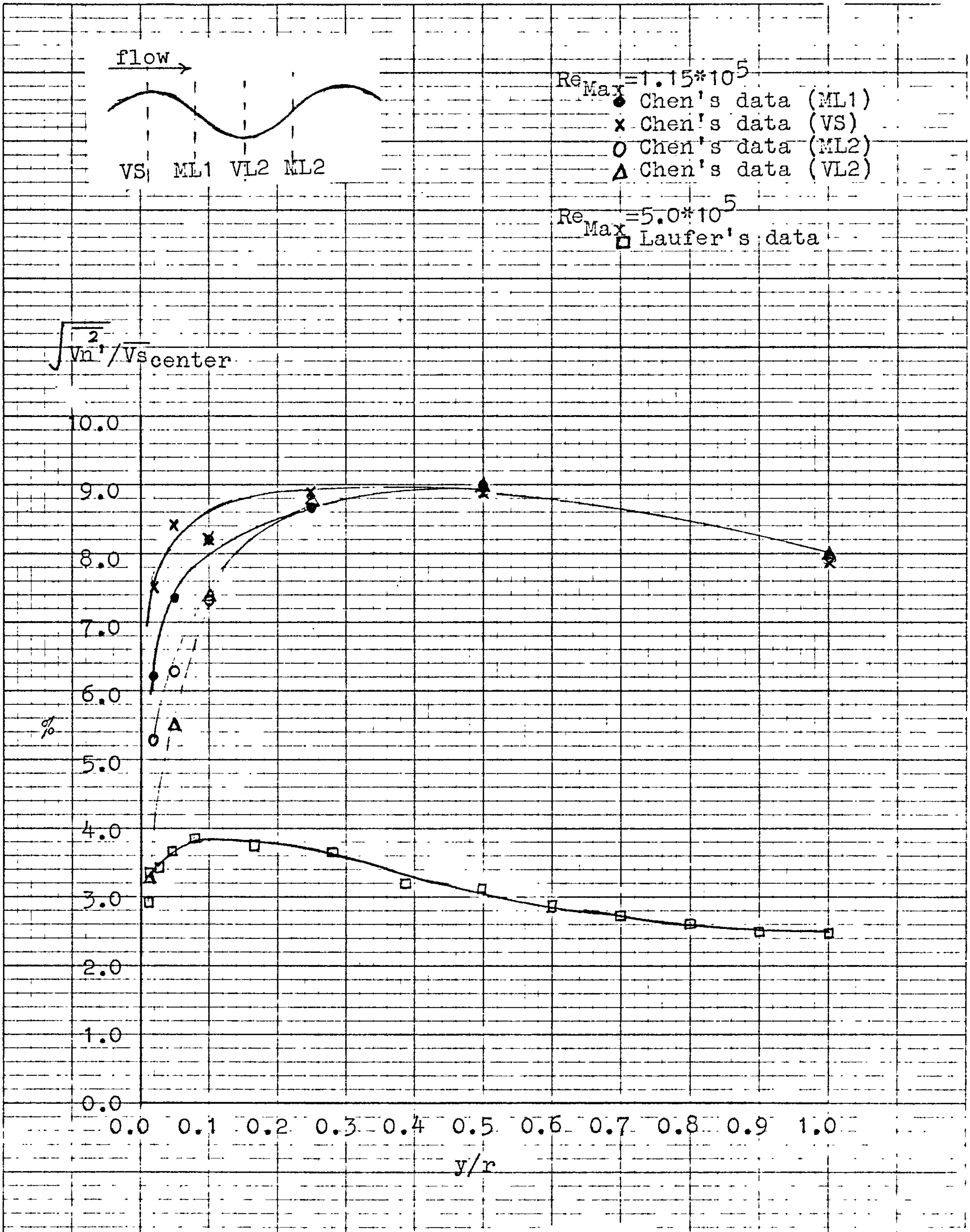

FIGURE IX-7. RADIAL TURBULENT INTENSITIES RELATIVE TO CENTERLINE MEAN VELOCITY ACROSS FLOW CHANNEL.

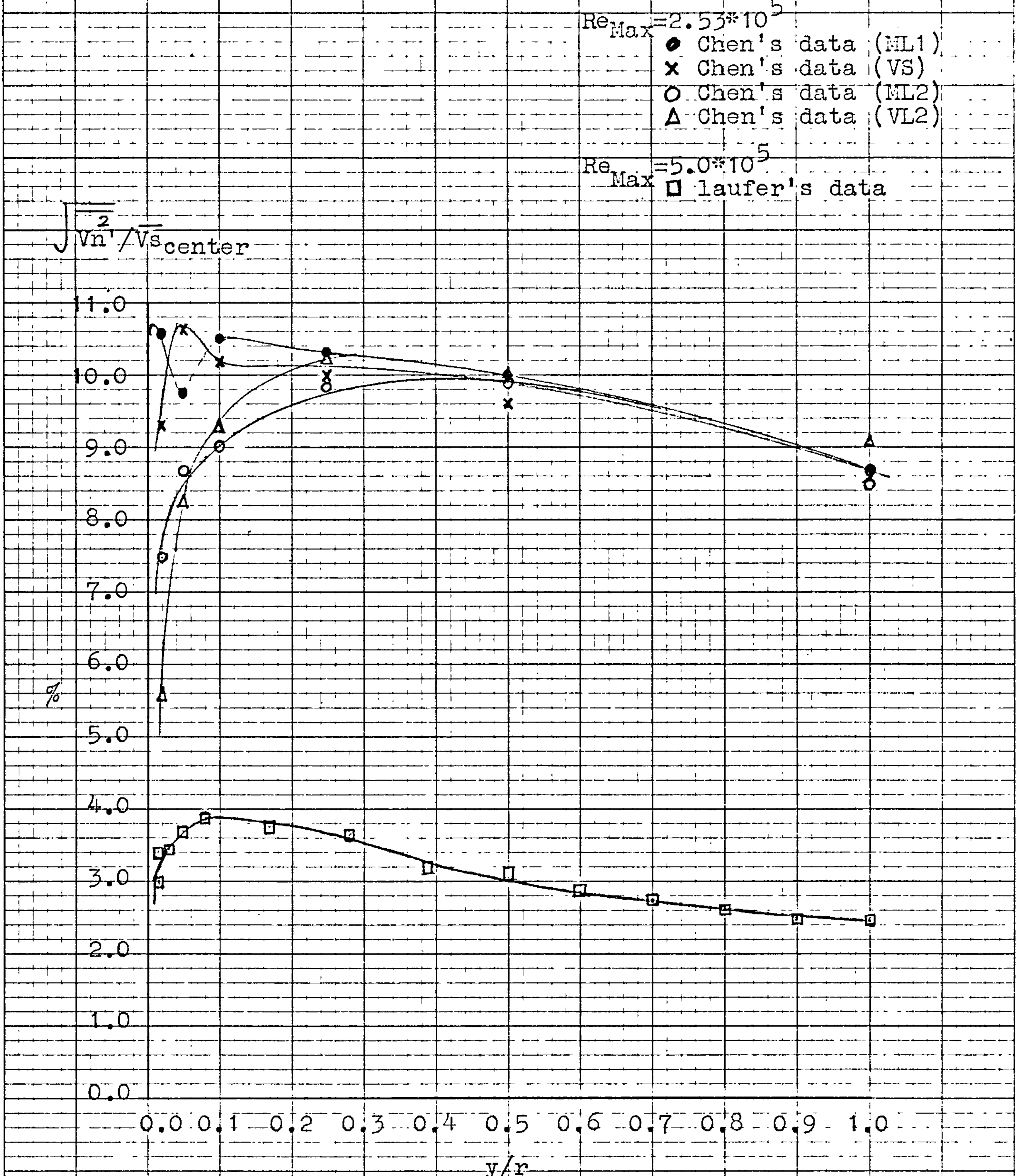

FIGURE IX-8. RADIAL TURBULENT INTENSITIES RELATIVE TO CENTERLINE MEAN VELOCITY ACROSS FLOW CHANNEL.

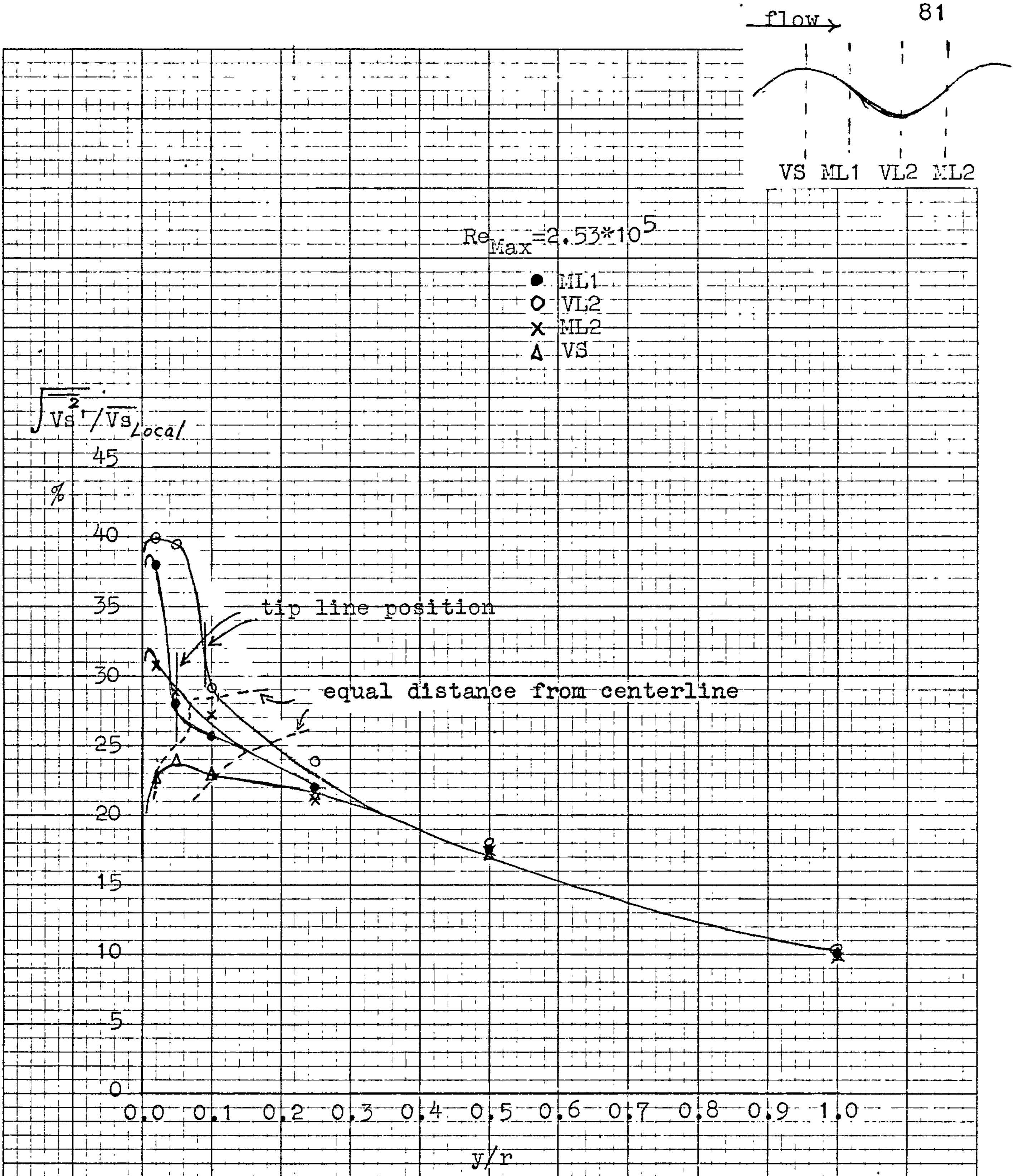

FIGURE IX-9. LONGITUDINAL TURBULENT INTENSITIES RELATIVE TO LOCAL MEAN VELOCITY ACROSS FLOW CHANNEL.

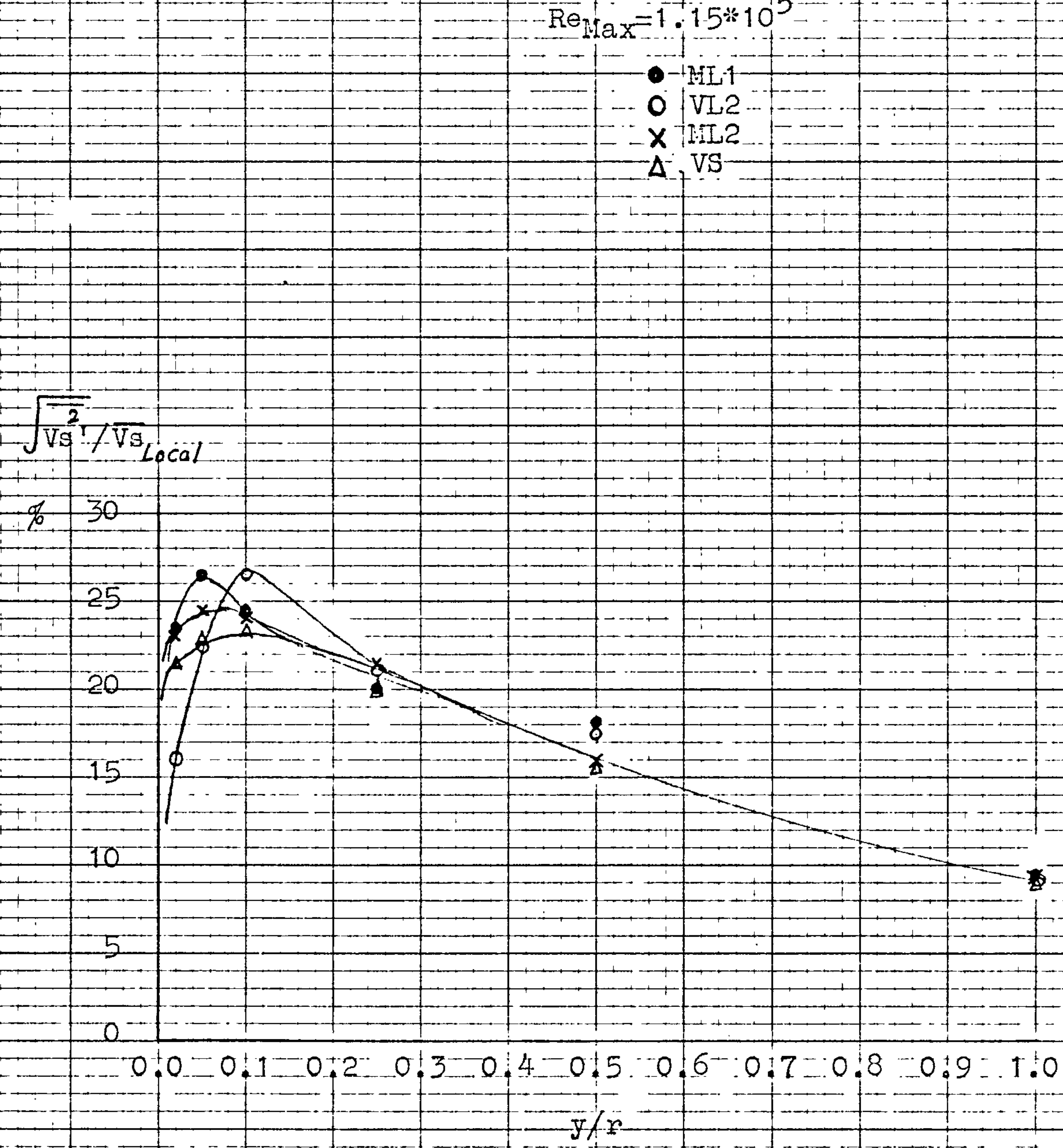

FIGURE IX-10. LONGITUDINAL TURBULENT INTENSITIES RELATIVE TO LOCAL MEAN VELOCITY ACROSS FLOW CHANNEL.

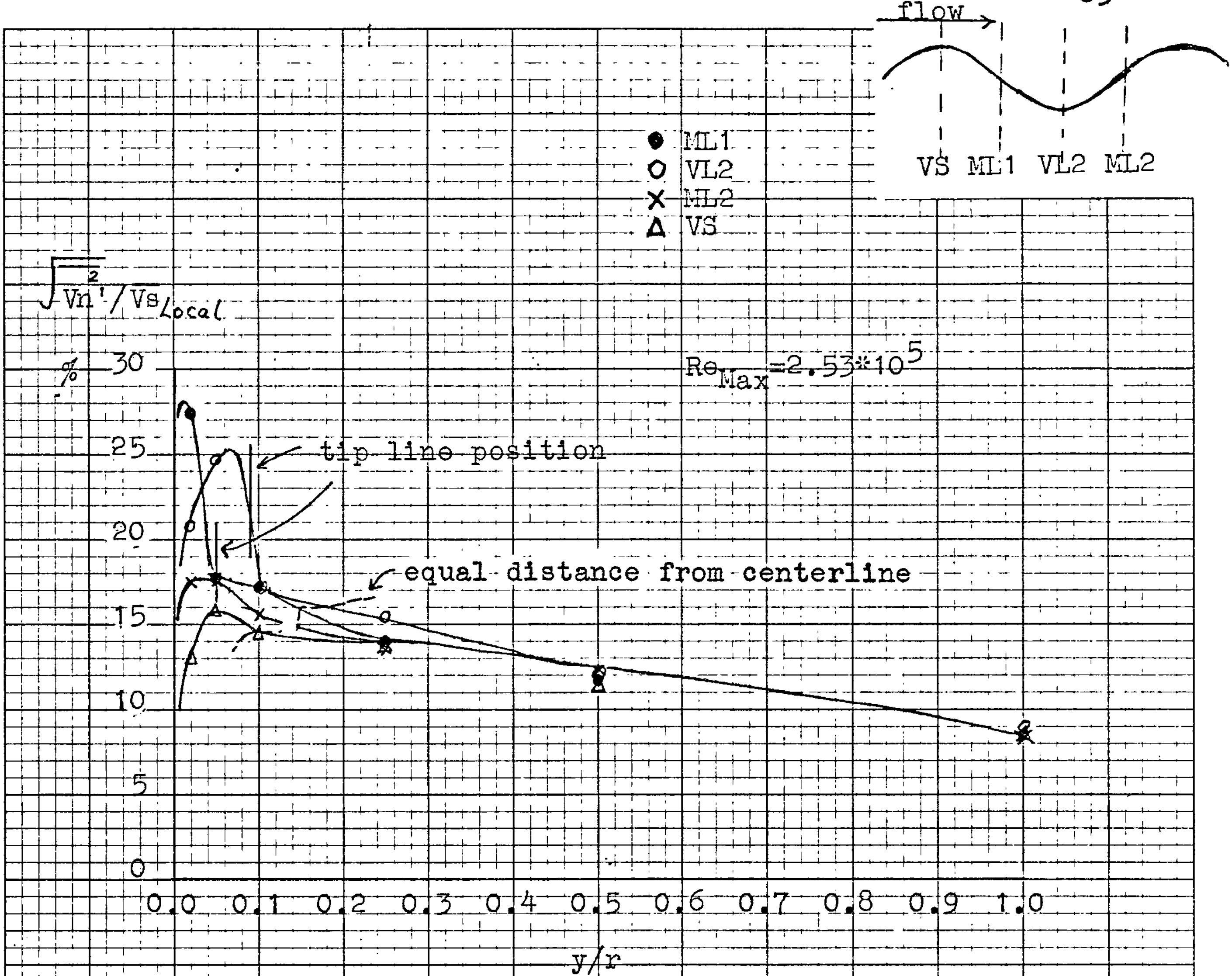

FIGURE IX-11. RADIAL TURBULENT INTENSITIES RELATIVE TO LOCAL MEAN VELOCITY ACROSS FLOW CHANNEL.

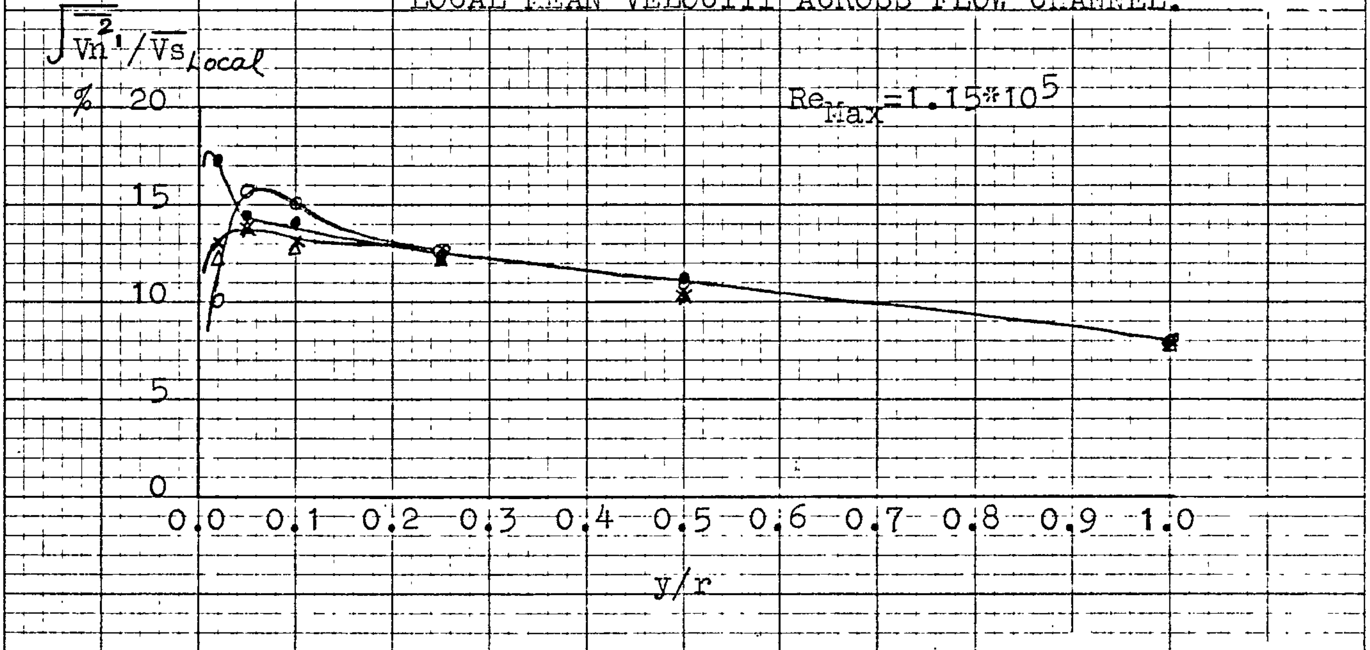

FIGURE IX-12. RADIAL TURBULENT INTENSITIES RELATIVE TO LOCAL MEAN VELOCITY ACROSS FLOW CHANNEL.

y/r=0.05 for ML1 section and at y/r=0.1 for VL2 section. This sharp increase in local relative turbulent intensity occurs around the tip line (the line connecting the tips of the peaks). This will be discussed latter in section F.

Another relative turbulent intensity calculated is one based on the friction velocity, V*, for $Re_{Max}=2.53*10^5$. This friction velocity, V*, calculated was based on the total average shear stress which is discussed in section C. This relative turbulent intensity data are plotted in Figure IX-13 and IX-14. They are compared to the Laufer's data.[19]

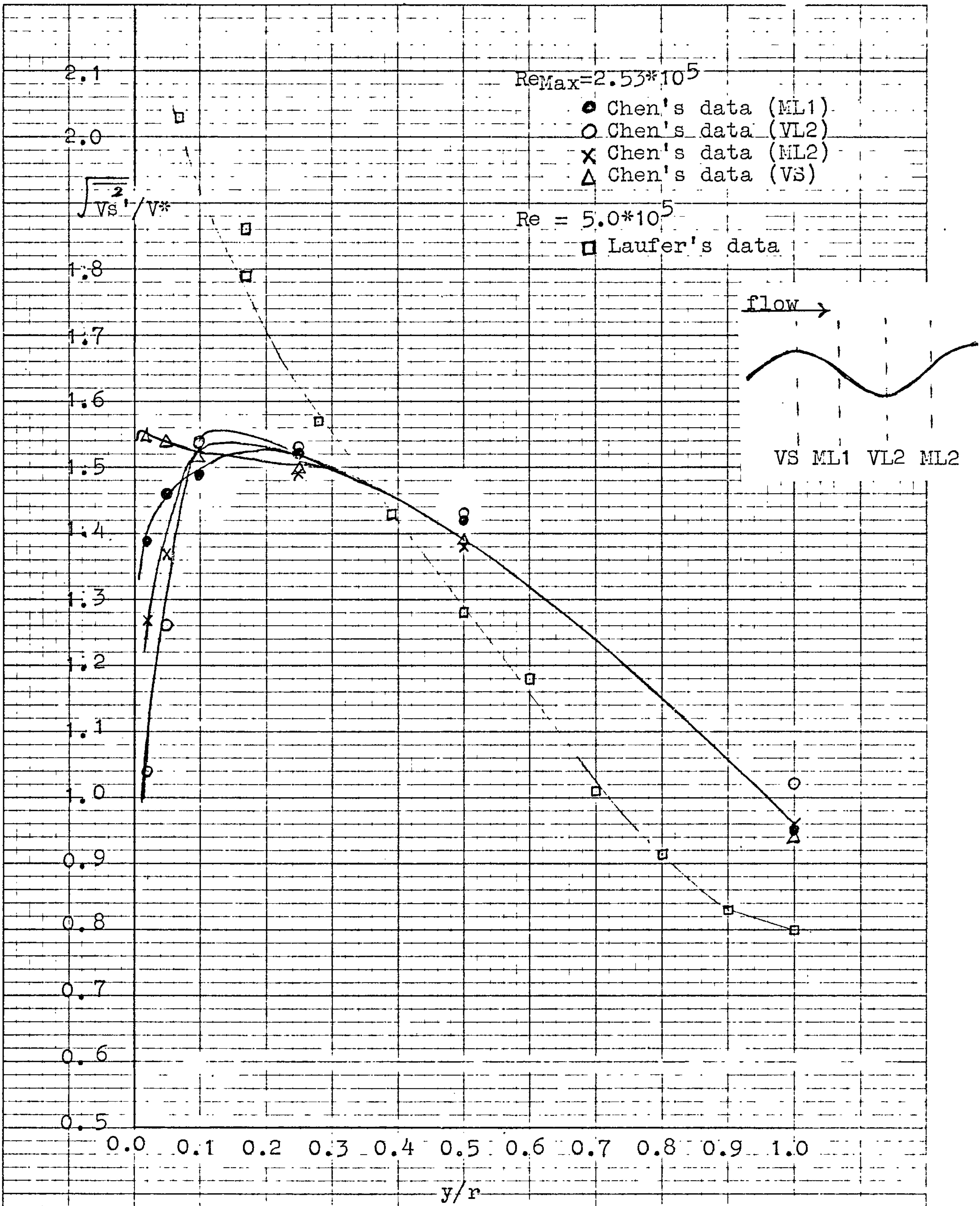

FIGURE IX-13. LONGITUDINAL TURBULENT INTENSITIES RELATIVE TO FRICTION VELOCITY ACROSS FLOW CHANNEL.

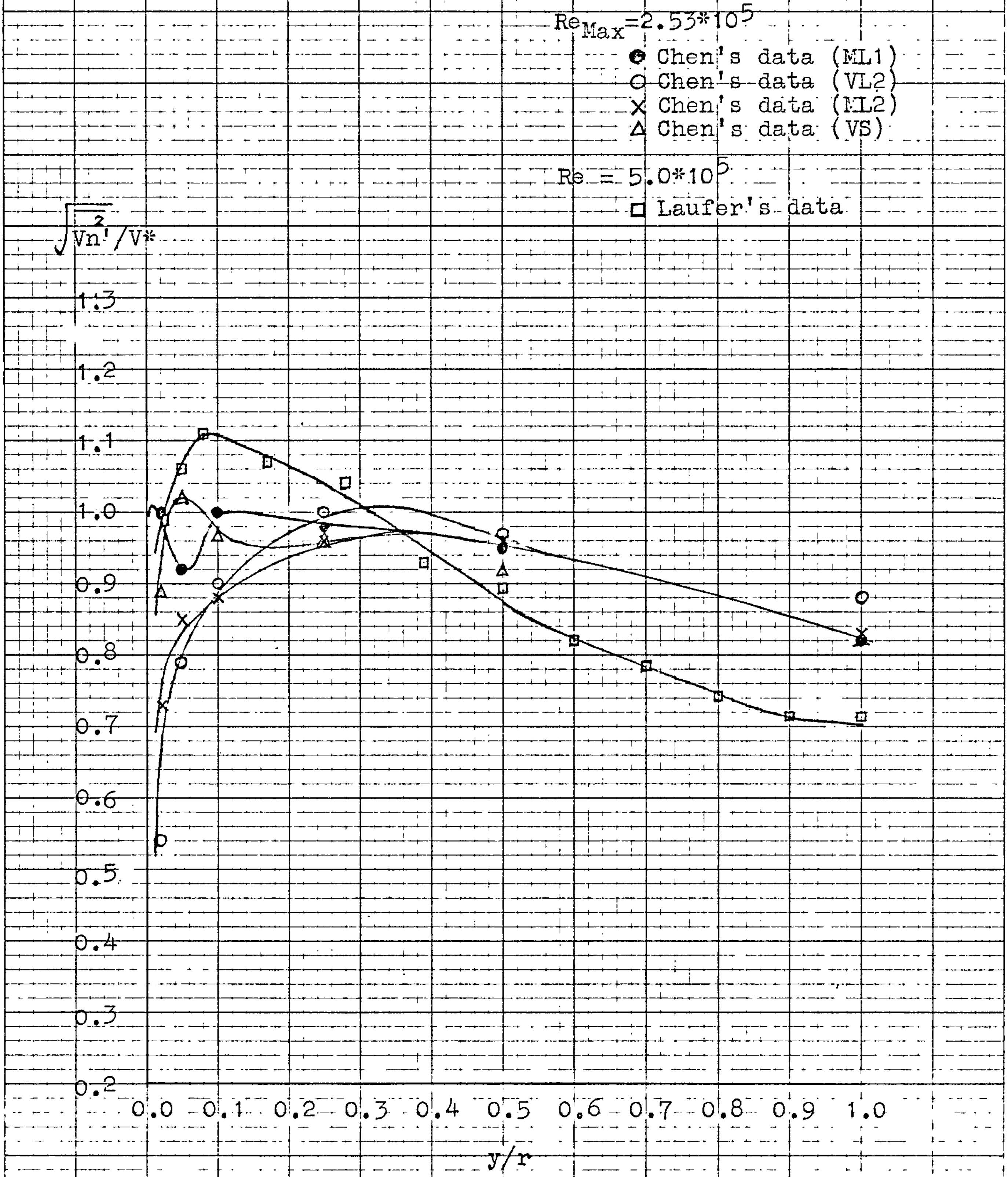

FIGURE IX-14. RADIAL TURBULENT INTENSITIES RELATIVE TO FRICTION VELOCITY ACROSS FLOW CHANNEL.

C. Turbulent Shear Stress Distribution

The measured turbulent shear stress data are tabulated in Table IX-1 and Table IX-2, and are also plotted in Figure IX-15 and Figure IX-16. From y/r=1.0 to y/r=0.5 the distributions coincide with each other for all sections of the roughness. Closer to the wall there is significant influence of section location. The ML1 curve has a very peculiar behavior. This observation along with the trend of $\overline{Vs}$, $\overline{Vn}$, $\sqrt{\overline{Vs'^2}}/\overline{Vs}_{local}$ and $\sqrt{\overline{Vn'^2}}/\overline{Vs}_{local}$ curves suggests a particular type of fluid motion and this will be discussed latter.

For a smooth circular pipe, the total shear stress equation[20] is,

$$\tau = -\left(\frac{\Delta P}{\Delta L}\right)\frac{D}{4} \qquad \text{(IX-1)}$$

where $\Delta P/\Delta L$ is pressure drop along longitudinal, S, direction, and D is pipe diameter. But one asks,"is there a similar equation which exists for corrugated pipe?"

The force acting on the control volume is given by the flux of momentum summed over the entire control volume surface and the rate of change of the momentum within the volume,

$$\frac{1}{g_c}\iint_{As}\overline{Vs}\,\rho\, V_I\cdot\cos\alpha_e\, dAs+\frac{d}{d\theta}\iiint_V\frac{\overline{Vs}\,\rho}{g_c}dV = Fsr-Fsp-Fsd$$

where Fsr = the external force in longitudinal, S, direction acting on the solid boundary of the volume

Fsp = the pressure force in S-direction

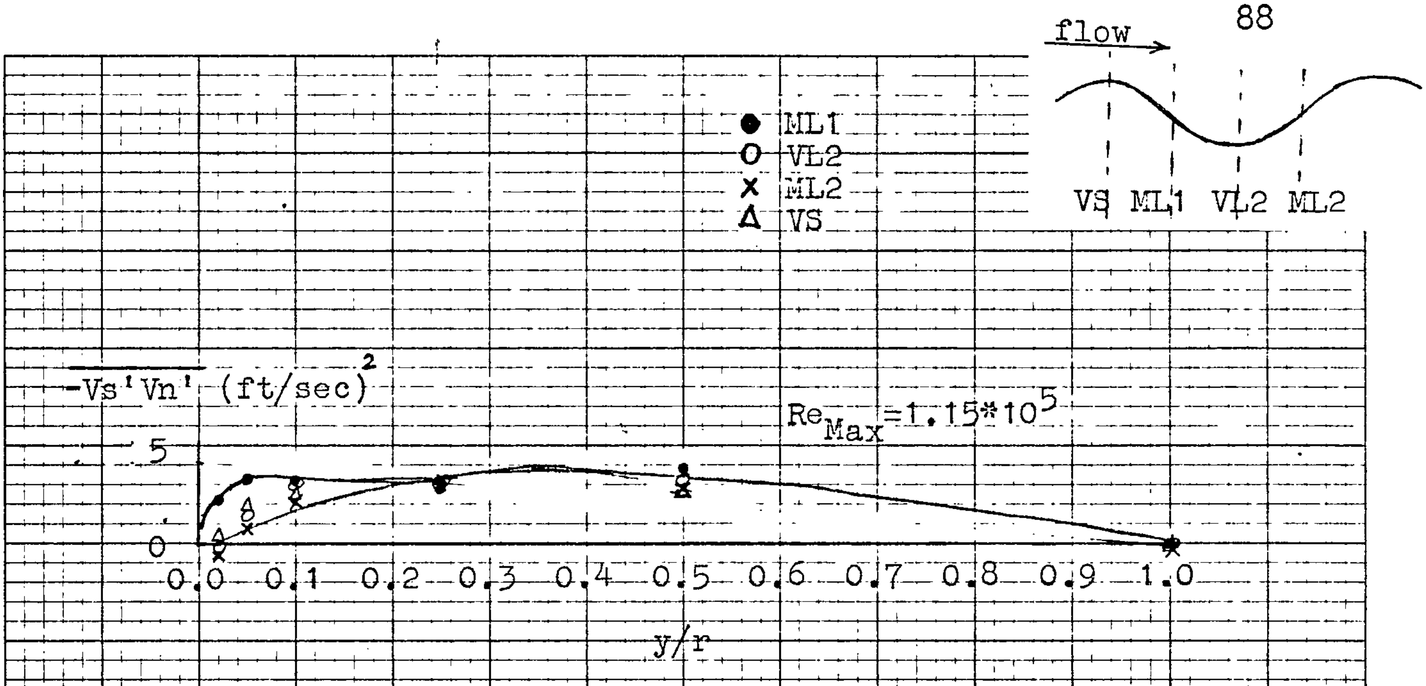

FIGURE IX-15. REYNOLD' SHEAR STRESS ACROSS FLOW CHANNEL.

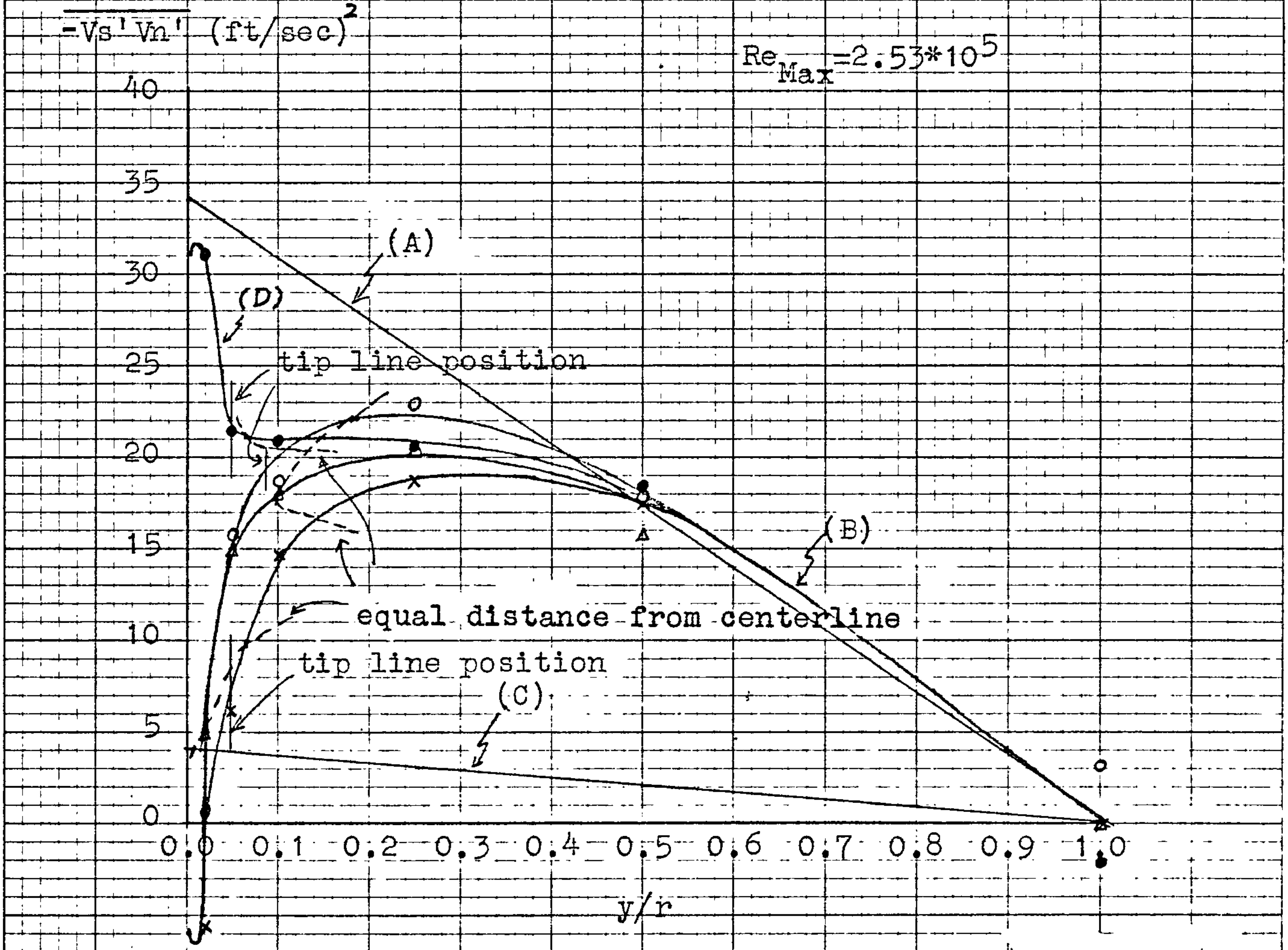

FIGURE IX-16. REYNOLD' SHEAR STRESS ACROSS FLOW CHANNEL.

Fsd = the shear stress caused by viscosity

α_e = angle between V_I and S-direction

As = surface area normal to the S-direction

V = control volume

At steady state, $\frac{d}{d\theta}\dot{-}=0$, and the control surfaces taken within the fluid or at its boundary, $Fsr=0$,

therefore,

$$\frac{1}{g_c}\iint_{As} \overline{Vs}\rho V_I \cdot \cos\alpha_e \, dAs = -Fsp-Fsd$$

If the condition is chosen at same cross-sectional area, we have,

$$\frac{1}{g_c}\iint_{As} \overline{Vs}\rho V_I \cdot \cos\alpha_e \, dAs = 0$$

therefore,

$$Fsp = -Fsd$$

Shear stress is tangential to curve surface at every point so that the shear stress at S-direction is

$$\tau_s = \tau * \cos\alpha_a$$

where α_a is the angle between the tangent to the wall boundary and the longitudinal, S, direction. The total drag force of length ΔL in S-direction is,

$$\tau_{total} = \int_{L_1}^{L_2} \tau \cdot \cos\alpha_a \cdot 2\pi r \, dS$$

where $r=f(s)$ and (L_1-L_2)=wave length or its multiple.

Define an average total shear stress of length $\Delta L(=L_1-L_2)$

$$\bar{\tau} = \frac{1}{2\pi\bar{r}(\Delta L)}\int_{L_1}^{L_2} \tau \cdot \cos\alpha_a \cdot 2\pi r ds$$

Where $r=(r_0+r_1)/2$ and r_1 is the radius at VL2 section, r_0 is the radius at VS section (see Figure IX-17).

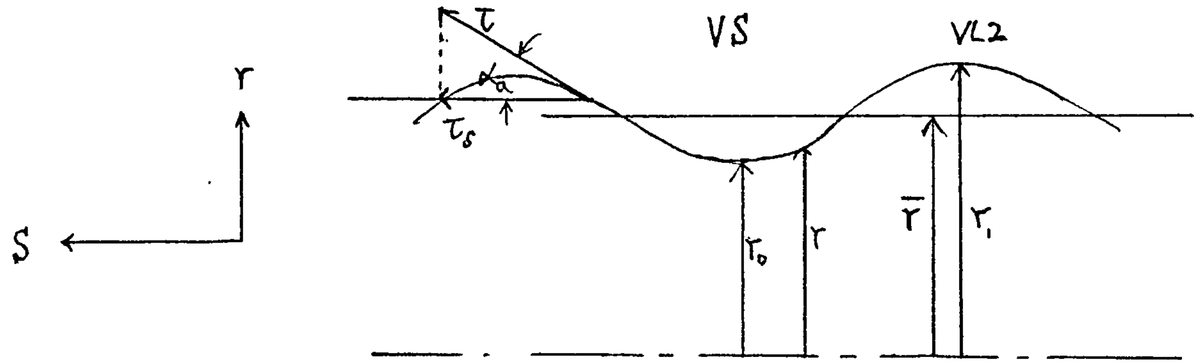

FIGURE IX-17. SHEAR STRESS COMPONENT DIAGRAM.

The pressure force, Fsp, at the corresponding area with radius r is,

$$Fsp = (-\Delta p)(\pi \bar{r}^2)$$

therefore,

$$(-\Delta p)(\pi \bar{r}^2) = 2\pi \bar{r}(\Delta L)\cdot\bar{\tau}$$

or,

$$\bar{\tau} = -\left(\frac{\Delta p}{\Delta L}\right)\left(\frac{\bar{r}}{2}\right) \qquad \text{(IX-2)}$$

This equation is very similar to equation (IX-1).

The wall shear stress is different along a wave length because the velocity profile at every cross-section at every point is different. The average pressure drop measured at $Re_{Max}=2.53*10^5$ is 0.00670 inH_2o/in which gives $\bar{\tau}=0.0783(lb_f/ft^2)$ or $V*^2=34.1$ $(ft/sec)^2$. Connecting $V*^2=34.1(ft/sec)^2$ at $y/r=0.0$ and $V*^2=0.0$ at $y/r=1.0$ gives a straight line which represents the average total shear stress curve. Observe that from $y/r=1.0$ to $y/r=0.5$ measured values of turbulent shear stress coincide with this line but closer to the wall the turbulent shear is significantly lower. For a smooth circular pipe with the diameter $2\overline{r}$, and with the empirical equation, $f=0.046R_e^{-\frac{1}{5}}$ and $V^*=V_b\sqrt{f/2}$ (21) where f is the friction factor and V_b is bulk average velocity, and for VL2 section with $V_b=42$ ft/sec, we have $V^{*2}=4.07$. Connecting $V^{*2}=4.07$ at $y/r=0.0$ and $V^{*2}=0.0$ at $y/r=1.0$ represents the total shear stress curve for a smooth pipe then it is seen that the shear stress from smooth circular pipe is much less than that from the corrugated pipe.

If we let,

$$\tau^{\text{total}} = \tau^{\text{turbulent}} + \tau^{\text{laminar}} + \tau^{\text{2nd}}$$

where τ^{2nd} is the shear stress caused by secondary flow, then the difference between curve A and curve C is caused by corrugations (see Figure IX-16). From $y/r=1.0$ to $y/r=0.5$ curve A and curve B almost coincide, this means that far from the wall the particular slope of the wall has no effect. This is completely reasonable since the core region "sees" an average of the local behavior and that connected from upstream locations. From $y/r=0.5$ to $y/r=0.0$ the difference between curve A and curve B is τ^{laminar} and τ^{2nd}. However, since τ^{laminar} is very small, we can regard this difference as due to τ^{2nd} only.

D. Energy Spectrum Measurement

The hot wire signal were processed through a hybrid digitizing and power spectrum program. (see Appendix E) These auto-power-spectrum measured at $Re_{Max}=2.53*10^5$ are plotted in Figure IX-20 through IX-31 and are presented as normalized values, $F_i(k_w)$, where $F_i(k_w)=E_i(k_w)/\overline{V_i^{2}}'$ in i-direction, k_w is the local wavenumber defined as $2\pi f/\overline{Vs}_{local}$, and f is the frequency.

In Figure IX-18, we compare the longitudinal centerline data made at the VS section to the Laufer's data.[19] We see that both sets of data have the same -5/3 power of the wavenumber, k_w, over a considerable range. But the Laufer's curve is lower than the VS one. This means that there is less longitudinal turbulent energy in Laufer's data. This is because the smooth circular pipe generates less longitudinal turbulent energy then does the corrugated pipe. If we plot this same data in dimensionless form as in Figure IX-19, we notice that when frequency approaches zero, the value $(\overline{Vs}\cdot E_s(f)/\overline{Vs^{2}}'\cdot \Lambda_f)=4.0$ agrees very satisfactorily with experimental data obtained from extrapolation of the measured $E_s(f)$ curve.

Figure IX-20 through IX-25 show that the spectrum is independent of position along the wall in the center region from y/r=1.0 to y/r=0.25. Thus $E_s(k_w)$ is the same for all four sections. However, the spectrum does depend on position, y/r.

The energy spectrum measurements have a bandwith of 32 cps and a record length of 3.75 sec which gives 240 degree of freedom. Thus there is a 90% confidence of the true value within 8.70 and 11.3.[27]

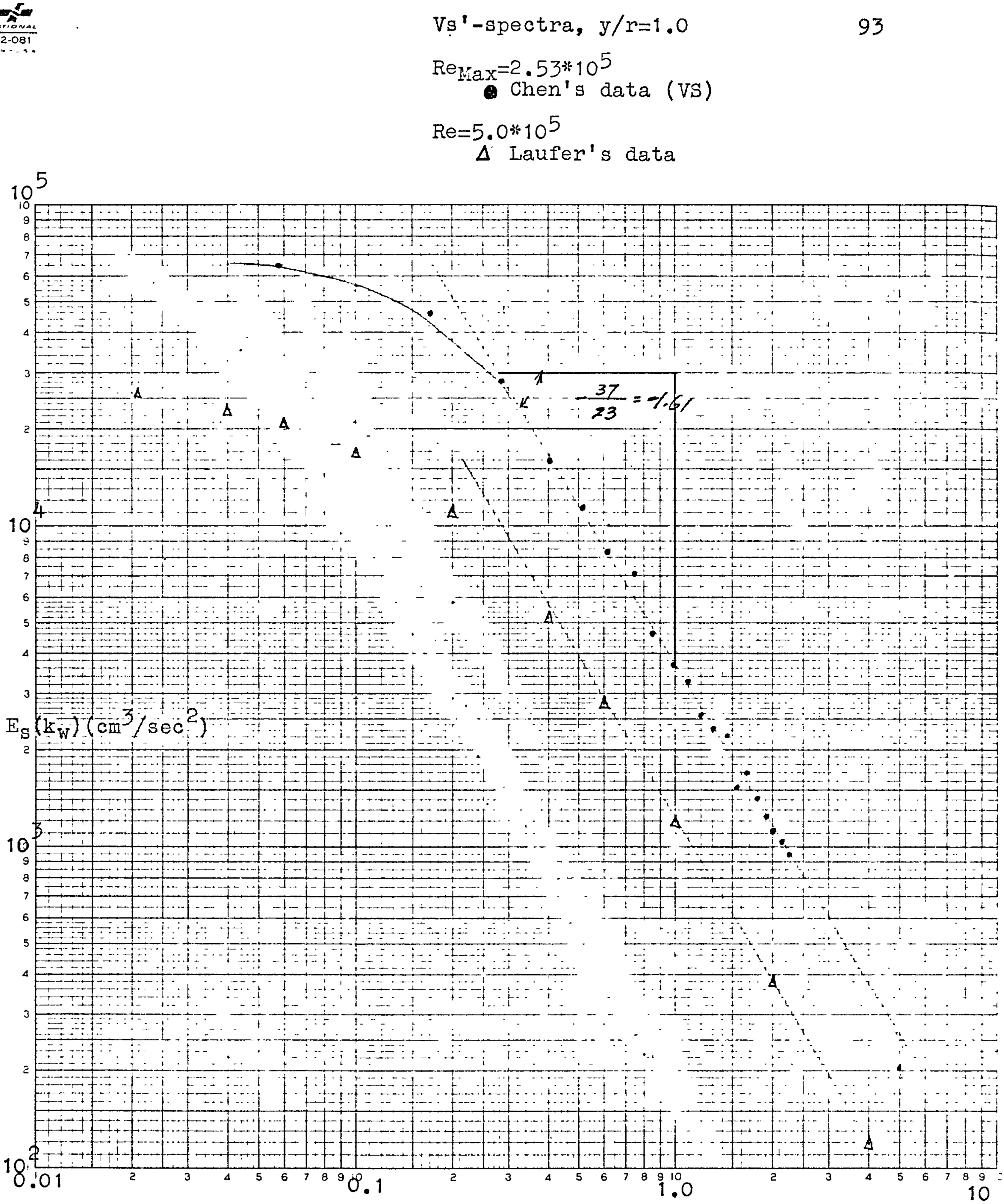

FIGURE IX-18. COMPRISON OF LAUFER'S AND CHEN'S DATA FOR Vs' AT y/r=1.0

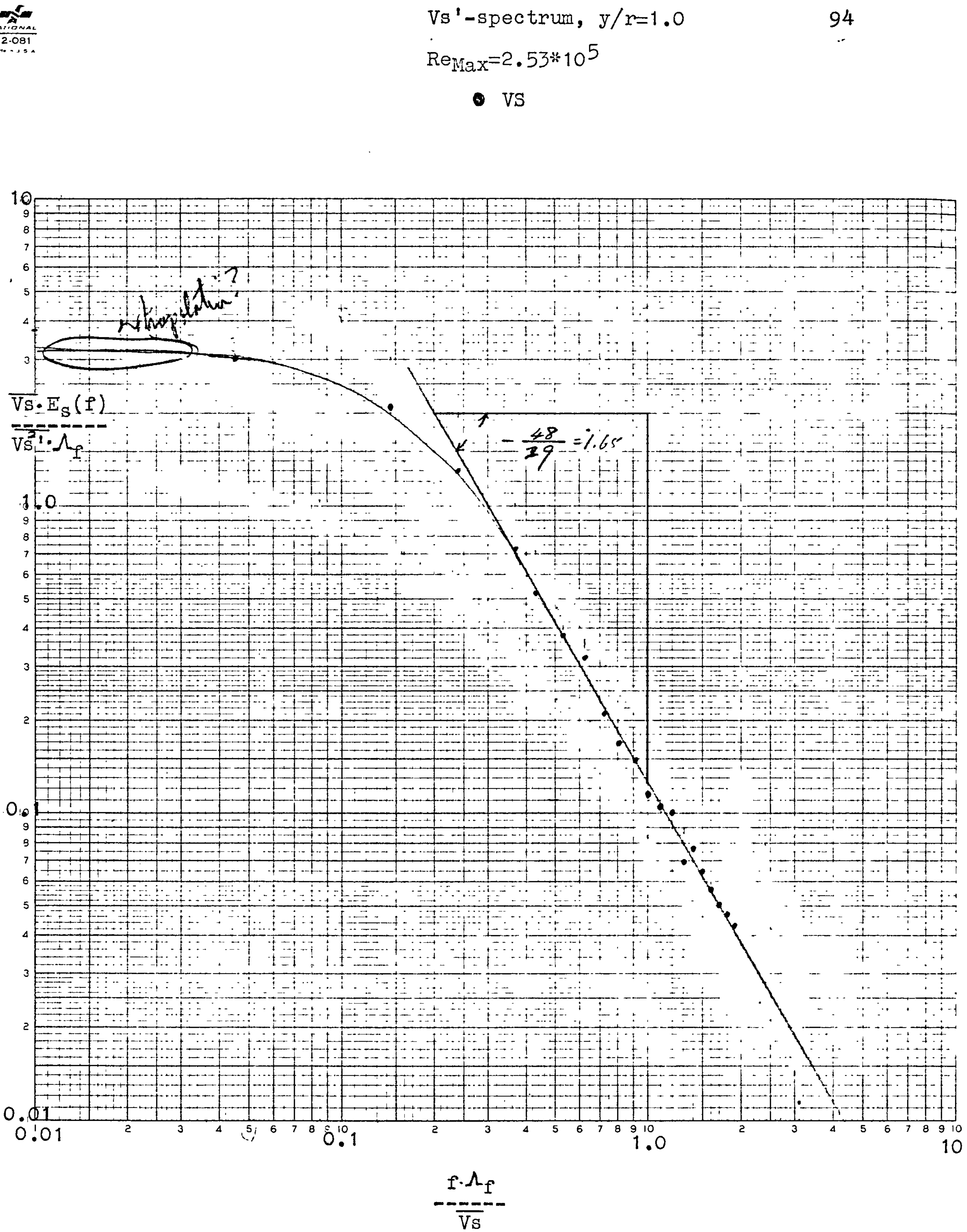

FIGURE IX-19, Vs'-SPECTRUM IN DIMENSIONLESS FORM.

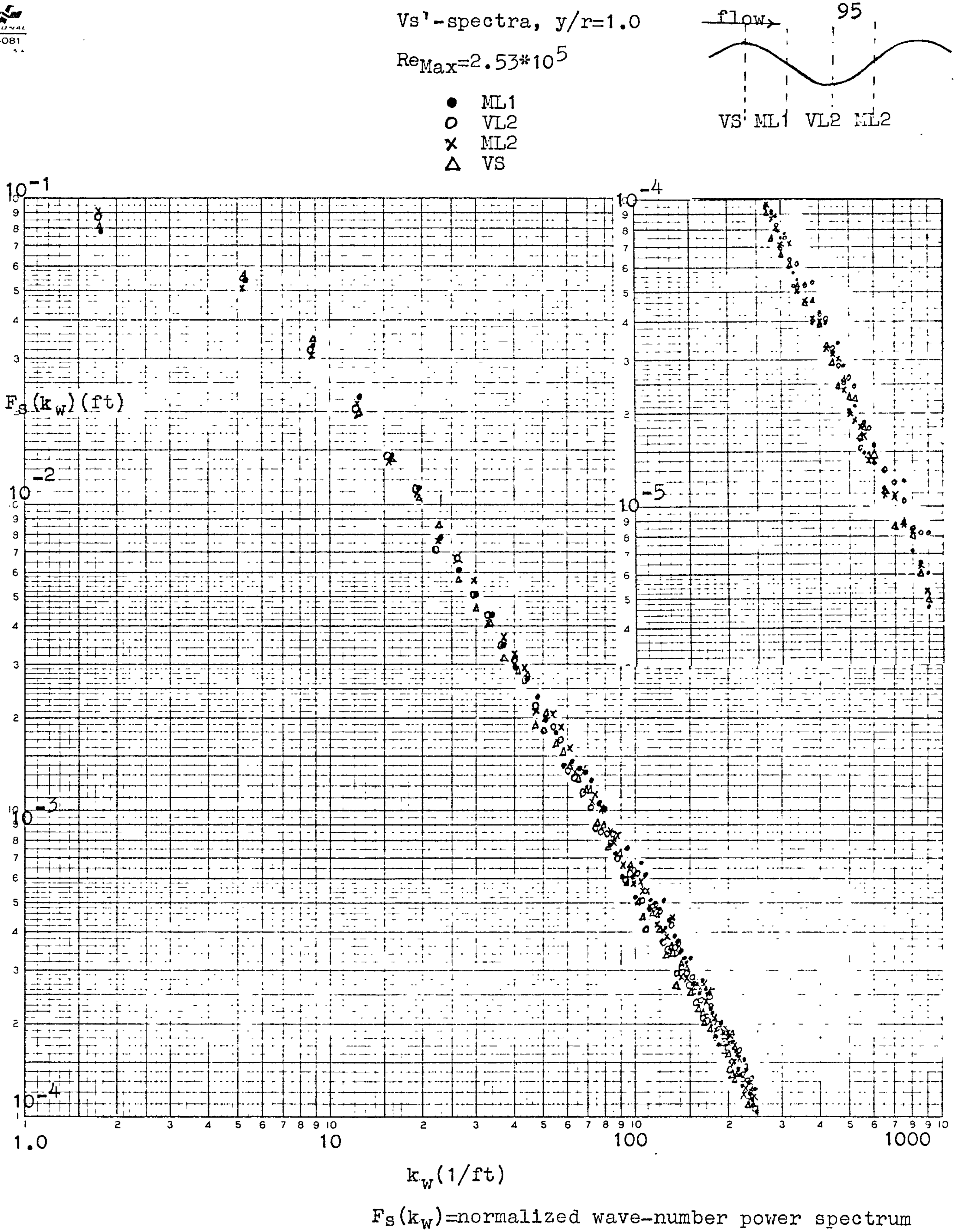

FIGURE IX-20. Vs'-SPECTRUM AT y/r=1.0

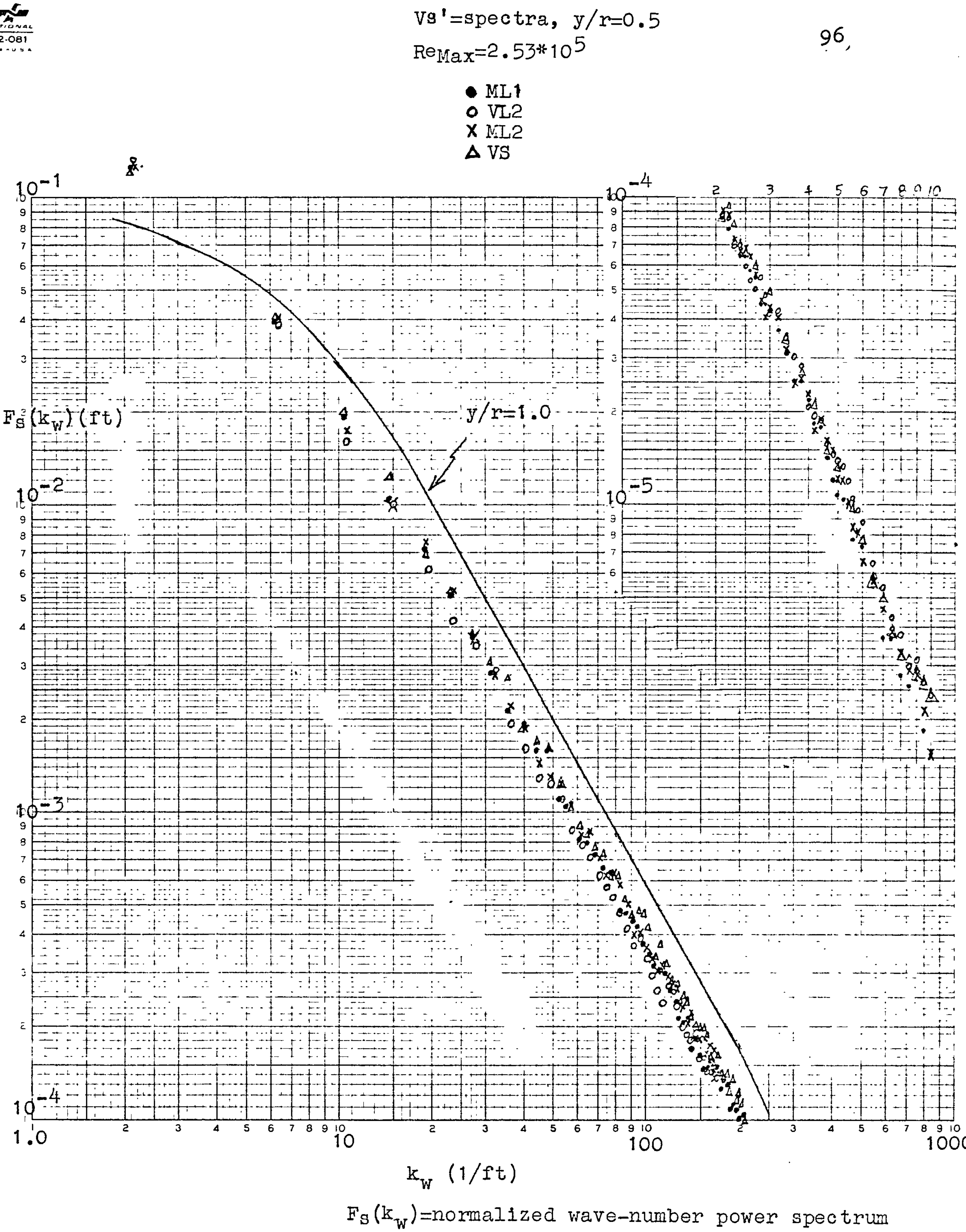

FIGURE IX-21. Vs'-SPECTRUM AT y/r=0.5

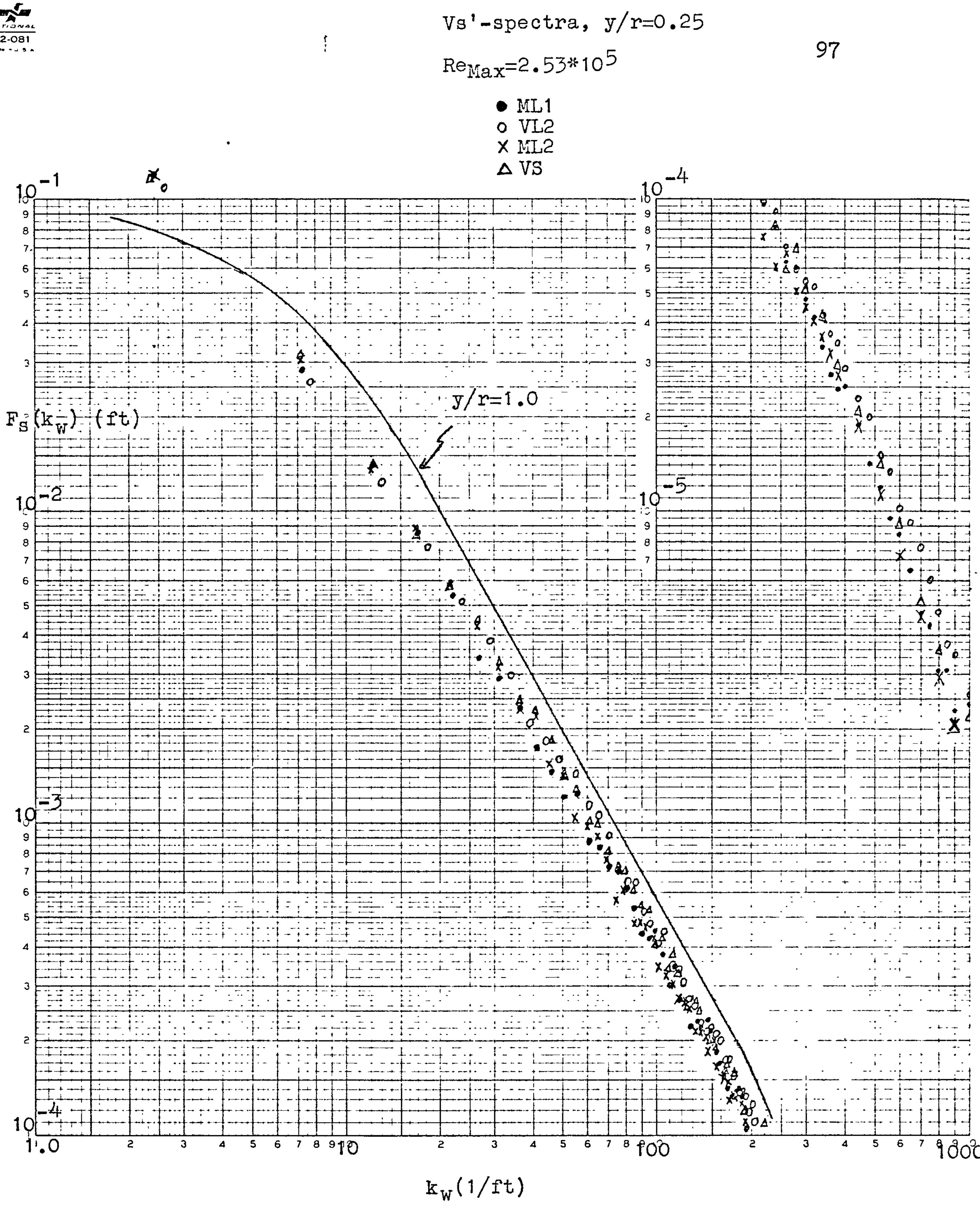

FIGURE IX-22. Vs'-SPECTRUM AT y/r=0.25

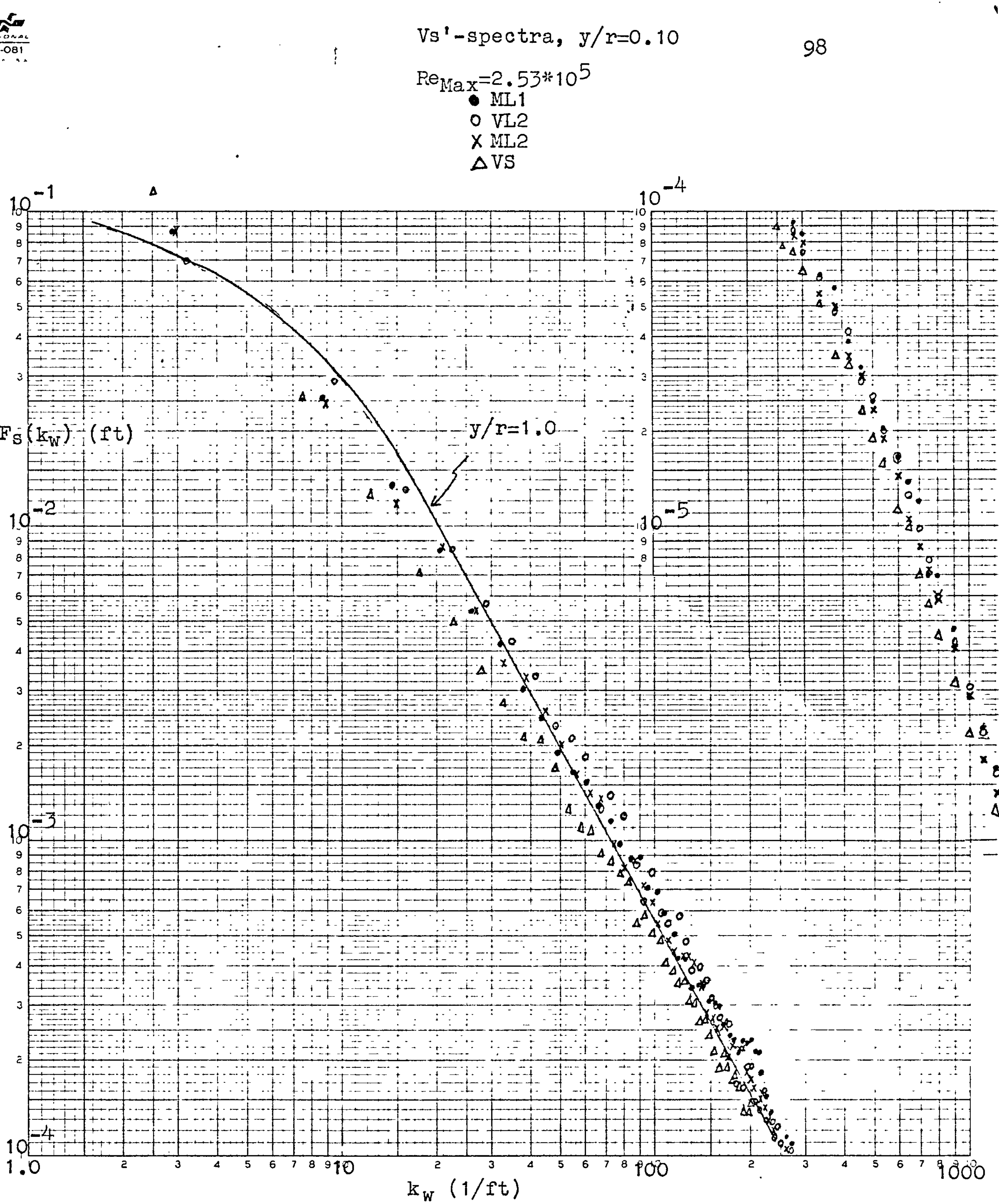

$F_s(k_w)$=normalized wavenumber power spectrum

FIGURE IX-23. Vs'-SPECTRUM AT y/r=0.10

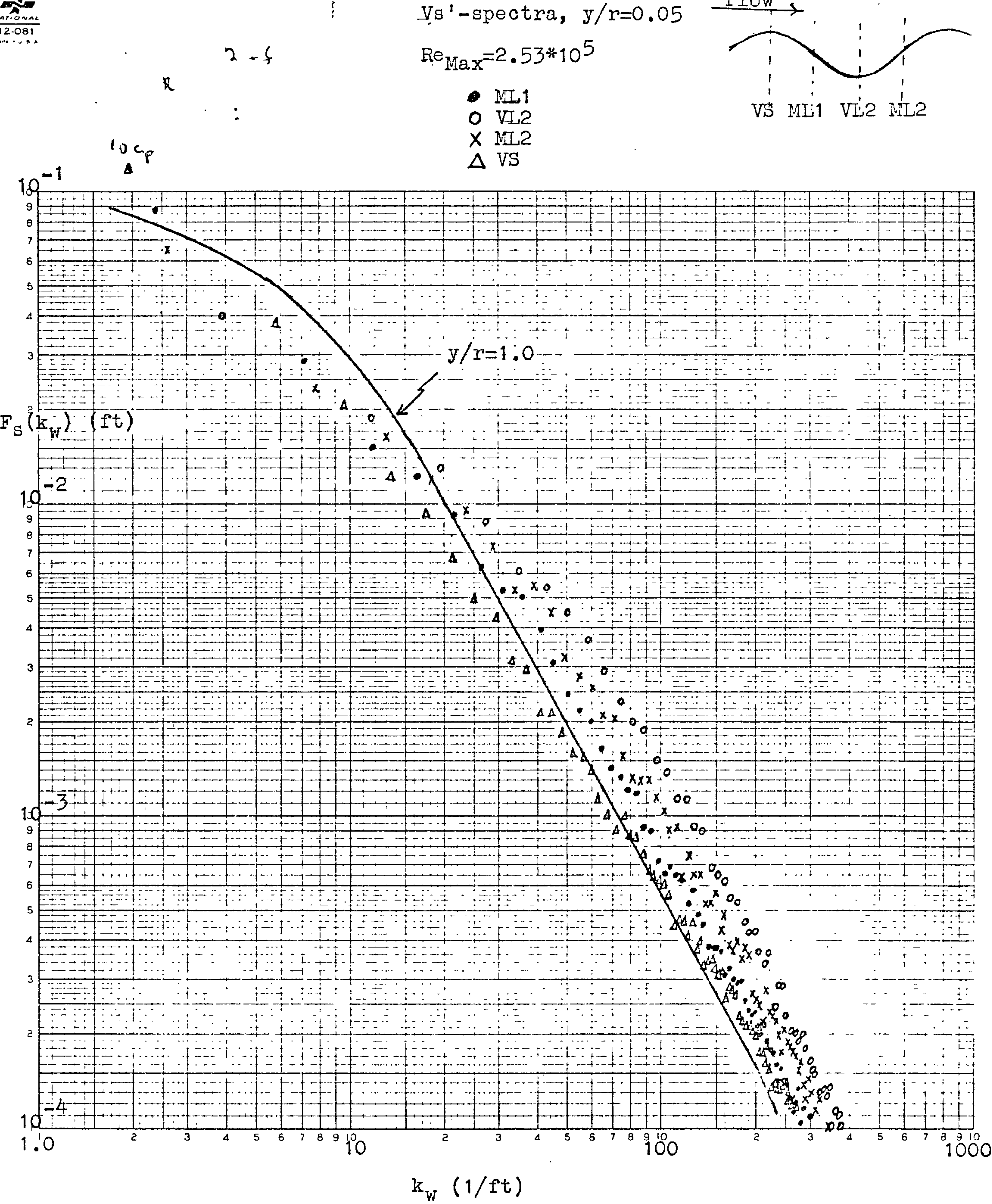

$F_s(k_w)$=normalized wavenumber power spectrum

FIGURE IX-24. Vs'-SPECTRUM AT y/r=0.05

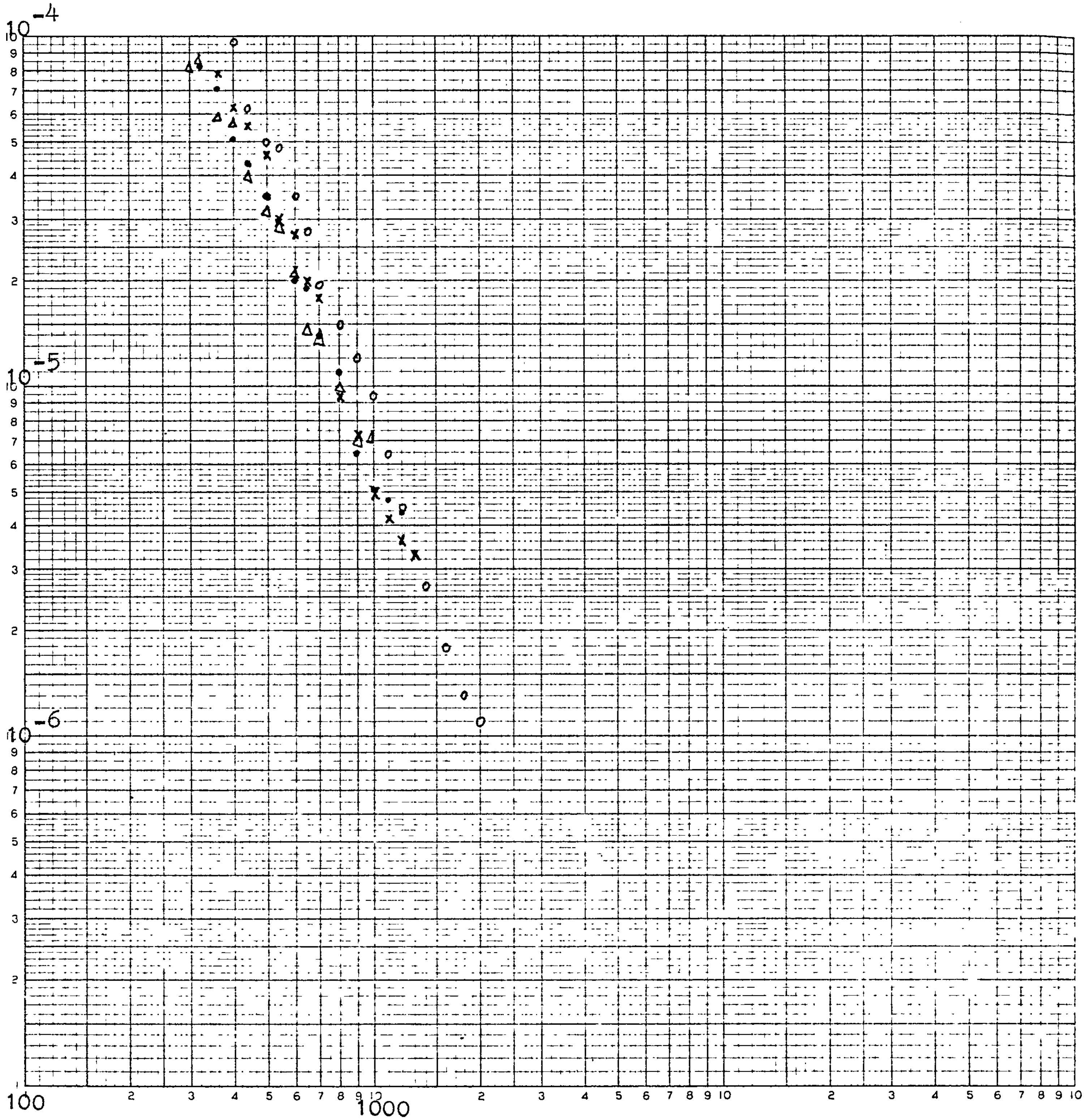
10^{-4}
10^{-5}
10^{-6}
100
1000

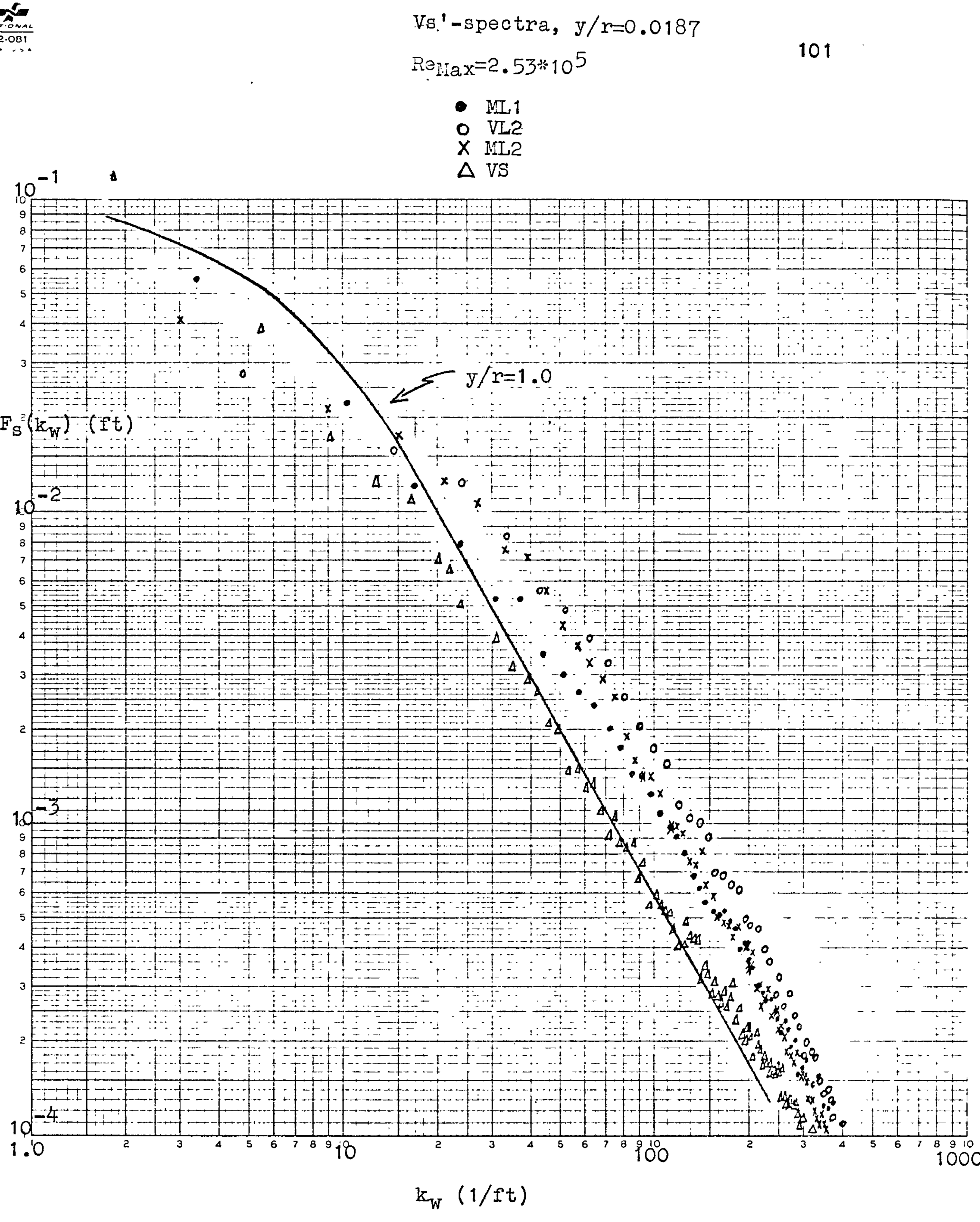

$F_s(k_w)$=normalized wavenumber power spectrum

FIGURE IX-25. Vs'-SPECTRUM AT y/r=0.0187

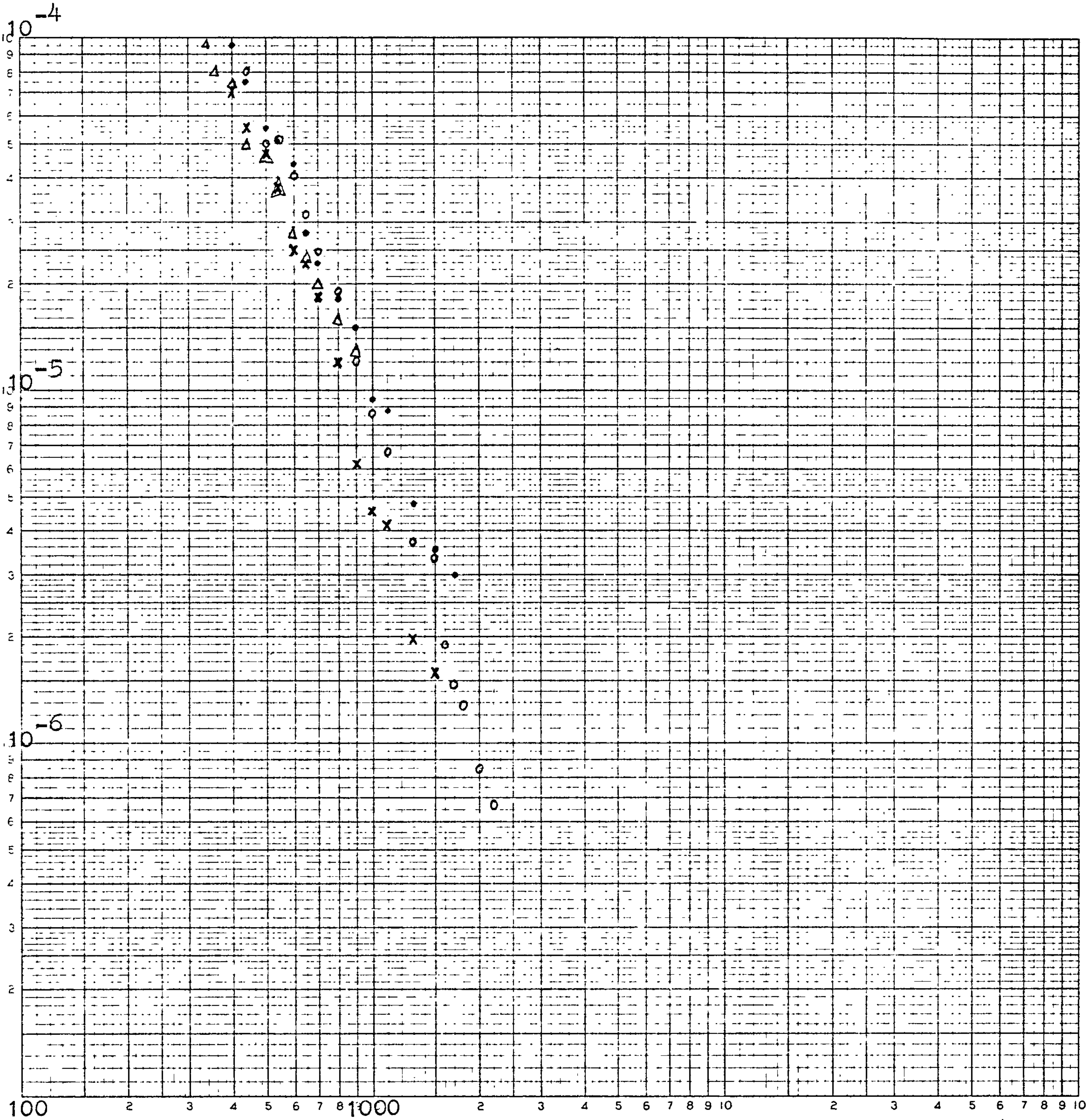
10^-4
10^-5
10^-6
100
1000

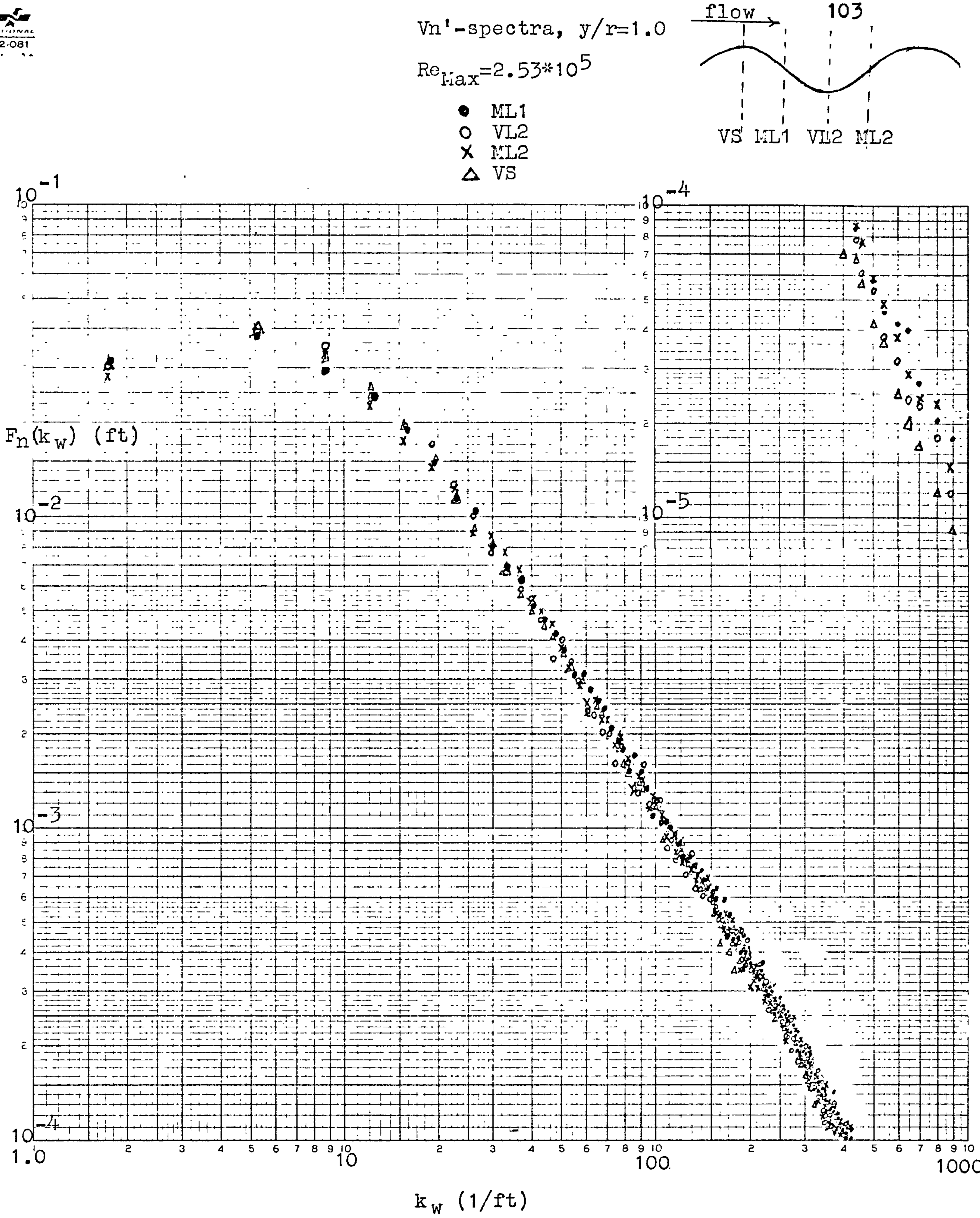

$F_n(k_w)$=normalized wavenumber power spectrum

FIGURE IX-26. Vn'-SPECTRUM AT y/r=1.0

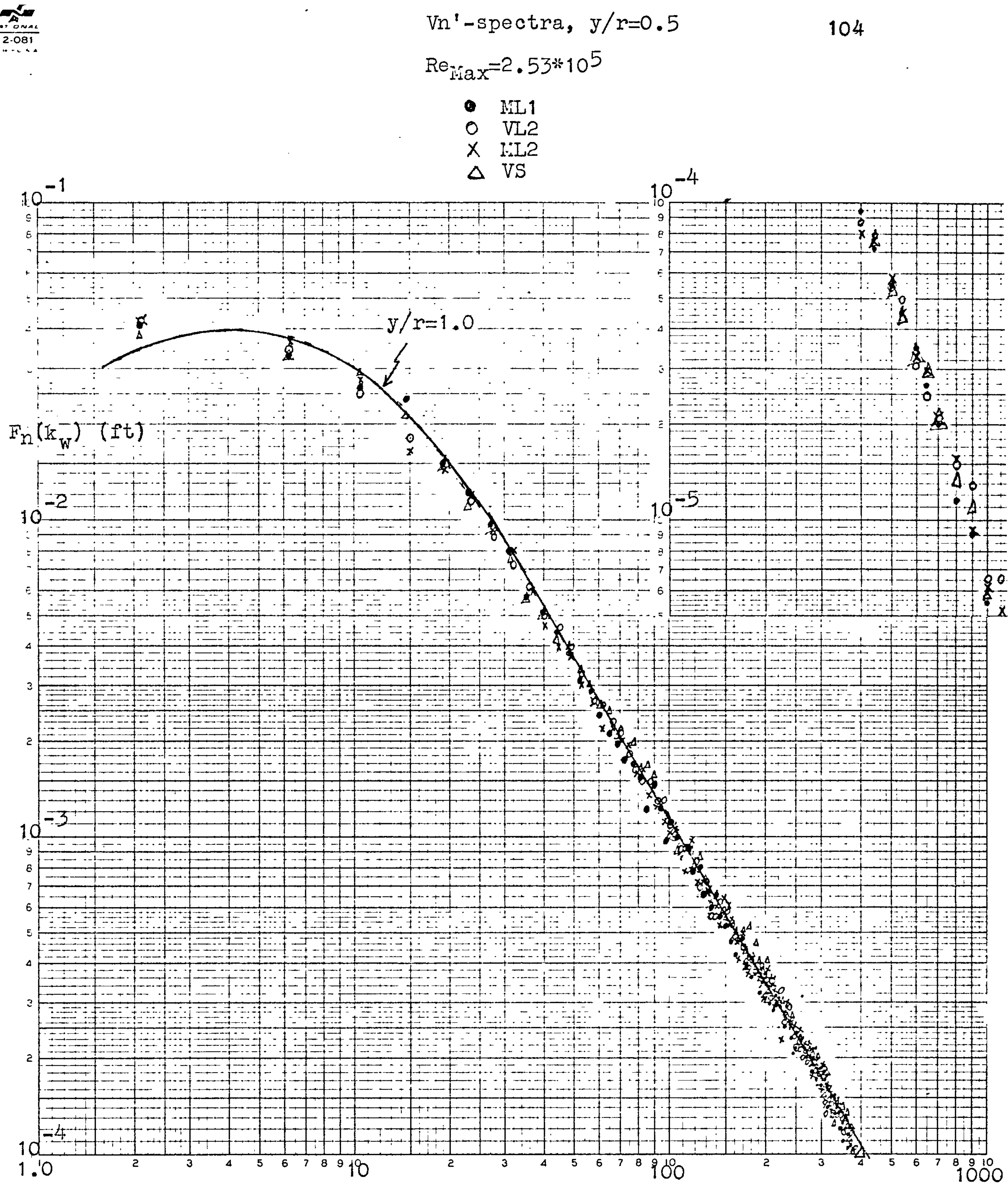

$F_n(k_w)$=normalized wavenumber power spectrum

FIGURE IX-27. Vn'-SPECTRUM AT y/r=0.5

Vn'-spectra, y/r=0.25
$Re_{Max}=2.53*10^5$

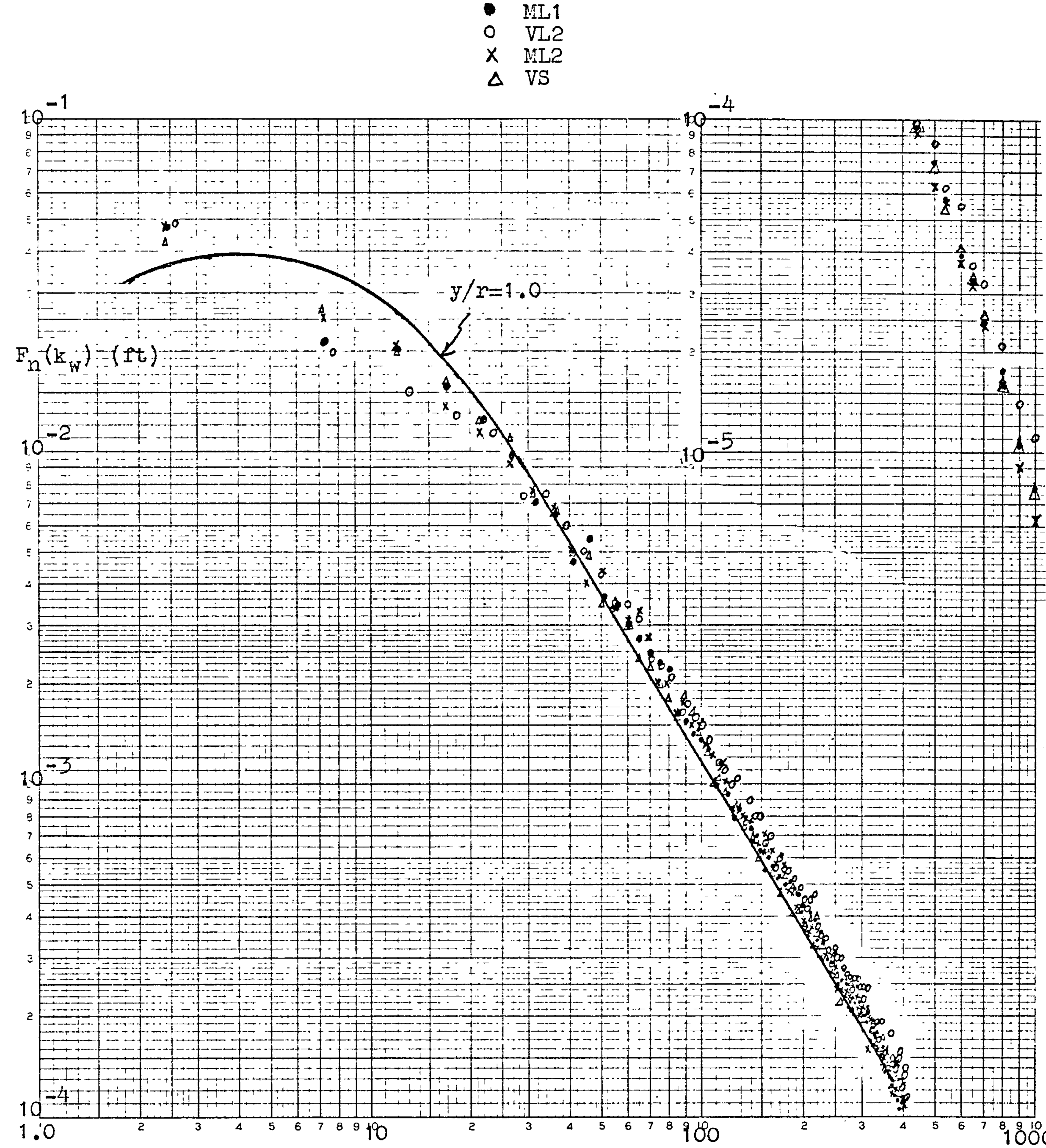

$F_n(k_w)$=normalized wavenumber power spectrum

FIGURE IX-28. Vn'-SPECTRUM AT y/r=0.25

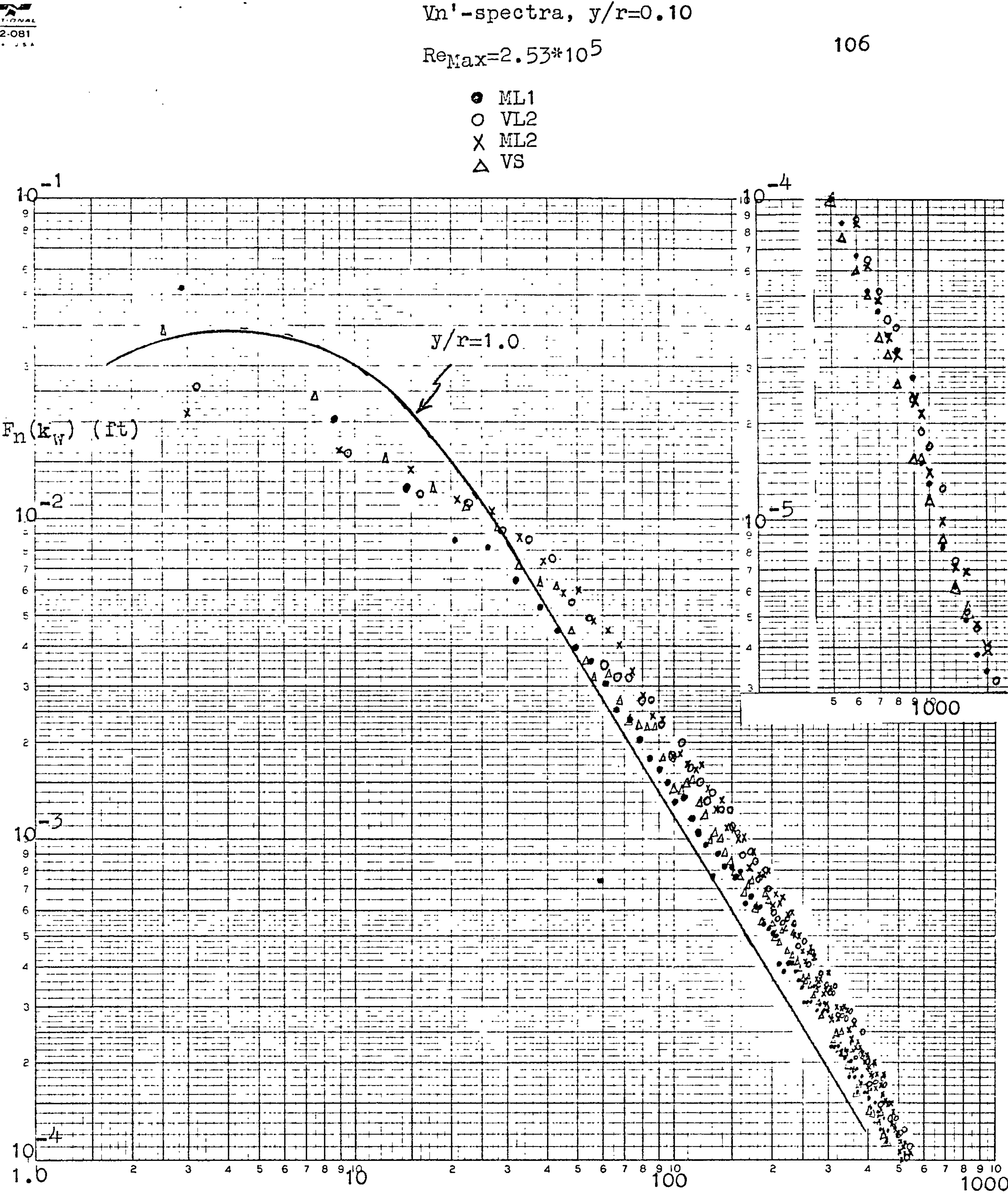

$F_n(k_W)$=normalized wavenumber power spectrum

FIGURE IX-29. Vn'-SPECTRUM AT y/r=0.10

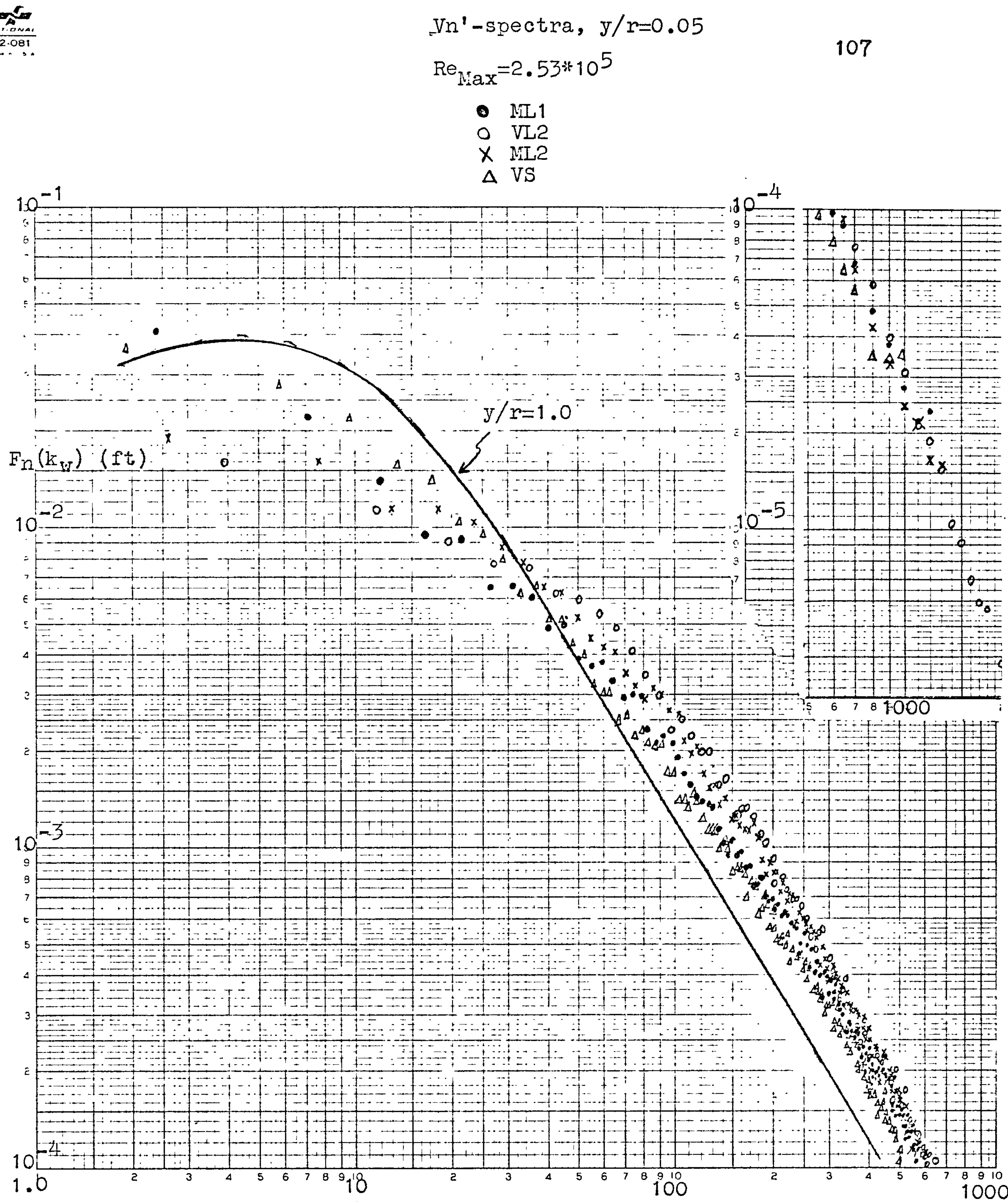

$F_n(k_W)$=normalized wavenumber power spectrum

FIGURE IX-30. Vn'-SPECTRUM AT y/r=0.05

ll Logarithmic, 3 × 3 Cycles

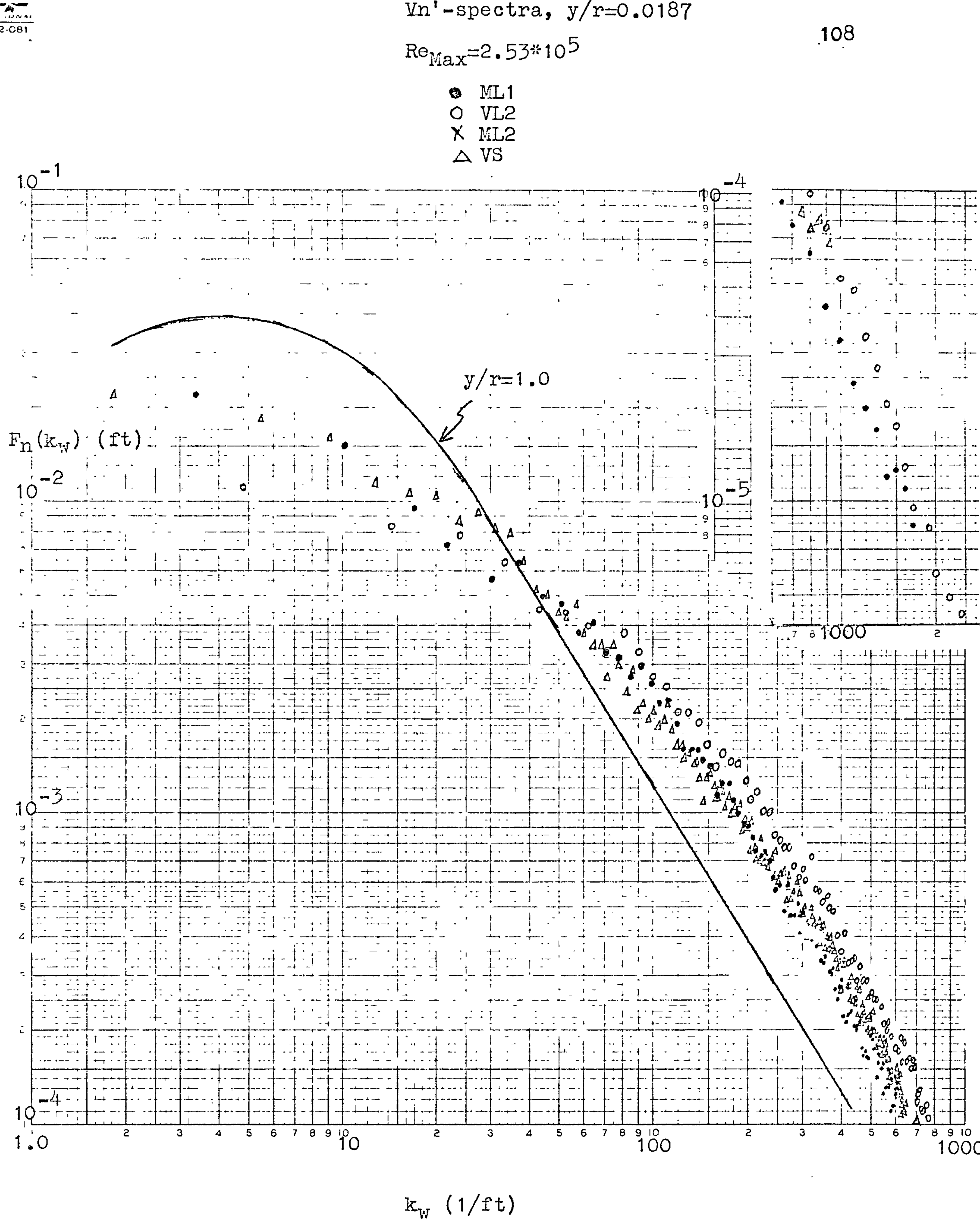

FIGURE IX-31. Vn'-SPECTRUM AT y/r=0.0187

E. Scale And Microscale Measurements

We assume that this field is stationary. There then exists a constant time average value of the contributions of all the frequencies.

Let $E_s(f)df$ be the contribution to $\overline{Vs'^2}$ of the frequencies between f and f+df; the distribution function $E_s(f)$ then has to satisfy the condition,

$$\int_0^\infty E_s(f)\,df = \overline{Vs'^2} \tag{IX-3}$$

or,

$$\int_0^\infty F_s(f)\,df = 1$$

where $F_s(f) = E_s(f)/\overline{Vs'^2}$.

The power spectrum $S^+(\omega)$ of a process $Vs'(t)$ is the Fourier Transform of its autocorrelation,

$$S^+(\omega) = \int_{-\infty}^{\infty} R(\tau) e^{-j\omega\tau} d\tau \tag{IX-4}$$

where $R(\tau)=\langle Vs'(t+\ )Vs'(t)\rangle$, $\langle\ \rangle$ is the expectation notation, and from the fourie's inversion formula it follows that,

$$R(\tau) = \frac{1}{2\pi}\int_{-\infty}^{\infty} S^+(\omega)\ e^{j\omega\tau}\,d\omega \tag{IX-5}$$

with $\tau=0$, the above becomes,

$$\frac{1}{2\pi}\int_{-\infty}^{\infty} S^+(\omega)\,d\omega = R(0) = \langle Vs'(t)\cdot Vs'(t)\rangle \tag{IX-6}$$

If the Ergodicity of the autocorrelation exists then [23]

$$\langle Vs'(t+\tau)\cdot Vs'(t)\rangle = \lim_{T\to\infty}\frac{1}{2T}\int_{-T}^{T} Vs'(t+\tau)\cdot Vs'(t)\,dt \tag{IX-7}$$

$$\therefore \quad \langle Vs'(t)Vs'(t)\rangle = \lim_{T\to\infty}\frac{1}{2T}\int_{-T}^{T} Vs'(t)Vs'(t)\,dt \qquad \text{(IX-8)}$$
$$= \overline{Vs'^2}$$

finally,

$$\int_{-\infty}^{\infty} S^+(f)\,df = \overline{Vs'^2} \qquad \text{with } \omega = 2\pi f \qquad \text{(IX-9)}$$

Since the process $Vs'(t)$ is real, then $R(\tau)$ and $S^+(\omega)$ are real and even, so that

$$\int_0^{\infty} S(f)\,df = \overline{Vs'^2} \qquad \text{(IX-10)}$$

where $S(f)=2S^+(f)$ for $0 \leq f < \infty$, otherwise zero. The physically measured quantity is $S(f)$ other than $S^+(f)$ because negative frequencies are just imaginary ones.[24] (IX-3) and (IX-10) are identical if we let $E_S(f)=S(f)$.

If Taylor's hypothesis[25] applies, then we have,

$$R(\tau) = \int_0^{\infty} E_S(f)\cdot\cos\left(\frac{2\pi f x}{\overline{Vs}}\right)df \qquad \text{(IX-11)}$$

for homogeneous turbulence where x is the coordinate distance, and[26]

$$\frac{1}{\lambda^2} = 2\cdot\lim_{x\to 0}\left(\frac{1-R(\tau)}{x^2}\right) \qquad \text{(IX-12)}$$

where λ is the micro scale.

when x is small,

$$\cos\left(\frac{2\pi f x}{\overline{Vs}}\right) \cong 1 - \frac{2\pi^2 x^2 f^2}{\overline{Vs}^2} \qquad \text{(IX-13)}$$

$$\therefore \quad R(\tau) = \int_0^{\infty} E_S(f)\left(1 - \frac{2\pi^2 x^2 f^2}{\overline{Vs}^2}\right)df \qquad \text{(IX-14)}$$

$$= \int_0^{\infty} F_S(f)\,df - \int_0^{\infty} F_S(f)\left(\frac{2\pi^2 x^2 f^2}{\overline{V_S}^2}\right)df$$

$$= 1 - \int_0^{\infty} F_S(f)\left(\frac{2\pi^2 x^2 f^2}{\overline{V_S}^2}\right)df \qquad \text{(IX-15)}$$

$$\therefore \quad \frac{1}{\lambda^2} = 2\cdot\lim_{x\to 0} \frac{\int_0^{\infty} F_S(f)\left(\frac{2\pi^2 x^2 f^2}{\overline{V_S}^2}\right)df}{x}$$

$$= 4\pi^2 \int_0^{\infty} \frac{F_S(f)\,f^2}{\overline{V_S}^2}\,df \qquad \text{(IX-16)}$$

The longitudinal and radial micro scales are shown in Table IX-5.

The integral scale of turbulence is defined by

$$\Lambda = \int_0^{\infty} R(\tau)\,d\tau \qquad \text{(IX-17)}$$

so it is easily determined. The longitudinal and radial integral scale are also tabulated in Table IX-5.

The micro-scale of turbulence calculated by Taylor[25] from a turbulent-producing grid with a mesh 3*3 in are compared to our data with a mesh 1*1 in in Table IX-6.

TABLE IX-5.

$Re_{Max}=2.53*10^5$

Longitudinal and Radial

Position	y/r	Micro-Scale λ_f (ft)	Micro-Scale λ_g (ft)	Integral-Scale Λ_f (ft)	Integral-Scale Λ_g (ft)
ML1	1.0	0.0137	0.00884	0.189	0.0589
	0.5	0.0186	0.00935	0.590	0.146
	0.25	0.0168	0.00807	0.570	0.170
	0.10	0.0121	0.00649	0.267	0.137
	0.05	0.0108	0.00525	0.244	0.0993
	0.0187	0.0071	0.00417	0.164	0.0570
VS	1.0	0.0143	0.01000	0.191	0.0619
	0.5	0.0171	0.00904	0.385	0.0638
	0.25	0.0161	0.00807	0.495	0.150
	0.10	0.0145	0.00677	0.418	0.0905
	0.05	0.0121	0.00631	0.333	0.0700
	0.0187	0.0108	0.00495	0.374	0.0381
ML2	1.0	0.0142	0.00911	0.186	0.0591
	0.5	0.0177	0.00906	0.600	0.143
	0.25	0.0174	0.00820	0.525	0.155
	0.10	0.0127	0.00573	0.312	0.0413
	0.05	0.0097	0.00497	0.190	0.0333
	0.0187	0.00894		0.0919	
VL2	1.0	0.0135	0.00940	0.195	0.0600
	0.5	0.0173	0.00893	0.592	0.140
	0.25	0.0147	0.00720	0.575	0.163
	0.10	0.0120	0.00557	0.204	0.0528
	0.05	0.00752	0.00420	0.0915	0.0334
	0.0187	0.00681	0.00310	0.0502	0.0221

TABLE IX-6.

data source	section	$\overline{Vs}$ (ft/sec)	λ_g (ft)
Taylor		15.0	0.0282
		20.0	0,0206
		35.0	0.0164
Chen	ML1	21.47	0.00407
		30.58	0.00525
		33.98	0.00649
		40.66	0.00807
Chen	VS	37.77	0.00631
Chen	ML2	28.02	0.00497
		33.17	0.00573
		41.24	0.00820
Chen	VL2	15.27	0.00310
		18.76	0.00420
		30.93	0.00557
		37.78	0.00720

F. Separation Flow Around ML1 Point

The local pressure along the corrugations as measured at the wall is plotted in Figure IX-32. This diagram suggests that there is a possible separation flow around ML1 section. The corrugate pipe approximates a sine wave in shape, the equation is (see Figure IX-33),

$$y = \left(\frac{0.437}{2}\right) \sin\left(\frac{8\pi}{11}x\right)$$

differentiated,

$$y' = \left(\frac{0.437}{2}\right)\left(\frac{8\pi}{11}\right) \cos\left(\frac{8\pi}{11}x\right)$$

at x=11/8,

$$y' = \left(\frac{0.437}{2}\right)\left(\frac{8\pi}{11}\right) \cos(\pi) = -0.499$$

However, from data at y/r=0.0187 for $Re_{Max}=2.53*10^5$ at ML1 section, we have

$$\frac{\overline{Vn}}{\overline{Vs}} = \frac{5.18}{21.47} = 0.241$$

Notice that $\overline{Vn}$ in this case is toward the wall .

With

$$\text{arc tan}\left|\frac{\overline{Vn}}{\overline{Vs}}\right| = \theta_1 \qquad \text{and} \qquad \text{arc tan}\left|y'\right| = \theta_2$$

we have (see Figure IX-34),

$$\theta_1 < \theta_2 \qquad\qquad \text{because } 0.241 < 0.499$$

This would suggest that there exists some separation flow in

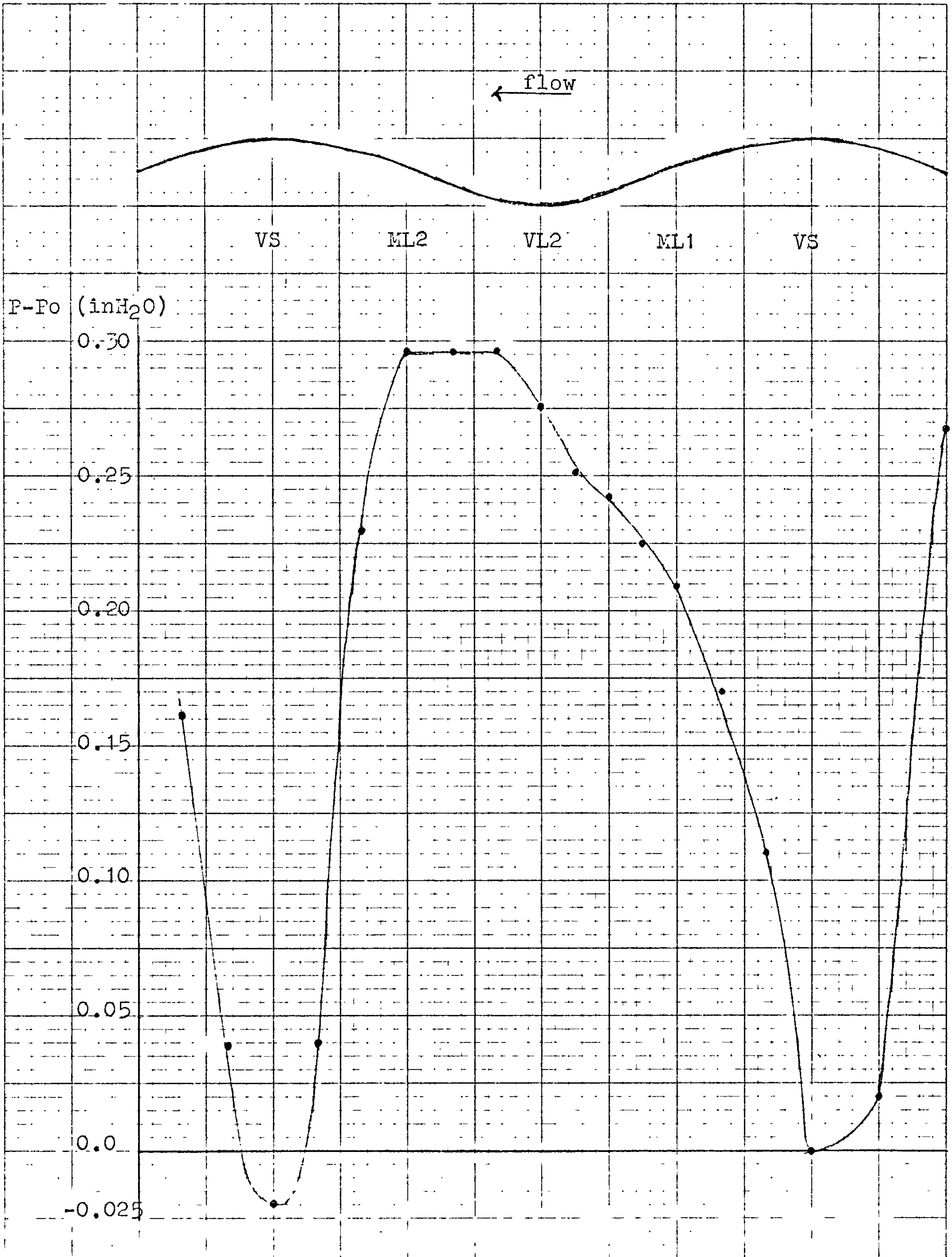

FIGURE IX-32. PRESSURE DISTRIBUTION ALONG A WAVE LENGTH.
Po = Atmosphere pressure

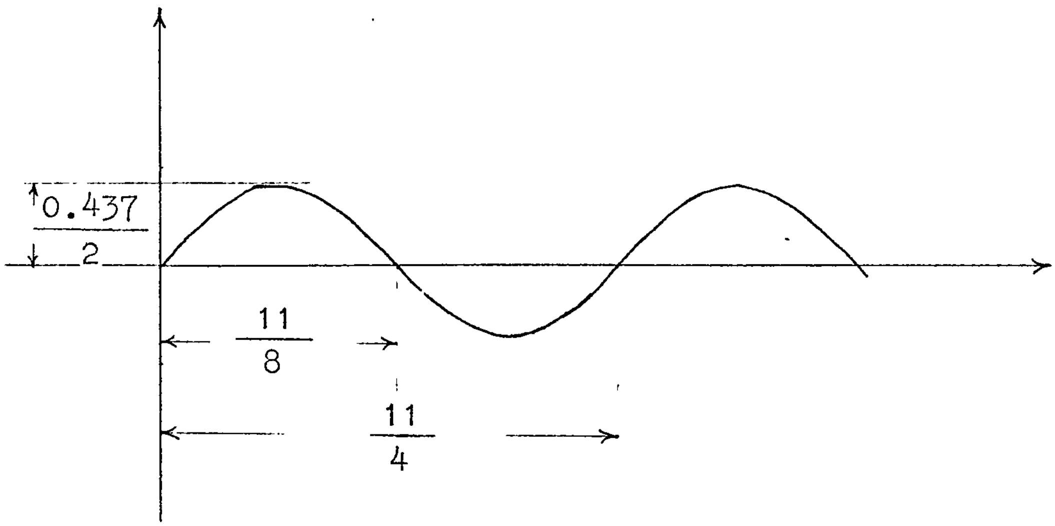

FIGURE IX-33. SCHEMATIC DIAGRAM OF CORRUGATION.

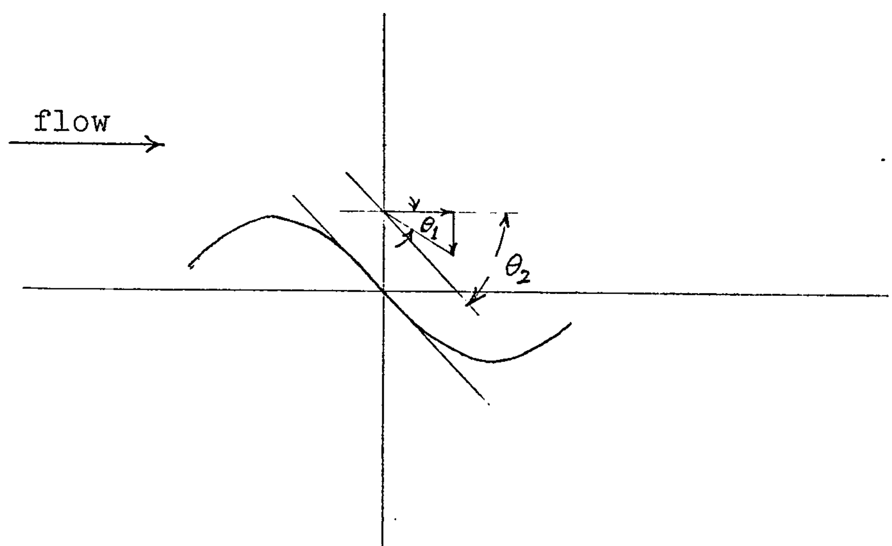

FIGURE IX-34. DIRECTION OF SHEAR STRESS VECTOR AT x=11/8.

the region very close to the wall such that the momentum displacement distance is pushed upward.

Also, if we make a close look at the data for ML1 section, we have the follow diagrams (Figure IX-35)

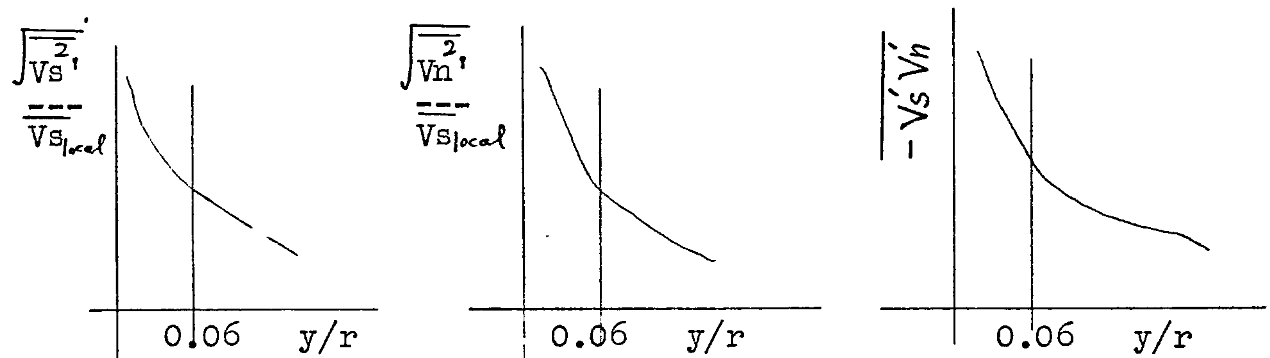

FIGURE IX-35. TURBULENT QUANTITIES RELATIVE TO LOCAL VELOCITY FOR ML1.

We know that at the region below y/r=0.05, there must exist some strong interaction between the fluid particles, because all these three curves have the unusually sharp change. When we examine the $\overline{Vs}$ curves at the ML1 and ML2 sections, these two are almost identical, for the $\overline{Vn}$ curves, they have a small difference. But the $\overline{Vs'Vn'}$ curves have quite different characteristics, so we could say that there must exist " separation flow" in ML1 section. The sudden jump can be regarded as the "thickness of the separation flow region", and the starting deviation point from ML2 curve as "its effective region". Also, in the separation region, the molecular momentum transfer becomes small and the inertia effect overcomes viscous effect, so the viscous shear stress is suppressed. The difference between curves A and D in Figure IX-16 at y/r=0.0187 is really quite small.

G. Flow Pattern

The corrugated pipe is not a pipe of uniform diameter so that equal y/r does not mean the equal position from centerline. Therefore, the velocity lines in Figure IX-1 and IX-2 do not tell the relative position of equal velocity at any section, and do not show the flow pattern. Equal velocity lines are plotted in Figure IX-36 for $\overline{Vs}$=40, 38, 35, 30, and 25 ft/sec for $Re_{Max}=2.53*10^5$. These five lines show that the equal velocity line is pushed upward near the region of tip line (line connecting the tips of the peaks) then it seems to be pushed backward toward the wall when it is closer to the wall at ML2 section. It is unfortunate that there is no data available below y/r=0.0187. Otherwise it may show the particular flow pattern at the wall region between VL2 and ML2 section because the data at turbulent shear stress Table IX-2 shows a negative $\overline{-Vs'Vn'}$ value at y/r=0.0187 at ML2 section for both Reynold number. Also, the pressure distribution along a wave length in Figure IX-32 suggests that there may exist a separation flow at the ML2 section. The negative value of $\overline{-Vs'Vn'}$ and the pressure distribution data seems to indicate a reverse flow existing at this region.

The flow pattern at VS section is apparantly shown by the equal velocity lines that the velocity is almost uniform at the region between y/r=0.25 and y/r=0.05. Between y/r=0.05 and y/r=0.0 there exists a local jet which is shown in Figure IX-2 and discussed in section A.

The flow pattern between VS and ML1 section is shown in Figure IX-36. From the discussion in section F we think that there is a separation flow around the tip line, below this line there is a strong eddy flow region.

The flow direction is shown in Figure IX-37.

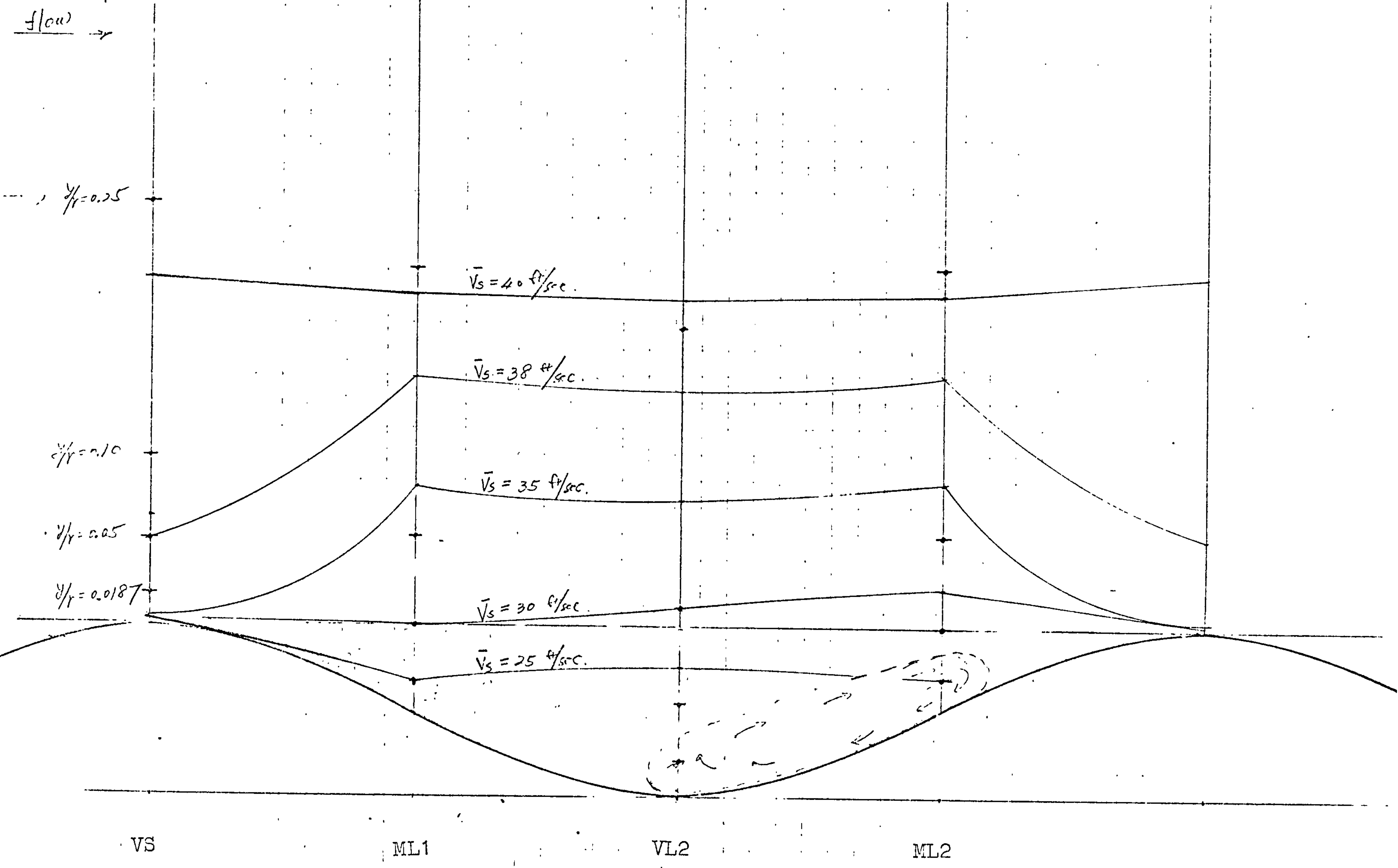

FIGURE IX-36. EQUAL VELOCITY LINES AND FLOW PATTERN

FIGURE IX-37. SCHEMATIC DIAGRAM OF FLOW DIRECTION

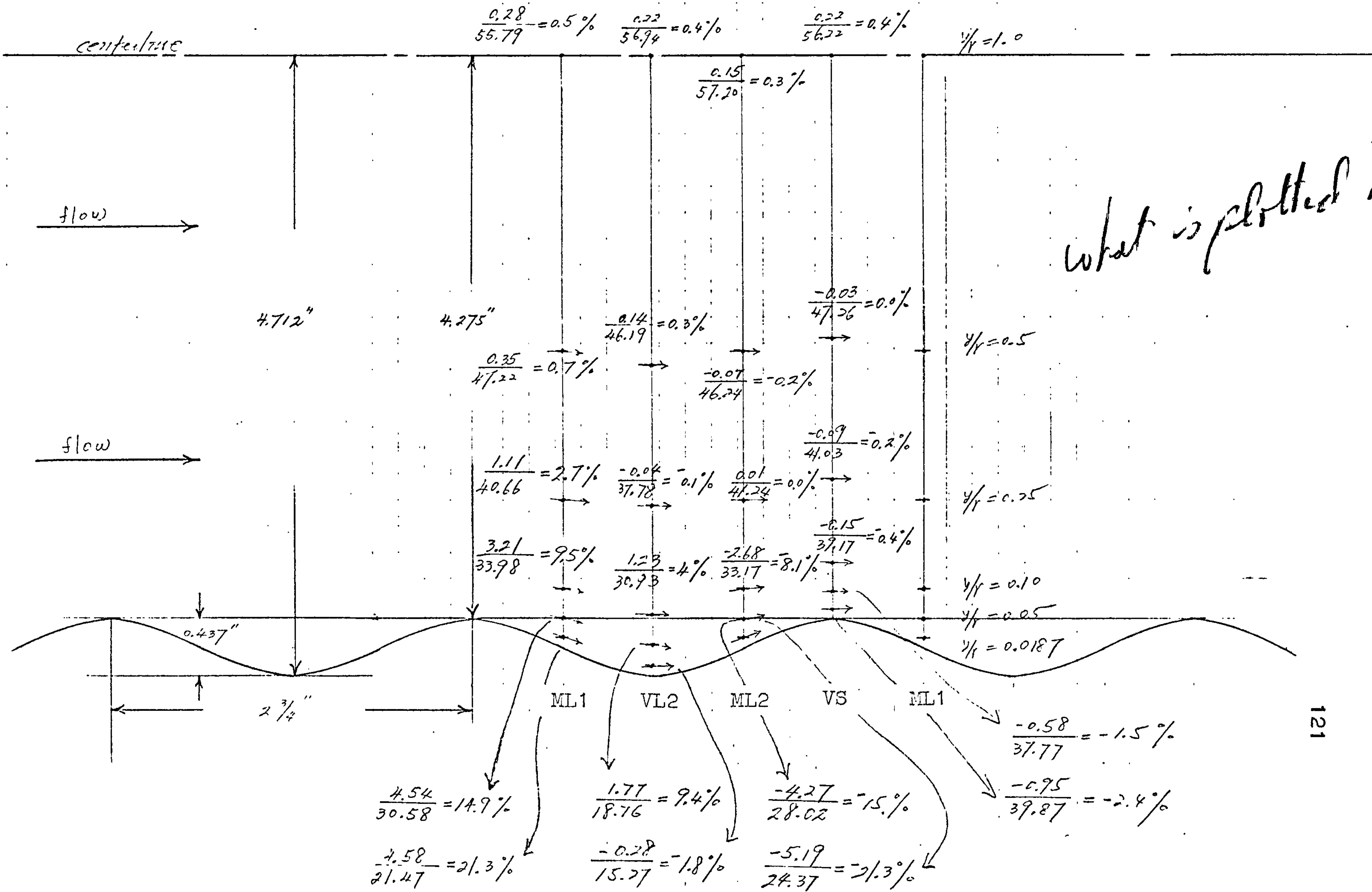

what is plotted?

A. The Measurement Of k Value

Recall from equation (II-3),

$$Ve^2 = V_I^2 \cdot (\cos^2\beta_3 + k^2 \cdot \sin^2\beta_3)$$

where Ve = Effective cooling velocity

V_I = Instantaneous velocity

k = Constant depended primarily on length-to-diameter ratio of the sensor

$\beta_3 = 90 - \alpha$, α is the anfle between the instantaneous velocity vector and the sensor axis

Solve for k, we have,

$$k = \frac{Ve^2/V_I^2 - \cos^2\beta_3}{\sin^2\beta_3} \qquad (x-1)$$

Also, recall from equation (III-5),

$$Eb\left(\frac{\Omega_\omega}{(\Omega_\omega + \Omega_3)}\right) = (C_1 + C_2 \cdot \sqrt{Ve})(Ts - Te)$$

where Ω_ω = The total electric resistance of the sensor

Ω_3 = Electric resistance in serie with Ω_ω

Ts = Sensor temperature

Te = Static stream temperature far from sensor

C_1 and C_2 = Experimental constants

Let

$$Ka = \frac{\Omega_\omega}{(\Omega_\omega + \Omega_3)(Ts - Te)}$$

therefore,

$$\sqrt{Ve} = \frac{Eb^2 \cdot Ka - C_1}{C_2} \qquad (x-2)$$

Substitute equation (x-2) into (X-1), gives

$$k = \frac{\left(\dfrac{Eb^2(\beta_3) - C_1}{Eb^2(0)Ka - C_2}\right) - \cos^2\beta_3}{\sin^2\beta_3} \qquad (X-3)$$

(Notice that $Ve = V_I$ with $\beta_3 = 0$) Therefore, if ka, C_1 , β_3 & Eb(0), Eb(β_3) are known, then k can be measured.

The experiment was carried out as follows:
Placed the single sensor (wire or film) at the cinter line position of the rectangular channel as shown in figure x-1. Rotate the sinsor in the horizontal plane and change the flow rate then we will obtain a series of values of Eb vs β_3. Feed these values into equation (x-3) we get the value of k.

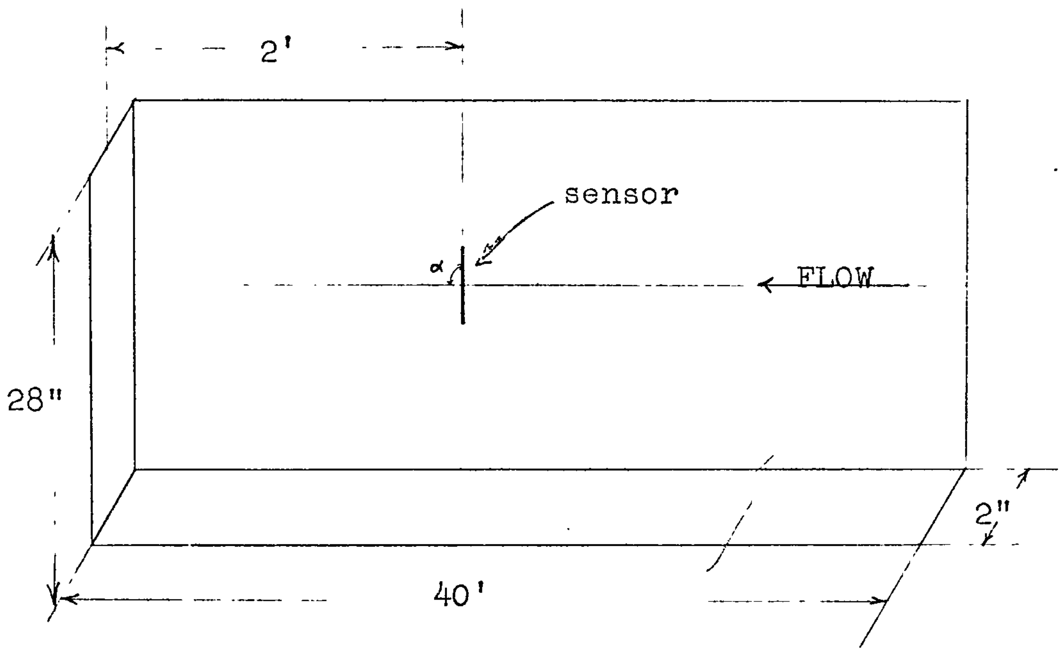

figure x-1.

FIGURE X-1. SCHEMATIC DIAGRAM OF RECTANGULAR CHANNEL AND PROBE POSITION.

Appendix A.


```
      C     THE MEASUREMENT OF K VALUE
            DIMENSION A(20),EBO(20),EB(20),VEDVO(20),FK(20)
        100 FORMAT (8F10.4)
        200 FORMAT (3X,'EBO(I)')
        205 FORMAT (3X,'EB(I)')
        210 FORMAT (3X,'VE/VEO')
        215 FORMAT (3X,'SK')
            A1 = 2.418*2.418
            M = 3
            N = 11
            A(1) = SIN(2.0*3.1416/9.0)
            A(2) = 1.0/SQRT(2.0)
            A(3) = COS(2.0*3.1416/9.0)
            READ (5,100) (EBO(I),I=1,N)
            DO 98 K=1,M
            READ (5,100) (EB (I),I=1,N)
            WRITE (6,200)
            WRITE(6,100) (EBO(I),I=1,N)
            WRITE (6,205)
            WRITE(6,100) (EB (I),I=1,N)
            DO 10 I=1,N
        10  VEDVO(I) = ((EB(I)**2-A1)/(EBO(I)**2-A1))**2
            WRITE (6,210)
            WRITE(6,100) (VEDVO(I),I=1,N)
            DO 20 I=1,N
        20  FK(I) = SQRT(1.0+(VEDVO(I)**2-1.0)/A(K)**2)
            WRITE (6,215)
            WRITE(6,100) (FK(I),I=1,N)
            WRITE(6,105)
        105 FORMAT (//)
        98  CONTINUE
            END
```

```
C      (KCON .EQ. 1), FIND FRDV & RGDF AND USING "SEPARATION SECTION #1"
C      (KCON .EQ. 2), FIND MEAN VALUE OF EMI (I=1,12) AND USING "SEPARAT
C      ON SECTION #2"
C      GRDV IS GROUND VALUE HYBRID OUTPUT
C      RANG IS RANGE VALUE HYBRID OUTPUT
C      GCAL AND RCAL ARE CALIBRATOR OUTPUT
C
C
       DIMENSION X(08000),Y(08000),RTSAVE(61)
       REAL*8 CCWAD(2), RCBAD(4), FSAVE(4)
       REAL*8 XSUM2,YSUM2,X2SY2,XSUM4,YSUM4,X2SY4,X4SY2,XSUM6,YSUM6,
     .        X4SY4,XSUM8,YSUM8,EM1,EM2,EM3,EM4,EM5,EM6,EM7,EM8,EM9,
     .        EM10,EM11,EM12,TEMPX,TEMPY,VMEANX,VMEANY
       INTEGER*2 LOCAD(16002)
       EQUIVALENCE (X(1), LOCAD(2))
  100  FORMAT (I5)
  105  FORMAT (/10X,'NN =',I5)
  106  FORMAT (2I5,2F10.4)
  110  FORMAT (5F10.5)
  115  FORMAT (4F10.5,F15.5)
  200  FORMAT ('TYPE NO. OF SAMPLES-I5 FORMAT')
  205  FORMAT (/10X,10F10.5)
       LOCAD(1)=1
       WRITE (15,200)
       READ (15,100) N
       READ (5,106) MM,KCON,AMP1,AMP2
       WRITE(6,106) MM,KCON,AMP1,AMP2
       READ (5,110) XDC,YDC,VMEANX,VMEANY,YR
       WRITE(6,110) XDC,YDC,VMEANX,VMEANY,YR
       READ (5,110) GRDVX,RANGX,GRDVY,RANGY,TIMER
       WRITE(6,115) GRDVX,RANGX,GRDVY,RANGY,TIMER
       READ (5,110) AX,BX,CX,   GCALX,RCALX
       WRITE(6,110) AX,BX,CX,   GCALX,RCALX
       READ (5,110) AY,BY,CY,   GCALY,RCALY
       WRITE(6,110) AY,BY,CY,   GCALY,RCALY
       TKX = (RANGX-GRDVX)/(RCALX-GCALX)
       TKY = (RANGY-GRDVY)/(RCALY-GCALY)
       TLX = (GRDVX*RCALX-RANGX*GCALX)/(RCALX-GCALX)
       TLY = (GRDVY*RCALY-RANGY*GCALY)/(RCALY-GCALY)
       WRITE(6,110) TKX,TLX,TKY,TLY,YR
       K2N = 2*N
       CALL READAD (CCWAD,K2N,3,LOCAD)
       CALL FRCBSU (RCBAD,28,CCWAD)
       M=N
       E1 = 0.0
       E2 = 0.0
       E11 = 0.0
       E12 = 0.0
       E22 = 0.0
       E14 = 0.0
       E24 = 0.0
       EM1 = 0.0
       EM2 = 0.0
       EM4 = 0.0
```

```
      EM5 = 0.0
      EM6 = 0.0
      EM7 = 0.0
      EM8 = 0.0
      EM9 = 0.0
      EM10 = 0.0
      EM11 = 0.0
      EM12 = 0.0
      NN = 1
   20 CONTINUE
      WRITE (6,105) NN
      CALL FRTIO (RCBAD,IRET)
      CALL FCHECK (RCBAD,IRET,1)
      FAMP1= 819.1*AMP1
      FAMP2 = 819.1*AMP2
      DO 10 I=1,N
      J=N-I+1
      Y(J) =-LOCAD(2*J+1)/FAMP2
   10 X(J) =- LOCAD(2*J)/FAMP1
      WRITE (6,205) (X(J),Y(J),J=1,5)
      IF (KCON .EQ. 1) GO TO 30
      DO 14 I=1,N
      X(I) = (X(I)-TLX)/TKX
   14 Y(I) = (Y(I)-TLY)/TKY
C     ********** SEPARATION SECTION #1 **********
      DO 17 I=1,N
      X(I) = (XDC-X(I))
   17 Y(I) = (YDC-Y(I))
      IF (KCON .EQ. 2) GO TO 30
      DO 12 I=1,N
      X(I) = AX+BX*X(I)*X(I)+CX*X(I)**4-VMEANX
   12 Y(I) = AY+BY*Y(I)*Y(I)+CY*Y(I)**4-VMEANY
      IF (KCON .EQ. 3) GO TO 33
   30 CONTINUE
C     INPUT SIGNAL IS FROM BRIDGE VOLTAGE OUTPUT
      XSUM = 0.0
      YSUM = 0.0
      XSUMX = 0.0
      YSUMY = 0.0
      DO 11 I=1,N
      XSUM = XSUM + X(I)
      XSUMX = XSUMX+X(I)*X(I)
      YSUMY = YSUMY+Y(I)*Y(I)
   11 YSUM = YSUM + Y(I)
      XMEAN = XSUM/FLOAT(N)
      XMEANX = XSUMX/FLOAT(N)
      YMEAN = YSUM/FLOAT(N)
      YMEANY = YSUMY/FLOAT(N)
      WRITE(6,235) XMEAN,XMEANX,YMEAN,YMEANY
      E1 = E1 + XMEAN
      E14 = E14+XMEANX
      E2 = E2 + YMEAN
      E24 = E24+YMEANY
      IF (KCON .NE. 3 ) GO TO 32
```

```
      33   CONTINUE
           XYSUM = 0.0
           XXSUM = 0.0
           YYSUM = 0.0
           DO 15 I=1,N
           XYSUM = XYSUM + X(I)*Y(I)
           XXSUM = XXSUM + X(I)*X(I)
      15   YYSUM = YYSUM + Y(I)*Y(I)
           XYMEAN = XYSUM/FLOAT(N)
           XXMEAN = XXSUM/FLOAT(N)
           YYMEAN = YYSUM/FLOAT(N)
           WRITE (6,240) XXMEAN,YYMEAN,XYMEAN
           E11 = E11+XXMEAN
           E12 = E12+XYMEAN
           E22 = E22+YYMEAN
      32   CONTINUE
           IF (NN .EQ. MM) GO TO 31
           NN = NN+1
           GO TO 20
      31   WRITE (6,245) E1,E14,E2,E24
           E1 = E1/FLOAT(NN)
           E14 = E14/FLOAT(NN)
           E24 = E24/FLOAT(NN)
           E2 = E2/FLOAT(NN)
           WRITE (6,245) E1,E14,E2,E24
           WRITE (6,250) E11,E22,E12
           E11 = E11/FLOAT(NN)
           E22 = E22/FLOAT(NN)
           E12 = E12/FLOAT(NN)
           WRITE (6,250) E11,E22,E12
     235   FORMAT (/10X,4F10.5)
     240   FORMAT (/3(10X,F10.5))
     245   FORMAT (/10X,'E1=',F10.5,5X,'E14=',F10.5,5X,'E2=',F10.5,5X,'E24='
          .        ,F10.5)
     250   FORMAT (/10X,'E11(XX)=',F10.5,5X,'E22(YY)=',F10.5,5X,'E12(XY)=',F
          .10.5)
           STOP
           END
```

```
C
C     ********** SEPARATION SECTION #2 **********
      DO 17 I=1,N
      X(I) = (XDC-X(I))**2
 17   Y(I) = (YDC-Y(I))**2
 30   CONTINUE
      XSUM2 = 0.0
      YSUM2 = 0.0
      X2SY2 = 0.0
      XSUM4 = 0.0
      YSUM4 = 0.0
      X2SY4 = 0.0
      X4SY2 = 0.0
      XSUM6 = 0.0
      YSUM6 = 0.0
      X4SY4 = 0.0
      XSUM8 = 0.0
      YSUM8 = 0.0
      DO 18 I=1,N
      TEMPX = X(I)
      TEMPY = Y(I)
      XSUM2 = XSUM2+TEMPX
      YSUM2 = YSUM2+TEMPY
      X2SY2 = X2SY2+TEMPX*TEMPY
      XSUM4 = XSUM4+TEMPX**2
      YSUM4 = YSUM4+TEMPY**2
      X2SY4 = X2SY4+TEMPX*TEMPY**2
      X4SY2 = X4SY2+TEMPY*TEMPX**2
      XSUM6 = XSUM6+TEMPX**3
      YSUM6 = YSUM6+TEMPY**3
      X4SY4 = X4SY4+TEMPX**2 * TEMPY**2
      XSUM8 = XSUM8+TEMPX**4
      YSUM8 = YSUM8+TEMPY**4
 18   CONTINUE
      XSUM2 = XSUM2 / FLOAT(N)
      YSUM2 = YSUM2 / FLOAT(N)
      X2SY2 = X2SY2 / FLOAT(N)
      XSUM4 = XSUM4 / FLOAT(N)
      YSUM4 = YSUM4 / FLOAT(N)
      X2SY4 = X2SY4 / FLOAT(N)
      X4SY2 = X4SY2 / FLOAT(N)
      XSUM6 = XSUM6 / FLOAT(N)
      YSUM6 = YSUM6 / FLOAT(N)
      X4SY4 = X4SY4 / FLOAT(N)
      XSUM8 = XSUM8 / FLOAT(N)
      YSUM8 = YSUM8 / FLOAT(N)
      WRITE(6,255) XSUM2,YSUM2,X2SY2,XSUM4,YSUM4,X2SY4,X4SY2,XSUM6,
     .             YSUM6,X4SY4,XSUM8,YSUM8
      EM1 = EM1 + XSUM2
      EM2 = EM2 + YSUM2
      EM3 = EM3 + X2SY2
      EM4 = EM4 + XSUM4
      EM5 = EM5 + YSUM4
```

```
      EM6 = EM6 + X2SY4
      EM7 = EM7 + X4SY2
      EM8 = EM8 + XSUM6
      EM9 = EM9 + YSUM6
      EM10 = EM10 + X4SY4
      EM11 = EM11 + XSUM8
      EM12 = EM12 + YSUM8
      IF (NN .EQ. MM) GO TO 31
      NN = NN+1
      GO TO 20
   31 CONTINUE
      EM1 = EM1 / FLOAT(NN)
      EM2 = EM2 / FLOAT(NN)
      EM3 = EM3 / FLOAT(NN)
      EM4 = EM4 / FLOAT(NN)
      EM5 = EM5 / FLOAT(NN)
      EM6 = EM6 / FLOAT(NN)
      EM7 = EM7 / FLOAT(NN)
      EM8 = EM8 / FLOAT(NN)
      EM9 = EM9 / FLOAT(NN)
      EM10 = EM10 / FLOAT(NN)
      EM11 = EM11 / FLOAT(NN)
      EM12 = EM12 / FLOAT(NN)
      WRITE(6,255) EM1,EM2,EM3,EM4,EM5,EM6,EM7,EM8,EM9,EM10,EM11,EM12
  255 FORMAT (/10X,2(F12.7,4X),3(F12.6,4X)/(10X,4(F12.5,4X),3(F12.3)))
      WRITE (7,249) EM1,EM2,EM3,EM4,EM5,EM6,EM7,EM8,EM9,EM10,EM11,EM12
  249 FORMAT (2F10.5,3F10.4,3F10.3,/,1F10.3,3F10.2)
      STOP
      END
```

```
      C        CALIBRATION CURVE PROGRAM
      C        IF X AND Y INPUT REVERSE,SOLUTION STILL SAME INDIVIDALLY
      C        X1 = EB1**2 MEAN
      C        Y1 = EB1**4 MEAN
      C        Z1 = VELOCITY FROM PITOT TUBE
      C        ZX = VELOCITY AFTER CORRECTION
      C
      C
               REAL*8     X1(15),X2(15),Y1(15),Y2(15),F1(15),F2(15),FCS(15),
              .           FCT(15),ZX(15),ZY(15),FXSUM2(15),FYSUM2(15),FX2SY2(15),
              .           FXSUM4(15),FYSUM4(15),FX2SY4(15),FX4SY2(15),FXSUM6(15),
              .           FYSUM6(15),FXSUM8(15),FYSUM8(15),FX4SY4(15) ,Z1(15),
              .           Z2(15),ASQURX(3,3),ASQURY(3,3),BCOLMX(3),BCOLMY(3)   ,
              .           AX,BX,CX,AY,BY,CY,XSUM2,YSUM2,X2SY2,XSUM4,YSUM4,
              .           X2SY4,X4SY2,XSUM6,YSUM6,X4SY4,XSUM8,YSUM8
        98     FORMAT(F10.5)
        100    FORMAT(8F10.5)
        105    FORMAT (10X,8F13.5)
        111    FORMAT(//)
        205    FORMAT(/10X,'COEFFICIENTS =',6F12.5)
        214    FORMAT (/10X,'C1=',F10.5,5X,'C2=',F10.5,5X,'AE11=',F10.5,5X,'AE22
              .'         ,F10.5,5X,'AE12 =',F10.5)
        215    FORMAT(/10X,'A1=',F10.5,5X,'A2=',F10.5,5X,'A3=',F10.5,5X,'A4=',F1
              .          .5,5X,'A5=',F10.5,5X,'S1=',F10.5)
        216    FORMAT(/10X,'B1=',F10.5,5X,'B2=',F10.5,5X,'B3=',F10.5,5X,'B4=',F1
              .          .5,5X,'B5=',F10.5,5X,'T1=',F10.5)
        220    FORMAT(/10X,'AFRS2=',F10.5,5X,'AFRN2=',F10.5,5X,'AFRSN=',F10.5)
        260    FORMAT(/10X,F10.4,5X,'***',5X,3F13.4)
        265    FORMAT (/10X,'FCS =',F10.5,5X,'F1  =',F10.5,5X,'FCT =',F10.5,5X,
              .          'F2 =',F10.5)
        270    FORMAT (/10X,'FCS1=',F10.5,5X,'FCS3=',F10.5,5X,'FCT1=',F10.5,5X,
              .          'FCT3=',F10.5)
        275    FORMAT(2X,'XSUM2',4X,'YSUM2',4X,'X2SY2',4X,'XSUM4',4X,'YSUM4',4X,
              .          'X2SY4',4X,'X4SY2',4X,'XSUM6',4X,'YSUM6',4X,'X4SY4',4X,
              .          'XSUM8',4X,'YSUM8')
        276    FORMAT(2X,'EB1**2')
        277    FORMAT(2X,'EB2**2')
        278    FORMAT(2X,'EB1**4')
        279    FORMAT(2X,'EB2**4')
        280    FORMAT(2X,'US1')
        281    FORMAT(2X,'US2')
        282    FORMAT(2X,'US1*SQRT((1.0+SK*SK)/2.0)*(1.0+F1)')
        283    FORMAT(2X,'US2*SQRT((1.0+SK*SK)/2.0)*(1.0+F2)')
               N = 14
               KCHEN = 1
               SK = 0.35
               READ (5,98) TEMPF
               WRITE(6,98) TEMPF
               READ (5,100) (Z1(I),I=1,N)
               READ (5,100) (Z2(I),I=1,N)
               DO 11 I=1,N
               Z1(I) = 2.90239404* DSQRT(Z1(I)*TEMPF)
        11     Z2(I) = 2.90239404* DSQRT(Z2(I)*TEMPF)
               WRITE(6,275)
```

```
             DO 14 I=1,N
             READ (5,255) FXSUM2(I),FYSUM2(I),FX2SY2(I),FXSUM4(I),FYSUM4(I),
            .             FX2SY4(I),FX4SY2(I),FXSUM6(I),FYSUM6(I),FX4SY4(I),
            .             FXSUM8(I),FYSUM8(I)
       14    WRITE(6,250) FXSUM2(I),FYSUM2(I),FX2SY2(I),FXSUM4(I),FYSUM4(I),
            .             FX2SY4(I),FX4SY2(I),FXSUM6(I),FYSUM6(I),FX4SY4(I),
            .             FXSUM8(I),FYSUM8(I)
      250    FORMAT (2F9.5,3F9.3,7F9.0)
      255    FORMAT(8F10.5)
             DO 13 I=1,N
             X1(I) = FXSUM2(I)
             X2(I) = FYSUM2(I)
             Y1(I) = FXSUM4(I)
       13    Y2(I) = FYSUM4(I)
             WRITE(6,276)
             WRITE(6,105) (X1(I),I=1,N)
             WRITE(6,277)
             WRITE(6,105) (X2(I),I=1,N)
             WRITE(6,278)
             WRITE(6,105) (Y1(I),I=1,N)
             WRITE(6,279)
             WRITE(6,105) (Y2(I),I=1,N)
             WRITE(6,280)
             WRITE(6,105) (Z1(I),I=1,N)
             WRITE(6,281)
             WRITE(6,105) (Z2(I),I=1,N)
             DO 12 I=1,N
             F1(I) = 0.0
       12    F2(I) = 0.0
        3    CONTINUE
             DO 15 I=1,N
             ZX(I) = Z1(I)*SQRT((1.0+SK*SK)/2.0)*(1.0+F1(I))
       15    ZY(I) = Z2(I)*SQRT((1.0+SK*SK)/2.0)*(1.0+F2(I))
             WRITE(6,111)
             WRITE(6,282)
             WRITE(6,105) (ZX(I),I=1,N)
             WRITE(6,283)
             WRITE(6,105) (ZY(I),I=1,N)
      C      GENERATE MATRIX
             DO 28 I=1,3
             DO 28 J=1,3
             BCOLMX(I) = 0.0
             BCOLMY(I) = 0.0
             ASQURX(I,J) = 0.0
       28    ASQURY(I,J) = 0.0
             ASQURX(1,1) = N
             DO 30 I=1,N
             ASQURX(1,2) = ASQURX(1,2)+X1(I)
             ASQURX(1,3) = ASQURX(1,3)+Y1(I)
             ASQURX(2,2) = ASQURX(2,2)+X1(I)*X1(I)
             ASQURX(2,3) = ASQURX(2,3)+X1(I)*Y1(I)
       30    ASQURX(3,3) = ASQURX(3,3)+Y1(I)*Y1(I)
             ASQURX(2,1) = ASQURX(1,2)
             ASQURX(3,1) = ASQURX(1,3)
```

```
            ASQURX(3,2) = ASQURX(2,3)
            DO 31 I=1,N
            BCOLMX(1) = BCOLMX(1)+ZX(I)
            BCOLMX(2) = BCOLMX(2)+ZX(I)*X1(I)
      31    BCOLMX(3) = BCOLMX(3)+ZX(I)*Y1(I)
            DO 33 I=1,3
      33    WRITE(6,260) BCOLMX(I),(ASQURX(I,J),J=1,3)
            WRITE(6,111)
            CALL SIMQ(ASQURX,BCOLMX,3,0)
            ASQURY(1,1) = N
            DO 34 I=1,N
            ASQURY(1,2) = ASQURY(1,2)+X2(I)
            ASQURY(1,3) = ASQURY(1,3)+Y2(I)
            ASQURY(2,2) = ASQURY(2,2)+X2(I)*X2(I)
            ASQURY(2,3) = ASQURY(2,3)+X2(I)*Y2(I)
      34    ASQURY(3,3) = ASQURY(3,3)+Y2(I)*Y2(I)
            ASQURY(2,1) = ASQURY(1,2)
            ASQURY(3,1) = ASQURY(1,3)
            ASQURY(3,2) = ASQURY(2,3)
            DO 35 I=1,N
            BCOLMY(1) = BCOLMY(1)+ZY(I)
            BCOLMY(2) = BCOLMY(2)+ZY(I)*X2(I)
      35    BCOLMY(3) = BCOLMY(3)+ZY(I)*Y2(I)
            DO 36 I=1,3
      36    WRITE(6,260) BCOLMY(I),(ASQURY(I,J),J=1,3)
            CALL SIMQ(ASQURY,BCOLMY,3,0)
            AX = BCOLMX(1)
            BX = BCOLMX(2)
            CX = BCOLMX(3)
            AY = BCOLMY(1)
            BY = BCOLMY(2)
            CY = BCOLMY(3)
            WRITE(6,205) AX,BX,CX,AY,BY,CY
            IF (KCHEN .EQ. 4) GO TO 654
            WRITE(6,111)
            DO 17 I=1,N
            XSUM2 = FXSUM2(I)
            YSUM2 = FYSUM2(I)
            X2SY2 = FX2SY2(I)
            XSUM4 = FXSUM4(I)
            YSUM4 = FYSUM4(I)
            X2SY4 = FX2SY4(I)
            X4SY2 = FX4SY2(I)
            XSUM6 = FXSUM6(I)
            YSUM6 = FYSUM6(I)
            X4SY4 = FX4SY4(I)
            XSUM8 = FXSUM8(I)
            YSUM8 = FXSUM8(I)
            YSUM8 = FYSUM8(I)
            A1 = 1.0+SK*SK
            A2 = 1.0-SK*SK
            A3 = A1
            A4 = A1
            A5 = 2.0*A2
```

```
      B1 = A1
      B2 = -A2
      B3 = A1
      B4 = A1
      B5 = -A5
      S1 = A1
      T1 = A1
      C1 = SQRT(S1*2.0)/Z1(I)
      C2 = SQRT(T1*2.0)/Z2(I)
      AE11 = BX*BX*(XSUM4-XSUM2*XSUM2) + 2.0*BX*CX*(XSUM6-XSUM2*XSUM4)
     .       + CX*CX*(XSUM8-XSUM4*XSUM4)
      AE22 = BY*BY*(YSUM4-YSUM2*YSUM2) + 2.0*BY*CY*(YSUM6-YSUM2*YSUM4)
     .       + CY*CY*(YSUM8-YSUM4*YSUM4)
      AE12 = BX*BY*(X2SY2-XSUM2*YSUM2) + BX*CY*(X2SY4-XSUM2*YSUM4) +
     .       CX*BY*(X4SY2-XSUM4*YSUM2) + CX*CY*(X4SY4-XSUM4*YSUM4)
      X422 = XSUM4-XSUM2*XSUM2
      Y422 = YSUM4-YSUM2*YSUM2
      X624 = XSUM6-XSUM2*XSUM4
      Y624 = YSUM6-YSUM2*YSUM4
      X844 = XSUM8-XSUM4*XSUM4
      Y844 = YSUM8-YSUM4*YSUM4
      X222 = X2SY2-XSUM2*YSUM2
      X424 = X2SY4-XSUM2*YSUM4
      X242 = X4SY2-XSUM4*YSUM2
      X444 = X4SY4-XSUM4*YSUM4
      WRITE(6,100)X422,X624,X844,Y422,Y624,Y844,X222,X424,X242,X444
      WRITE (6,214) C1,C2,AE11,AE22,AE12
      AFRS2 = ((B2*C1)**2*AE11-2.*B2*A2*C1*C2*AE12 +(A2*C2)**2*AE22)/
     .        (A1*B2-A2*B1)**2
      AFRN2 = ((B1*C1)**2*AE11-2.*B1*A1*C1*C2*AE12 +(A1*C2)**2*AE22)/
     .        (A1*B2-A2*B1)**2
      AFRSN = -((B1*B2*C1*C1*AE11) - (A1*B2+A2*B1)*C1*C2*AE12    + (A1*
     .        A2*C2*C2*AE22)) / (A1*B2-A2*B1)**2
      FCS1 = (A4/S1-(A1/S1)**2)*AFRS2
      FCS2 = (A3/S1-(A2/S1)**2)*AFRN2
      FCS3 = (A5/S1-2.0*A1*A2/S1**2)*AFRSN
      FCS(I) = 0.5*(FCS1+FCS2+FCS3)
      FCT1 = (B4/T1-(B1/T1)**2)*AFRS2
      FCT2 = (B3/T1-(B2/T1)**2)*AFRN2
      FCT3 = (B5/T1-2.0*B1*B2/T1**2)*AFRSN
      FCT(I) = 0.5*(FCT1+FCT2+FCT3)
      WRITE (6,265) FCS(I),F1(I),FCT(I),F2(I)
      WRITE (6,220) AFRS2,AFRN2,AFRSN
      WRITE(6,111)
   17 CONTINUE
      DO 77 I=1,N
      IF(DABS(FCS(I)-F1(I)).GT.0.0001.OR.DABS(FCT(I)-F2(I)).GT..0001)
     .                GO TO 61
   77 CONTINUE
      WRITE (6,215) A1,A2,A3,A4,A5,S1
      WRITE (6,216) B1,B2,B3,B4,B5,T1
      WRITE (6,270) FCS1,FCS3,FCT1,FCT3
      GO TO 91
   61 DO 23 I=1,N
```

```
          F1(I) = FCS(I)
     23   F2(I) = FCT(I)
          GO TO 3
    654   CONTINUE
     91   STOP
          END
```

```
C     FINAL PROGRAM
C     E1 REPRESENT --/ OR THE POSITIVE ANGLE IS LESS THAN 90 DEGREE
C     IMM CONTROLS SETS OF SK
C     IND CONTROLS SETS OF DATA
C
C
      DIMENSION FE1(60),FE2(60),      FXSUM2(60),FYSUM2(60),FX2SY2(60),
     .          FXSUM4(60),FYSUM4(60),FX2SY4(60),FX4SY2(60),FXSUM6(60),
     .          FYSUM6(60),FXSUM8(60),FYSUM8(60),FX4SY4(60)
      REAL*8    E1,E2,F1,F2,FCT,UN,TINTS,TINTN,TSHEAR,TF,
     .          XSUM2,YSUM2,X2SY2,XSUM4,YSUM4,X2SY4,X4SY2,XSUM6,YSUM6,
     .          X4SY4,XSUM8,YSUM8,AEK,ACO,ACE,ACP1,ACP2,SK,R1,R2,S1,T1,
     .          QS,QST,C1,C2,AE11,AE22,AE12,A1,A2,A3,A4,A5,B1,B2,B3,B4,
     .          B5,AFRS2,AFRN2,AFRSN,FCS1,FCS2,FCS3,FCS,FCT1,FCT2,FCT3
  103 FORMAT (F10.5)
  104 FORMAT (4I3)
  105 FORMAT (6F10.5)
  210 FORMAT (/10X,'QS=',F10.5,10X,'QST=',F10.5)
  214 FORMAT (/10X,'E1=',F10.5,5X,'E2=',F10.5,5X,'AE11=',F10.5,5X,'AE22
     .'     ,F10.5,5X,'AE12 =',F10.5)
  215 FORMAT(/10X,'A1=',F10.5,5X,'A2=',F10.5,5X,'A3=',F10.5,5X,'A4=',F1
     .          .5,5X,'A5=',F10.5,5X,'S1=',F10.5)
  216 FORMAT(/10X,'B1=',F10.5,5X,'B2=',F10.5,5X,'B3=',F10.5,5X,'B4=',F1
     .          .5,5X,'B5=',F10.5,5X,'T1=',F10.5)
  217 FORMAT (/10X,'C1=',F10.5,5X,'C2=',F10.5)
  220 FORMAT(/10X,'AFRS2=',F10.5,5X,'AFRN2=',F10.5,5X,'AFRSN=',F10.5)
  225 FORMAT (/// )
  227 FORMAT(/10X,'US=',F10.5,5X,'UN=',F10.5,5X,'TINTS=',F10.5,5X,'TINT
     .=',F10.5,5X,'TSHEAR=',F10.5)
  245 FORMAT (/10X,'IMAGINARY ROOT')
  249 FORMAT (2F9.5,3F9.3,7F9.0)
  250 FORMAT (/10X,'SK = ', F10.5)
  251 FORMAT (/10X,8F10.5)
  255 FORMAT (/10X,'(R1=',F10.5,')',9X,'R2=',F10.5)
  256 FORMAT(8F10.5)
  260 FORMAT (/10X,'R1=',F10.5,10X,'(R2=',F10.5,')')
  265 FORMAT (/10X,'FCT1=',F10.5,5X,'FCT2=',F10.5,5X,'FCT3=',F10.5,5X,
     .          'FCT=',F10.5,5X,'F2=',F10.5)
  270 FORMAT (/10X,'FCS1=',F10.5,5X,'FCS2=',F10.5,5X,'FCS3=',F10.5,5X,
     .          'FCS=',F10.5,5X,'F1=',F10.5)
  274 FORMAT (/10X,'AEK =',F10.5,5X,'ACO =',F10.5,5X,'ACE =',F10.5,5X,
     .          'ACP1=',F10.5,5X,'ACP2=',F10.5)
  275 FORMAT(2X,'XSUM2',4X,'YSUM2',4X,'X2SY2',4X,'XSUM4',4X,'YSUM4',4X,
     .          'X2SY4',4X,'X4SY2',4X,'XSUM6',4X,'YSUM6',4X,'X4SY4',4X,
     .          'XSUM8',4X,'YSUM8')
      READ  (5,104) N,IND,IMM,NN
      WRITE (6,104) N,IND,IMM,NN
      READ (5,105) AX,BX,CX,AY,BY,CY
      WRITE(6,105) AX,BX,CX,AY,BY,CY
      READ(5,103) SK
      WRITE(6,275)
      DO 10 I=1,N
      READ (5,256) FXSUM2(I),FYSUM2(I),FX2SY2(I),FXSUM4(I),FYSUM4(I),
     .              FX2SY4(I),FX4SY2(I),FXSUM6(I),FYSUM6(I),FX4SY4(I),
```

```
      .                  FXSUM8(I),FYSUM8(I)
       WRITE(6,249) FXSUM2(I),FYSUM2(I),FX2SY2(I),FXSUM4(I),FYSUM4(I),
      C                  FX2SY4(I),FX4SY2(I),FXSUM6(I),FYSUM6(I),FX4SY4(I),
      .                  FXSUM8(I),FYSUM8(I)
   10  CONTINUE
  1    CONTINUE
       MM = 1
  4    CONTINUE
       XSUM2 = FXSUM2(NN)
       YSUM2 = FYSUM2(NN)
       X2SY2 = FX2SY2(NN)
       XSUM4 = FXSUM4(NN)
       YSUM4 = FYSUM4(NN)
       X2SY4 = FX2SY4(NN)
       X4SY2 = FX4SY2(NN)
       XSUM6 = FXSUM6(NN)
       YSUM6 = FYSUM6(NN)
       X4SY4 = FX4SY4(NN)
       XSUM8 = FXSUM8(NN)
       YSUM8 = FYSUM8(NN)
       E1 = AX+BX*XSUM2     +CX*XSUM4
       E2 = AY+BY*YSUM2     +CY*YSUM4
       A3 = 1.0 + SK*SK
       A4 = 1.0 + SK*SK
       A5 = 2.0*(1.0-SK*SK)
       B3 = 1.0 + SK*SK
       B4 = 1.0 + SK*SK
       B5 = 2.0*(SK*SK-1.0)
  2    F1 = 0.0
       F2 = 0.0
       AE11 = BX*BX*(XSUM4-XSUM2*XSUM2) + 2.0*BX*CX*(XSUM6-XSUM2*XSUM4)
      .       + CX*CX*(XSUM8-XSUM4*XSUM4)
       AE22 = BY*BY*(YSUM4-YSUM2*YSUM2) + 2.0*BY*CY*(YSUM6-YSUM2*YSUM4)
      .       + CY*CY*(YSUM8-YSUM4*YSUM4)
       AE12 = BX*BY*(X2SY2-XSUM2*YSUM2) + BX*CY*(X2SY4-XSUM2*YSUM4) +
      .       CX*BY*(X4SY2-XSUM4*YSUM2) + CX*CY*(X4SY4-XSUM4*YSUM4)
  3    CONTINUE
       AEK = ((E1    )/(E2    )) * ((1.+F2)/(1.+F1))
       ACO = (AEK*AEK+1.0)/(AEK*AEK-1.0)
       ACE = (1.0-SK*SK)/(1.0+SK*SK)
       ACP1 = ACE*ACO
       ACP2 = ACP1*ACP1
       IF ( ACP2-1.0 ) 20,25,25
  20   WRITE (6,245)
       GO TO 61
  25   R1 = ACP1+DSQRT(ACP2-1.)
       R2 = ACP1-DSQRT(ACP2-1.)
       IF (ACO .LE. 0.0 ) GO TO 30
       WRITE (6,255) R1,R2
       R1 = R2
       GO TO 31
  30   WRITE (6,260) R1,R2
       GO TO 31
  31   S1 = (1.0+SK*SK)+2.0*(1.0-SK*SK)*R1+(1.0+SK*SK)*R1*R1
```

```
      T1 = (1.0+SK*SK)-2.0*(1.0-SK*SK)*R1+(1.0+SK*SK)*R1*R1
      TF=1.0
      QS = E1/(TF* DSQRT(S1/2.0)*(1.0+F1))
      QST= E2/(TF* DSQRT(T1/2.0)*(1.0+F2))
      C1 =DSQRT(2.0*S1) / (TF* QS)
      C2 =DSQRT(2.0*T1) / (TF* QST)
      A1 = (1.0+SK*SK)-(SK*SK-1.0)*R1
      A2 = (1.0-SK*SK)+(1.0+SK*SK)*R1
      B1 = (1.0+SK*SK)+(SK*SK-1.0)*R1
      B2 = (SK*SK-1.0)+(1.0+SK*SK)*R1
      AFRS2 = ((B2*C1)**2*AE11-2.*B2*A2*C1*C2*AE12 +(A2*C2)**2*AE22)/
     .         (A1*B2-A2*B1)**2
      AFRN2 = ((B1*C1)**2*AE11-2.*B1*A1*C1*C2*AE12 +(A1*C2)**2*AE22)/
     .         (A1*B2-A2*B1)**2
      AFRSN = -((B1*B2*C1*C1*AE11) - (A1*B2+A2*B1)*C1*C2*AE12    + (A1*
     .         A2*C2*C2*AE22)) / (A1*B2-A2*B1)**2
      FCS1 = (A4/S1-(A1/S1)**2)*AFRS2
      FCS2 = (A3/S1-(A2/S1)**2)*AFRN2
      FCS3 = (A5/S1-2.0*A1*A2/S1**2)*AFRSN
      FCS = 0.5*(FCS1 + FCS2 + FCS3)
      FCT1 = (B4/T1-(B1/T1)**2)*AFRS2
      FCT2 = (B3/T1-(B2/T1)**2)*AFRN2
      FCT3 = (B5/T1-2.0*B1*B2/T1**2)*AFRSN
      FCT = 0.5*(FCT1 + FCT2 + FCT3)
      IF(DABS(FCS-F1) .LE.0.00001.AND.DABS(FCT-F2) .LE.0.00001) GO TO 6
      F1 = FCS
      F2 = FCT
      GO TO 3
   61 UN = QS*R1
      TINTS =DSQRT(AFRS2)
      TINTN =DSQRT(AFRN2)
      TSHEAR = AFRSN*QS*QS
      WRITE (6,250) SK
      WRITE (6,274) AEK,ACO,ACE,ACP1,ACP2
      WRITE (6,210) QS,QST
      WRITE (6,214) E1,E2,AE11,AE22,AE12
      WRITE (6,215) A1,A2,A3,A4,A5,S1
      WRITE (6,216) B1,B2,B3,B4,B5,T1
      WRITE (6,217) C1,C2
      WRITE (6,270) FCS1,FCS2,FCS3,FCS,F1
      WRITE (6,265) FCT1,FCT2,FCT3,FCT,F2
      WRITE (6,220) AFRS2,AFRN2,AFRSN
      WRITE(6,227) QS,UN,TINTS,TINTN,TSHEAR
      IF (MM .EQ. IMM) GO TO 65
      MM = MM+1
      GO TO 4
   65 IF (NN .EQ. IND) GO TO 70
      NN = NN+1
      WRITE (6,225)
      GO TO 1
   70 STOP
      END
```

```
      C
      C     AUTO POWER SPECTRUM
      C
            DIMENSION X(08194),DATA(2,4097),RCOR(4098),FR(4098),NX(1),S(280)
            EQUIVALENCE (X(1),DATA(1,1))
            EQUIVALENCE (FR(1),RCOR(1))
       201  FORMAT (//5X,'TIMER',21X,'=',F8.0,//5X,'FREQUENCY',17X,'=',F10.6,
           .//5X,'NO. OF ITERATION',10X,'=',I4,  //5X,    'FREQUENCY AVERAGE D
           .OMAIN  =',I4,//5X,'MEAN-SQUARE VALUE',9X,'=',F8.4,//5X,'TOTAL SAMP
           .LED POINTES      =',I8,//5X,'EXPERIMENT POSITION ',6X,'=',I3,//5X,'
           .EXPERIMENT  DATE',10X,'=',I3//5X,'REYNOLD NUMBER',12X,'=',F8.0//
           .5X,'TAPE  SPEED',15X,'=',I3)
       202  FORMAT (    10E11.3/(10E11.3))
       205  FORMAT (1H1)
       206  FORMAT (//5X,'FREQUENCY  (CYCLES/SEC.)'/)
       207  FORMAT (//5X,'NORMALIZED AUTO CORRELATION WITH TIME DELAY = 1/TIME
           .R'/)
       209  FORMAT (//5X,'AUTO CORRELATION WITH TIME DELAY = 1/TIMER'/)
       210  FORMAT (I5,F10.5,F10.5,F10.5)
       220  FORMAT (1X)
       226  FORMAT (5X,I6,10X,1E11.3)
       240  FORMAT (//5X,'INTEGREL TIME SCALE ',5X,'=',E13.5,10X,'INTERGRAL LE
           .NGTH SCALE',5X,'=',E13.5,3X,'(FT)')
       246  FORMAT (//5X,'NORMALIZED WAVENUMBER POWER SPECTRUM ',3X,'(FT)')
       248  FORMAT (//5X,'FREQUENCY WITH WAVENUMBER   (1/FT)')
       250  FORMAT (//5X,'MICRO SCALE OR DESSIPATION SCALE   =',E13.5,3X,
           .        '(FT)')
       252  FORMAT (//5X,'MEAN SQUARE VALUE FROM TURBULENT INTENSITY   =',
           .        F10.5)
       254  FORMAT (//5X,'PHYSICAL NORMALIZED ONE_SIDE POWER SPECTRUM',3X,
           .        '(SEC)')
       400  FORMAT (45F8.4)
       401  FORMAT (I3,I6,F8.0,I3,F8.0,I3)
       402  FORMAT (I3,I6,F8.0,I3,F8.0,I3,14F10.5)
       403  FORMAT (I3,I6,F8.0,I3,F8.0,I3,6F10.5/(10F10.5))
      C
            KKK = 3
       1    CONTINUE
            READ (1,402) MM, N  , TIMER, KCOND ,REY,ISPEED,AX,BX,CX,AY,BY,CY,
           .                R1,R2,Q1,Q2,XDC,YDC,UEMX,UEMY
            WRITE(6,403) MM, N  , TIMER, KCOND ,REY,ISPEED,AX,BX,CX,AY,BY,CY,
           .                R1,R2,Q1,Q2,XDC,YDC,UEMX,UEMY
            MM = MM-1
            READ (5,210) MD, DATE , US ,TINSTS
            WRITE(6,210) MD, DATE ,US  ,TINSTS
            RMSV = (TINSTS*US)**2
            FRECY = TIMER / FLOAT(N)
            NN = 0
            NX(1) = N
            NO = N * MM
            M2 = N/2
            M3 = M2+1
            N2 = M2
            MD2 = (N+2)/2
```

```
          MO4 = N/(2*MD)
          DO 3C I=1,MD2
   30     RCCR(I) = 0.0
          DO 31 I=1,MO4
   31     S(I) = 0.0
   20     CONTINUE
          IOUT1 = 256
          DO 33 I=1,N2,256
          DO 351 J=1,6
   351    READ (1,220)
   33     IOUT1 = 256 + IOUT1
          IOUT2 = 256
          DO 35 I=1,N2,256
          READ (1,400) (X(J),J=I,IOUT2)
   35     IOUT2 = 256 + IOUT2
          IOUT1 = 4352
          DO 37 I = 4097,N,256
          DO 381 J=1,6
   381    READ (1,220)
   37     IOUT1 = 256+IOUT1
          IOUT2 = 4352
          DO 38 I=4097,N,256
          READ (1,400) (X(J),J=I,IOUT2)
   38     IOUT2 = 256+IOUT2
          WRITE (6,202) (X(I),I=4090,4096)
          CALL FOUR2 (X   ,NX,1,-1,0)
          DO 44 I=1,MD2
   44     RCCR(I)=RCOR(I)+(DATA(1,I)*DATA(1,I)+DATA(2,I)*DATA(2,I))/FLOAT(N)
          DO 64 J=1,MO4
          SAVE = 0.0
          DO 61 I=1,MD
          IJ=I+(J-1)*MD
   61     SAVE = SAVE + DATA(1,IJ)*DATA(1,IJ)+DATA(2,IJ)*DATA(2,IJ)
   64     S(J) = S(J) + SAVE
          NN = NN + 1
          IF (NN .LT.MM)   GO TO 20
          FMSU = 0.0
          DO 51 I=2,M2
   51     FMSU = FMSU + RCOR(I)
          FMSU = (2.*FMSU+RCOR(1)+RCOR(MD2))/FLOAT(MM*N)
          WRITE(6,205)
          WRITE(6,201) TIMER, FREQY, MM, MD, FMSU,NO,POSITN,DATE,REY,ISPEED
          WRITE (6,252) RMSV
          DO 21 I=1,MD2
          DATA(1,I) = RCOR(I)/FLOAT(MM)
   21     DATA(2,I) = 0.0
          CALL FOUR2 (X, NX, 1,1,-1)
          DO 55 I=1,MD2
   55     FR(I) = FLOAT(I-1)/TIMER
          DO 22 I=1,MD2
   22     X(I) = X(I)/(FLOAT(N)*(1.-FREQY*FR(I)))
          WRITE (6,209)
          WRITE(6,202) (X(I),I=1,31)
          XOF1 = X(1)
```

```
      DO 29 I=1,MD2
29    X(I) = X(I)/XOF1
      WRITE (6,207)
      WRITE (6,202) (X(I),I=1,301)
      TINTER = 0.0
      DO 27 I=1,MD2
      IF (X(I) .LT. 0.00001 ) GO TO 28
27    TINTER = TINTER + X(I)
28    WRITE (6,226) I   ,X(I)
      TINTER = TINTER * 1.0 / TIMER
      TLENGT = TINTER * US
      WRITE (6,240)  TINTER ,TLENGT
      DO 62 I=1,MO4
62    S(I) = S(I)/(FLOAT(MD*NO)*TIMER*FMSU)  *2.0
      WRITE (6,254)
      WRITE (6,202) (   S(I),I=1,MO4)
      DO 63 I=1,MO4
63    FR(I) = (FLOAT((I-1)*MD) + FLOAT(MD)/2.)*FREQY
      WRITE(6,206)
      WRITE (6,202) (FR(I),I=1,MO4)
      TMICRO = 0.0
      DO 80 I=1,MO4
80    TMICRO = TMICRO+S(I)*FR(I)*FR(I)
      TMICRO =  TMICRO*FLOAT(MD)*FREQY*4.0*3.1416*3.1416/(US*US)
      TMICRO = SQRT(1.0/TMICRO)
       WRITE (6,250) TMICRO
      DO 72 I=1,MO4
72    S(I) = US *S(I) / 6.2832
      WRITE (6,246)
      WRITE (6,202) (S(I),I=1,MO4)
      DO 73 I=1,MO4
73    FR(I) = 6.2832 * FR(I) / US
      WRITE (6,248)
      WRITE (6,202) (FR(I),I=1,MO4)
      IF (KCOND .LT. KKK ) GO TO 1
      END
```

XI BIBLIOGRAPHY

1. Prandtl, L. Ministry of Aircraft Production Völkenrode, Rept. and Trans. No.64, 1946.

2. Jones, R.T. NACA Tech. Note, No.1402, 1947.

3. Sears, W.R. J.Aero. Sci. 15,49. 1948.

4. Schubauer, G.B. & Klebanoff, P.S. NACA Adv. Conf. Rept. No.5K27, Wartime Report W-86, 1946.

5. Kronauer, R.E. Pratt and Whitney Res. Rept. No.137, 1953.

6. Champagne, F.H., Sleicher, C.H., & Wehrmann, O.H. "Turbulence measurements with inclined hot wires," J. Fluid Mech., vol.28, pt.1, pp. 153-175, 1967.

7. Champagne, F.H. & Sleicher, C.H. "Turbulence measurements with inclined hot wire," J. Fluid Mech., vol.28, pt.2, pp. 177-182, 1967.

8. Bullock, K.J. & Bremhorst, K. "Hot-wire anemometer measurements in flow where direction of mean velocity change during a traverse," IEEE Transaction on Instrumentation & measurement, vol.IM-18, No3, 1969.

9. Mccroskey, W.J. & Durbin, E.J. "Flow angle and shear stress measurements using heated films and wires," ASME paper No.71-WA/FE-17, 1971.

10. King, L.V. "On the convection of hear from small cylinders in a stream of fluid," Phil. Trans. Roy. Soc. (London), 214A, 373, 1914.

11. Kovasznay, L.S. & Tormarck, S.I. "Heat loss of hot-wire in supersonic flow," Bumblebee Rep. No.127, Johns Hopkins, 1950.

12. Lowell, H.H. "Design and application of hot wire anemometer," NACA TN2117, 1950.

13. Spangenburg, W.G. "Heat loss characteristics of hot wire anemometers," NACA, TN3381, 1955.

14. Collins, D.C. & Williams, M.J. "Two-dimensional convection from heated wires at low Reynolds number," J. Fluid Mechanics, vol.6, 1959.

15. Morkovin, M.V. "Fluctuations and hot wire anemometry in compressible flows," Agardagraph 24, 1956.

16. Hinze,J.O. "Turbulence, An Introduction To Its Mechanism And Theory," pp. 75-80, Mcgraw-Hill Co., New York, 1959.

17. Van der Hegge Zijnen,B.G. Appl. Sci. Research 6A,129, 1956.

18. Kramers,H. Physica, 12, 61, 1946.

19. Laufer,J. "The Structure Of Turbulence In Fully Developed Pipe Flow," Report 1174, National Advisory Committee For Aeronautics, 1954.

20. Bennett,C.O., & Myers,J.E. "Momentum, Heat, And Mass Transfer," pp. 62, Mcgraw-Hill co., New York, 1962.

21. Bennett,C.O., & Myers,J.E. "Momentum, Heat, And Mass Transfer," pp. 137-138, Mcgraw-Hill., New York, 1962.

22. Hinze,J.O. "Turbulence, An Introduction To Its Mechanism And Theory," pp. 60-61, Mcgraw-Hill Co., New york, 1959.

23. Athanasios Papoulis, "Probability, Random Variables, And Stochastic Processes," pp. 329, Mcgraw-Hill Co., New york, 1965.

24. Bendat,J.S., & Piersol,A.G. "Measurement And Analysis Of Random Data," pp. 82, John Wiley & Sons., 1966.

25. Taylor,G.I. "The Spectrum Of Turbulence," Proc. Roy. Soc. London, 157A,537, 1936.

26. Taylor,G.I. "The Spectrum Of Turbulence," Proc. Roy. Soc. London, 151A,421, 1935.

27. Schiesser,W.E. "Statistical Uncertainty Of Power Spectral Estimates," TM 711-C-1 Weston-Boonshaft And Fuchs, Weston Instruments, Inc.

28. Yost,A.M. "An Investigation Of Turbulent Flow Over A Triangular Roughness," M.S. Thesis, Univ. Of Houston, 1969.

29. Jorgensen,F.E. "Directional Sensitivity Of Wire And Fiber-film Probes--An Experimental Study," DISA Information NO. 11, 1971.

NOMENCLATURE

A	Instantaneous bridge voltage from hot wire anemometer
A_1	$(1+k^2\tan\alpha) - R\cdot\tan\alpha\,(k^2-1)$
A_2	$(1-k^2)\tan\alpha + R(k^2+\tan^2\alpha)$
A_3	$(k^2+\tan^2\alpha)$
A_4	$(1+k^2\cdot\tan^2\alpha)$
A_5	$2(1-k^2)\tan\alpha$
A_s	Surface area normal to S-direction
B_1	$(k^2+\tan^2\alpha) + R(k^2-1)\tan\alpha$
B_2	$(k^2-1)\tan\alpha + R(1+k^2\cdot\tan^2\alpha)$
B_3	$(1+k^2\cdot\tan^2\alpha)$
B_4	$(k^2+\tan^2\alpha)$
B_5	$2(k^2-1)\tan\alpha$
C_1, C_2, C_3	Calibration constant
C_p, C_v	Specific heat at constant pressure, and volume respectively
D	Diameter
E_b	Bridge voltage
$E_s(f)$	Power spectrum in S-direction
F_1	$\overline{\gamma_s^2}\left(\frac{A_4}{2S_1}-\frac{A_1^2}{2S_1^2}\right) + \overline{\gamma_n^2}\left(\frac{A_3}{2S_1}-\frac{A_2^2}{2S_1^2}\right) + \overline{\gamma_s\gamma_n}\left(\frac{A_5}{2S_1}-\frac{A_1A_2}{S_1^2}\right)$
F_2	$\overline{\gamma_s^2}\left(\frac{B_4}{2T_1}-\frac{B_1^2}{2T_1^2}\right) + \overline{\gamma_n^2}\left(\frac{B_3}{2T_1}-\frac{B_2^2}{2T_1^2}\right) + \overline{\gamma_s\gamma_n}\left(\frac{B_5}{2T_1}-\frac{B_1B_2}{T_1^2}\right)$
F_{sd}	Shear stress caused by viscosity in S-direction
F_{sp}	Pressure force in S-direction
F_{sr}	External force in S-direction acting on the solid

	boundary of the volume
$F_s(K_w)$	Normalized power spectrum in S-direction
f	Frequency
G_1	$\frac{S_2}{2S_1} + \frac{S_3}{2S_1} - \frac{1}{8}\frac{S_2^2}{S_1^2}$
G_2	$\frac{T_2}{2T_1} + \frac{T_3}{2T_1} - \frac{1}{8}\frac{T_2^2}{T_1}$
H	Rate of heat transfer to stream per unit length of sensor
H_0, H_1	Known input signal to tape recorder
H_{00}, H_{10}	Corresponding output of H_0, H_1 respectively from hybrid computer
H_2	Hybrid computer output
I	Sensor heating current
k, k_0	Constant depending on sensor
Kg	Thermal conductivity
K_0, K_1, K_2	Gain value of adjustable DC offset, tape recorder, and hybrid computer, respectively
K_w	Local wave number, $2\pi f/\overline{Vs}_{local}$
L	Length
Nu	Nusselt number, $H/(\pi Kg(Ts-Te))$
Pr	Prandtl number, $\mu Cp/Kg$
P	Pressure
Po	Atmosphere pressure
R	$\overline{Vn}/\overline{Vs}$

$R(\tau)$	Auto correlation
Re	Reynold number, $\rho VeD/\mu$
Re_{Max}	Reynold number defined at VS section
r	Radius
γs	$Vs'/\overline{Vs}$
γn	$Vn'/\overline{Vs}$
S, N, T	Coordinates in longitudinal, radial, and binormal direction, respectively
S_1	$(1+k^2\cdot\tan^2\alpha) + 2R(1-k^2)\tan\alpha + R^2(k^2+\tan^2\alpha)$
S_2	$2A_1\gamma s + 2A_2\gamma n$
S_3	$A_3\gamma n^2 + A_4\gamma s^2 + A_5\gamma s\gamma n$
$S(w)$, $S^+(w)$	Power spectrum in mathematical notation
T_1	$(k^2+\tan^2\alpha) - 2R(1-k^2)\tan\alpha + R^2(1+k^2\tan^2\alpha)$
T_2	$2B_1\gamma s + 2B_2\gamma n$
T_3	$B_3\gamma n^2 + B_4\gamma s^2 + B_5\gamma s\gamma n$
Te	Ambient air temperature
Ts	Sensor temperature
V_I	Instantaneous velocity
$\overline{V_i}$	Mean velocity in i-direction
V_i'	Fluctuating velocity in i-direction
Ve	Effective cooling velocity
$\overline{Ve}$	Mean effective cooling velocity
Ve'	Fluctuating effective cooling velocity
V	Volume
V_b	Bulk average velocity
y	Distance from wall

V^*	Friction velocity, $(\tau_o/\rho)^{\frac{1}{2}}$
α_{si}, α_{ti}	Calibration coefficients
α_e	Angle between V_I and S-direction
$-\alpha_a$	Angle between tangent to the wall boundary and S-direction
α	Angle between the mormal to the sensor and the S-direction in three-dimensional plane
β_2	Angle between V_I and $(Vs^2 + Vt^2)^{\frac{1}{2}}$ vector
β_3	Angle between V_I and the normal to the sensor
β_4	Angle between Vs and $(Vs^2 + Vt^2)^{\frac{1}{2}}$ vector
δ	Angle between V_I and the sensor axis in one-dimensional plane
$\delta_0, \delta_1, \delta_2$	Offset value of adjustable DC offset, tape recorder, and hybrid computer, respectively
Ω_w	Total electric resistance of sensor
Ω_3	Electric resistance in serie with sensor
τ	Shear stress
τ_o	Shear stress at wall
ϕ	$(S_1/T_1)^{\frac{1}{2}}$
Φ	$(Ve_1(1+G_2))/(Ve_2(1+G_1))$
ψ	$(\Phi^2+1)(1-k^2)/(\Phi^2-1)(1+k^2)$
λ	Micro scale of turbulence
Λ	Integral scale of turbulence
$\langle\ \rangle$	Expectation notation
ρ	Density
μ	Viscosity

LIST OF TABLES

LIST OF FIGURES